Università degli Studi di Napoli Federico II
Ph.D. Program in
Information Technology and Electrical Engineering
XXXV Cycle

Thesis for the Degree of Doctor of Philosophy

Project, Development and Experimental Setting of Wearable E-Textile Systems for Remote Health Monitoring

by

Federica Amitrano

Advisor: Prof. Mario Cesarelli

Scuola Politecnica e delle Scienze di Base
Dipartimento di Ingegneria Elettrica e delle Tecnologie dell'Informazione

"La rotta di un navigatore in mare spiega i venti e le correnti.
Quando i venti e le correnti vengono da dietro, la rotta è diretta;
quando i venti e le correnti vengono da davanti, la rotta è indiretta.
La rotta diretta non è precipitosa; la rotta indiretta non è tortuosa.
In tutti i venti e le correnti del mondo, non essere nè precipitoso nè tortuoso.
Quando il mare è indurito dalla forza di una burrasca, l'inclinazione di una barca a vela si piega al montare dei venti, e il movimento della barca cede al montare delle onde.
Piegandoci e cedendo riconosciamo la forza del mondo; indurendoci e resistendo riconosciamo la forza di noi stessi."

Ray Grigg

Project, Development and Experimental Setting of Wearable E-Textile Systems for Remote Health Monitoring

Ph.D. Thesis presented
for the fulfillment of the Degree of Doctor of Philosophy
in Information and Communication Technology for Health
by

Federica Amitrano

October 2022

Approved as to style and content by

_____

Prof. Mario Cesarelli, Advisor

_____

Università degli Studi di Napoli Federico II
Ph.D. Program in Information and Communication Technology for Health
XXXV cycle - Chairman: Prof. Daniele Riccio

https://icth.dieti.unina.it/index.php/it/

Candidate's declaration

I hereby declare that this thesis submitted to obtain the academic degree of Philosophiæ Doctor (Ph.D.) in Information and Communication Technology for Health is my own unaided work, that I have not used other than the sources indicated, and that all direct and indirect sources are acknowledged as references.
Parts of this dissertation have been published in international journals and/or conference articles (see list of the author's publications at the end of the thesis).

Napoli, December 13, 2022

_____

Federica Amitrano

Abstract

Wearable devices are electronic systems that, due to their characteristics, can be worn and used to detect, analyse and transmit vital signs. The interest of the clinical field in wearable systems thus arises from the opportunity to follow and monitor the patient for long periods of time and in any environment, according to the principles of telemedicine and overcoming the limitations of the ambulatory approach. The current trend shifts the focus from the general concept of wearable technology to the more specific concept of Electronic Textiles. E-Textiles are textiles that integrate electronic components and represent an ideal solution for the realisation of sensors in direct contact with the body, ensuring comfort and ease of use at the same time. The development of e-textile devices for medical applications therefore represents an interesting challenge to face up in the near future, while large companies, that are active in the sector, are already engaged in the development of wearable systems to be placed on the market.
This work presents the design and development of several devices based on e-textile technology that can be applied to the medical field, according to the typical patterns of remote monitoring and telemedicine systems. The prototype devices realised are: a smart T-shirt, smart socks and a sensorised ankle-foot orthosis. The smart T-shirt integrates textile electrodes for measuring ECG and EMG signals and a wearable sensor for detecting trunk accelerations. The smart socks integrate sensors capable of detecting foot plantar pressures and angular velocities of the lower limbs while walking. These devices have also been tested on patients to verify their performance, using gold standard systems employed in clinical settings as a reference. The ankle-foot orthosis uses similar textile pressure sensors, EMG electrodes and accelerometers, in order to show how e-textile solutions can be applied to different areas of medicine for different purposes. In the end, it was tested a commercially available medical system based on textile technologies, with the aim of providing support to the manufacturing company in the validation and engineering of the device.

Keywords: wearable device, e-textile, telemedicine, healthcare, health monitoring.

Sintesi in lingua italiana

I dispositivi indossabili sono sistemi elettronici che, per le loro caratteristiche, possono essere indossati ed utilizzati per rilevare, analizzare e trasmettere biosegnali. L'interesse dell'ambito clinico per i sistemi indossabili deriva dunque dall'opportunità di seguire e monitorare il paziente per lunghi periodi di tempo ed in qualsiasi ambiente, secondo i principi della telemedicina e superando le limitazioni dell'approccio ambulatoriale. La tendenza attuale sposta l'attenzione dal concetto generale di tecnologia indossabile a quello più specifico di Electronic Textile. Gli E-Textile sono tessuti che integrano componenti elettronici e rappresentano una soluzione ideale per la realizzazione di sensori a diretto contatto con il corpo, garantendo allo stesso tempo comfort e semplicità di utilizzo. Lo sviluppo di dispositivi tessili per applicazioni mediche rappresenta dunque una interessante sfida da affrontare nel futuro prossimo, mentre già grandi aziende, attive nel settore, sono impegnate nello sviluppo di sistemi indossabili da immettere sul mercato.
In questo lavoro viene presentata la progettazione e realizzazione di diversi dispositivi basati su tecnologia e-textile applicabili al campo medico, secondo i tipici schemi propri dei sistemi di monitoraggio remoto e telemedicina. I dispositivi prototipali realizzati sono: una maglietta, dei calzini ed un'ortesi caviglia-piede. La maglietta integra elettrodi tessili per la misura di segnali ECG ed EMG ed un sensore indossabile per la rilevazione delle accelerazioni del tronco. I calzini integrano sensori in grado di rilevare le pressioni dell'arco plantare e le velocità angolari degli arti inferiori durante la deambulazione. Tali dispositivi sono stati anche testati su pazienti per verificarne le prestazioni, adottando come riferimento sistemi gold standard utilizzati in ambito clinico. L'ortesi caviglia-piede prevede l'impiego dei medesimi sensori tessili di pressione, elettrodi per EMG ed accelerometri, allo scopo di mostrare come le soluzioni offerte dall'e-textile possano essere applicate ai diversi ambiti della medicina per varie finalità. Per concludere, è stato testato un sistema commerciale disponibile in ambito medico basato su tecnologie tessili, con l'obiettivo di fornire supporto all'azienda produttrice nella validazione ed ingegnerizzazione del dispositivo.

Parole chiave: dispositivi indossabili, tecnologie tessili, telemedicina, sanità, tele-monitoraggio.

Contents

Acknowledgements

The author's work has been partially carried out in the framework of the European Union projects of the Horizon program 2014-2020:

- "SWEET—Smart WEarable E-Textile based m-health system". Leading companies: Adiramef S.p.A (Carinaro, CE, Italy), Corpora Centro Ortopedico S.u.r.l (Carinaro, CE, Italy).
- "APTIS—Advanced Personalized Three-dimensional printed SensorIzed orthosiS". Leading companies: ICS Maugeri SPA SB (Pavia, PV, Italy), Officine Ortopediche Tombolini (Taranto, TA, Italy).

funded by the Italian Ministry of Economic Development.

List of Acronyms

The following acronyms are used throughout the thesis.

ADC	Analogue-to-Digital Converter
AFO	Ankle-Foot Orthosis
AgNW	Silver Nanowire
AI	Artifical Intelligence
AP	Antero-Posterior
BA	Bland–Altman
BLE	Bluetooth Low Energy
CI	Confidence Intervals
CNT	Carbon Nanotubes
COP	Center Of Pressure
CRS	Comfort Rating Scale
DFA	Detrended Fluctuation Analysis
ECG	Electrocardiogram
EDA	Electrodermal Activity
EMG	Electromyography
EOG	Electroocoulography

FDA	Fractal Dimension Analysis
GCT	Gait Cycle Time
GO	Graphene Oxide
GSR	Galvanic Skin Response
HC	Healthy Control
HF	High Frequency
HIPAA	Health Insurance Portability and Account-ability Act
HR	Heart Rate
HRT	Heart Rate Turbulence
HRV	Heart Rate Variability
ICT	Information and Communications Technology
IMU	Inertial Measurement Unit
IoT	Internet of Things
IT	Information Technology
I2C	Inter-Integrated Circuit
LEVOP	Lower Extremity Venous Occlusion Plethysmography
LF	Low Frequency
LoA	Limits of Agreement
MAC	Media Access Control
ML	Medio-Lateral
MWCNTs	Multi-Walled Carbon Nano-Tubes
NFC	Near Field Communication
PB	Passing–Bablok
PDMS	Polydimethylsiloxane
PP	Pathological Patients

PSD	Power Spectral Density
PVC	Premature Ventricular Contraction
PVDF	Polyvinylidene Fluoride
RIP	Respiratory Inductive Plethysmograph
RLS	Restless Legs Syndrome
RMS	Root Mean Square
RMSE	Root Mean Square Error
SBS	Styrene–Butadiene–Styrene
SDNN	Standard Deviation of Normal-to-Normal beats
SEI	Skin-Electrode Impedance
sEMG	Surface Electromyography
SIDS	Sudden Infant Death Syndrome
SKC	Skin Conductance
SLS	Selective Laser Sintering
SNR	Signal-to-Noise Ratio
SWS	Smart Wearable System
TO	Turbulence Onset
TS	Turbulence Slope
VLF	Very Low Frequency
WL	Wearability Level

List of Figures

List of Tables

Chapter 1

Introduction

The rapid progress in the electronic and digital fields continuously produces innovative resources available for several applications in every-day life, including healthcare, determining the increase in human life expectancy and quality of life. A classic example is the use of mobile devices, which, at present, have no longer communication purposes only, but are used for various activities of daily life, including banking, health monitoring and fitness [24]. Similarly, textiles are no longer only used to be worn, but also assume a functional role [169, 178, 161]. Initially, these concepts originated and were developed in the medical sector, in order to monitor, diagnose and treat several pathological conditions. Nowadays, the use of smart textiles has extended to numerous sectors, including sports, military and in various defence projects [77, 165, 143]. The 'smart' textiles are usually also referred to as e-textiles, wearable electronics, smart clothing, textronics, etc. [178, 122]. This name is derived from the innovative solution of integrating electronic components into textiles, extending the utility and functionality of ordinary garments. These components can be textile or non-textile in nature, integrated with the various techniques available, such as weaving, embroidery, knitting, etc. Depending on the requirements, these components may include sensors, active or passive, actuators, LEDs, antennas, processing units, devices for storing, producing and collecting energy, and transmitting energy [1, 81].

1.1 Smart Textile

According to the definition by Stoppa *et al.* [152] and Simegnaw *et al.* [149], an e-textile can be defined as "A textile structure (fibre, yarn, fabric or finished product) permanently integrated, sewn or attached, etc., with electrical and/or

electronic functionality" [149]. Consequently, the e-textile system is configured as a complex system, with different inputs from textiles, wearable electronics and information technology [152, 36, 113]. The discovery of shape memory materials in the 1960s and smart polymer gels in the 1970s has been generally accepted as the birth of smart materials [123]. However, the term smart material was first introduced in Japan in 1989. The first textile material in history that was referred to as 'smart fabric' was a shape memory silk yarn. The introduction of the first smart material in textiles took place in the late 1990s, while the first semiconductor electronic components for textiles was created in the early 2000s [123]. Intelligent textiles are able to sense and respond to stimuli from the external environment, and can therefore be distinguished into: passive and active smart textiles. The former change their properties according to external inputs, while active smart textiles detect external signals (e.g. temperature, light intensity, etc.) and react accordingly through textile-based, flexible or miniaturised sensors and actuators. Thus, e-textile systems are widely used in different applications and their use depends on customer requirements.

1.2 E-textile Market

Considering the features offered by smart textiles, several digital applications can potentially be developed on a textile substrate. This interesting opportunity is causing a revolution in the wearable device market, with large companies aiming to move from wearable electronic hardware to more convenient electronic textiles. In fact, the market of smart textiles is constantly growing and this is due to changes in daily habits that have underlined the potentialities of e-textiles in the common textile market. This progressive development has also had an impact on the reduction of production costs resulting in easy access to these emerging systems by customers. However, it cannot yet be said that e-textile systems are fully integrated into the Internet of Things (IoT) infrastructure, but as the infrastructure (5G technology) progresses, there will be an increase of such products in the market. A survey conducted by 'Markets And Markets' (wearable healthcare devices market) underlines that the global wearable healthcare market is expected to reach USD 46.6 billion in 2025.

Healthcare remains one of the most interesting and promising markets: e-textile features are very suitable for the development of innovative medical devices or applications that can potentially lead to significant cost reductions for healthcare systems. Wearable health monitoring devices can be easily used by the patient in the home environment and, when integrated in a complete communication infrastructure, enable intelligent remote monitoring with great benefits for healthcare professionals and the patient himself. Electronics-sensitive garments

can be developed to acquire and react to biophysical and biochemical signals from the human body, with some interesting advantages: firstly, the nature of textiles makes them the best solution to realise sensors in direct contact with the skin; secondly, textiles are flexible and well adaptable to the human body, offering technological possibilities not available with common electronics; thirdly, textiles are cheap, comfortable, washable and easily customisable [40]. Therefore, the proper integration of these e-textiles into garments potentially represents an innovative tool for continuous biomonitoring of vital signs, combining the function of sophisticated medical devices with the comfort and ease of use of clothing products. Such systems can thus be exploited to assess the patient state of health at an early stage, allowing clinicians to quickly detect critical conditions, thereby reducing the time needed to obtain a diagnostic result and, finally, enabling the transition from a healthcare model focused on treating illness to one focused on prevention and health promotion [109]. Furthermore, the opportunity to integrate these innovative devices into IoT networks makes it possible to create smart solutions for remote health monitoring, exploring the growing field of m-health and supporting cost reduction in the healthcare system by facilitating early hospital discharge. The possibility of remote diagnosis plays a key role in healthcare worldwide by facilitating timely, convenient and rapid assessment of health status and providing surveillance data for emergencies and chronic diseases. Many E-Textile solutions for health monitoring have been proposed in the literature, but most of them are stuck in the research field and are not destined to flow into the pragmatic healthcare world. Regulatory issues regarding patient safety, privacy, data management, and the need for a secure degree of reliability for device performance are the main obstacles to the widespread commercial deployment of these types of devices. Two of the main issues to be addressed are the washability and reliability of wearable textiles [77, 164, 137]. Washing reliability is assessed by testing the functioning of the entire textile system after a predefined number of washing cycles. There are standard protocols for washing textiles, but these cannot be applied to electronic textiles. Currently, there is not much work addressing this issue applied in the healthcare sector, and for this reason there are not many commercial systems available for purchase. Nevertheless, some experiments on washing reliability have been conducted by some researchers for their products; but reliability issues are still a major obstacle for these products [140, 82, 147, 137, 139, 94].

This thesis is the result of the research activity conducted on wearable and e-textile solutions for the remote health monitoring. The research was firstly focused, but not limited, on the information-theoretic aspects, then flowing to the practice, with the development of several wearable e-textile prototypical devices for health remote monitoring. The aim of the work was to demonstrate the feasibility and the advantages of this kind of approach based on textile electronics in

healthcare, also exploring the reliability of such devices. The innovative features of the proposed systems lie in their multi-parameter approach to health monitoring and their ease of use. The "wearabilit" of the system and its convenience of use make it very suitable for use in the home environment for continuous remote health monitoring of dehospitalized patients. In addition, the literature review work, reported below, revealed the lack of wearable devices in e–textile technology fully integrated into an Information and Communications Technology (ICT) infrastructure for health monitoring. The solutions proposed in this dissertation work aim to fill this gap.
The outline of the thesis is the following:

In this **Chapter 1** it is presented a review of the literature about the biomedical application of e-textile sensors and system. The review explores the progress in smart e–textiles design and manufacturing, with a focus on biomedical devices developed for healthcare monitoring. The main aim is to provide a complete overview of the state-of-art in this promising area, investigating the various applications and the different approaches and solutions proposed by research groups working on these themes.

Chapter 2 presents the first prototypical device developed during the research activity: a smart T-shirt. The smart garment integrates textile electrodes for measuring Electrocardiogram (ECG) and Electromyography (EMG) signals and a wearable sensor for detecting trunk accelerations. The wearable device is integrated in a complete infrastructure for telemedicine service, including a mobile application as access point for collecting data, a dedicated cloud and a user interface to present raw and processed data to the clinician. Details about the design and development of the system are provided and a validation analysis is also performed in order to verify the reliability of the system in comparison with gold-standard methods used in clinical practice.

Chapter 3 introduces another application based on e-textile smart socks. The smart socks were developed using textile pressure sensors, placed on the sole of the garments, and a wearable gyroscope. The system allows the detection of the distribution of plantar pressures and angular velocities of lower limbs, providing static postural and dynamic gait analysis. This prototypical device is integrated in a health monitoring system analogous to the above-mentioned, demonstrating the potentialities of these solutions that can be used for several applications in healthcare sector. The reliability of the system in performing gait analysis is also explored through experimental trials.

Chapter 4 addresses the development of a passive ankle-foot orthosis with embedded textile sensors. This orthotic device exploits similar textile pressure sensors, EMG electrodes and accelerometers, in order to show how e-textile solutions can be applied to different areas of healthcare for different purposes.

Finally **Chapter 5** addresses the experimental validation of a commercially

available medical system for gait analysis based on smart wearable socks. The study was conducted on the request of the manufacturing company, with the aim of providing support to the developers in the validation and development of the device.

1.3 Biomedical Applications of E-Textile

In this Section a review of biomedical applications of e-textile sensors and systems presented in literature is presented, in order to provide a complete overview of the state-of-art in this promising area. Table 1.1 organises the scientific articles included in this review according to the type of acquired data. The researches are also organized in macro-categories regarding the medical field of potential diagnosis. The following paragraphs analyse each macro-categories with insights about the selected works.

1.3.1 The Applications in Cardiology

The first line of Table 1.1 have summarized in a concise and schematic form the principal acquired data – in the field of cardiology diagnostics – using e-textiles systems.

The electrocardiographic signal – called equivalently Electrocardiogram (ECG) – has been over years one of the most appropriate tools to diagnose in advance and, consequently, try to prevent the clinical complications caused by chronic and cardiovascular diseases [146, 110]; in recent years, wearable sensors have proved as novel possible alternatives for the ECG acquisition [28], because the e-textiles (used as ECG diagnostic systems) have indicated to address – or potentially address – several advantages[146].

The researches in this field are summarized in Table 1.2. A first prototype of ECG e-textile system was presented by Wu *et al.* [172]. The authors fabricated a cloth electrode into which Multi-Walled Carbon Nano-Tubes (MWCNTs) were randomly distributed into the fabric which one side was connected and fastened with traditional Ag/AgCl electrodes. The ECG acquisition performed on a single Healthy Control (HC) demonstrated the novel cloth electrode showed similar performances to the traditional Ag/AgCl electrodes, which might be potentially replaced for the daily and long-term monitoring of the ECG [172]. Similar studies were performed by Acar and Le and the respective co-workers [2, 89] which also tested the e-textiles applying the electrodes on smart garments. In particular, Acar *et al.* fabricated nylon Graphene Oxide (GO) coated fibers which were later embedded in an elastic armband; the evaluations on a single HC showed a 96% correlation between the ECG waveforms acquired with graphene textile

Table 1.1. Number of instances for each acquired data, data type and potential diagnosis combined with the related references.

Potential Diagnosis	Acquired Data	Instances
Cardiac	ECG	17 [22, 87, 129, 50, 150, 53, 90, 173, 89, 80, 2, 172, 104, 99, 148, 5, 11]
	Heart Rate	3 [31, 104, 99]
	Blood Pulse	2 [5, 154]
	LEVOP	1 [62]
Muscular	EMG	9 [142, 150, 120, 119, 12, 173, 80, 117, 116]
	Pressure signal from muscles	1 [26]
Physiatry/Orthopaedics	Finger flexion angle	3 [167, 69, 174]
	Acceleration data	3 [52, 14, 157]
	Angle of inclination	2 [104, 99]
	Body motion	2 [173, 154]
	Motion tracking	2 [80, 131]
	Elbow and knee bending angles	1 [91]
	Knee flexion angle	1 [174]
	Knee and scapular flexion angles	1 [101]
	Motion signals	1 [168]
	Sleep posture	1 [142]
	FS and LL indexes	1 [67]
	Back movements	1 [54]
	Strain signals	1 [92]
Respiratory	Respiratory Rate	4 [75, 96, 142, 50]
	Breath Pressure	2 [26, 93]
	Breathing Patterns	1 [132]
Other Themes	EOG	3 [58, 57, 56]
	EDA	2 [150, 63]
	SKC	1 [129]
	GSR	1 [68]
	Skin Temperature	4 [102, 99, 104, 50]
	Biomedical microwave sensing	1 [108]
	Pharynx motion	1 [167]
	Sodium and lactate concentration in human sweat	1 [179]
	Humidity	1 [79]
	Resistance signals	1 [25]
	Alert of the volume of leaked urine	1 [97]

electrodes and the conventional Ag/AgCl ones [2]. More accurate statistical data, on the other hand, were presented by Le *et al.* to compare the performances of

silver-based textile electrodes (embedded in a smart bra) and Ag/AgCl gel counterparts [89]. A similar bra was designed and fabricated by Shathi *et al.* [148] which proved their reduced GO/poly(3,4-ethyelenedioxythiophne polystyrene sulfonate) (PEDOT:PSS) electrodes showed an improved ECG signal response in both wet and dry conditions; additionally, their e-textile electrodes demonstrated an improved flexibility, bendability, and stretchability if compared with conventional electrodes. The manufactured ones – integrated in the sport bra – were the final product of a fabrication study in which even other kinds of e-textile electrodes were analysed [5]. Sinha *et al.* [150] fabricated and analysed in the same period similar PEDOT:PSS coated electrodes demonstrating the capability of such devices to record ECG – and even Electrodermal Activity (EDA) and Electromyography (EMG) – for a single HC in both dry and wet conditions.

Another interesting approach to fabricate e-textiles for ECG monitoring was proposed by Li *et al.* [90]. The authors designed and fabricated an e-textile solution combining the advantages of both the Japanese Kirigami pattering and the inkjet printing strategy demonstrating an ECG stable signal acquisition on a single HC with more than 100% strain of the electrodes. Another solution based on micro/nanofabrication strategies was proposed by Yao *et al.* [173] who manufactured Silver Nanowire (AgNW)/thermoplastic polyurethane electrodes to be later integrated on commercial patches. The authors demonstrated these devices were capable to acquire EGC – in dry state – of a quality comparable to the commercial gel electrodes; moreover, they did not find signal degradation up to 50% strain and 100 cycles. As shown in Table 1.2, in addition to ECG, even EMG and body motion signals were collected. Similar signals were analysed even by Jin *et al.* [80] who used an e-textile sportswear in which an EMG sensor, a strain sensor and a fluoroelastomer conductor - reinforced with Polyvinylidene Fluoride (PVDF) nanofibers - were integrated. The system showed the possibility to acquire ECG signal without significant degradation during a 1h exercise of an HC.

In the last few years, although the research on the ECG monitoring in the field of wearable e-textiles seems still in a preliminary stage, few authors have anyway tried to develop slightly complex e-textile solutions. For instance, in 2013 Kuroda *et al.* [87] proposed two prototypes of e-textile sensing vests, where different combinations of conductive and non-conductive yarns were investigated. The first prototype demonstrated the Japanese NISHIJIN production process was suitable to acquire a clean ECG signal as well as the second more advanced prototype (albeit fabricated – for an eventual mass production – using a different manufacturing technique), although some limitations in the ECG acquisition appeared [87]. In the same period, Catarino *et al.* [22] investigated the capabilities of a novel shirt prototype; specifically, three electrodes were knitted with Elitex for a double purpose: firstly, to allow the integration of electrical connections in

the textile substrate, and secondly to fix the electrodes in specific areas of the shirt prototype. Even if the ECG signals demonstrated different in case of either dry or wet electrodes, the authors claimed the results were of acceptable quality (considering conventional gel electrodes performances) and a tailor-made design of the shirt (according to the target patient) could potentially maximize the ECG acquisition performance [22].

The literature on e-textile applications for ECG acquisition showed even approaches for which the signal acquisition was only one of the milestones. For instance, Lopez *et al.* [99, 104] designed and presented a medical Information Technology (IT) platform – based on multiple subsystems – for patients' localization and monitoring. The authors proposed as a healthcare monitoring subsystem for ECG acquisition a Nylon/Lycra shirt into which two e-textile electrodes were integrated. The results – after acquiring ECG on 5 patients with cardiological disease – showed ECG was of a higher quality (also in a dry state) when the subjects were still, while the signal slightly worsened when sudden movements took place. However, the authors demonstrated the use of a conductive gel and/or mechanisms to reduce motion artifacts could improve signal quality [99]. Similar conclusions were further presented in their more recent article [104]. Similarly, Ferreira *et al.* [50] designed and presented a Smart Wearable System (SWS), the Baby Night Watch IT platform, to monitor infants potentially affected by Sudden Infant Death Syndrome (SIDS). In this study, a chest belt – into which electrodes and silver coated polyamide yarns were integrated – was chosen as healthcare monitoring subsystem, demonstrating a comparable performance with counterpart commercial products in terms of ECG measurements.

Finally, it is worth mentioning a few research groups performed also experiments on a relatively significant number of subjects (if compared to the already cited contributions). For instance, Postolache *et al.* [129] presented a wheelchair prototype where e-textiles – namely, electrodes composed by fibers coated by conductive polymer and silver – were integrated in correspondence of the armrests. The data acquired by 7 HC demonstrated the proposed platform showed results comparable to the commercial counterparts. A similar number of HC were object of ECG acquisitions in the study of Arquilla *et al.* [11]. The authors manufactured a set of three electrodes – made of nylon coated by silver nanoparticles – stitched on an inextensive fabric baking. Two minutes ECG acquisitions on 8 HC demonstrated once again the capabilities of e-textile electrodes, showing the potential applicability across a wide range of anthropometries and skin types and signal invariance during stretch, bend, or wash tests. The most important diagnostic example, however, was such proposed by Fouassier *et al.* [53]. Specifically, the authors designed and manufactured a t-shirt prototype – into which electrodes made of silver yarn and hydrogel pads were integrated – aimed at working as a 12-lead ECG acquisition system. This solution allowed – to the best of the

authors' knowledge – short-duration 12-lead ECG acquisitions with quality levels comparable to conventional Holter recordings on 30 HC for 4 different analysed positions.

Often, in the context of cardiac field, diagnostic data can be acquired also using simpler and/or different strategies. For instance, Lopez *et al.* [99, 104] were also able to acquire simultaneously and show (on their IT platform) the hearth rate from 5 patients with cardiological disease (Pathological Patients (PP)), using the same shirt used for ECG acquisition. Later, Dabby *et al.* [31] showed similar conclusions using another e-textile prototype; specifically, they demonstrated their e-textile solutions (bras, shirts, and shorts) were capable to acquire a heart rate signal comparable to a commercial chest strap. Blood pulse rate is another potential diagnostic data e-textiles can collect from patients. Shathi *et al.* [148], for instance, acquired the pulse rate of a single HC demonstrating their e-textile electrode – in direct contact with the female volunteer's wrist – showed a pulse response in nearly accordance with normal kits; anyway, some deflections/distortions in pulse rate were found during running. Simultaneously, Tang *et al.* [154] designed and manufactured a non-woven fabric e-textile prototype which demonstrated capable to effectively monitor blood pulse. Finally, in recent years – to the authors' best knowledge – the last diagnostic solution in the field of cardiology, by means of e-textiles, was oriented to record Lower Extremity Venous Occlusion Plethysmography (LEVOP). To this aim, Goy *et al.* [62] developed and fabricated a custom-made battery powered plethysmograph, connected on the one side to an oscilloscope, and on the other side on a set of different e-textile electrodes. The authors conducted LEVOP recordings on 5 HC demonstrating all the three set of the proposed e-textiles materials can be used for LEVOP recordings, showing additionally a statistical in-depth analysis related to the recorded signals from the different materials.

Table 1.2. Insights regarding the cardiac literature: authors, aim, dataset and acquired data.

Authors	Aim	Dataset	Acquired Data
Lopez *et al.* (2010a) [99]	Describing a novel healthcare IT platform for localization and monitoring within hospital environments	5 PP	ECG, heart rate, angle of inclination, activity index, body temperature, location, level of battery, alert
Lopez *et al.* (2010b) [104]	Presenting a medical IT platform platform based on Wireless Sensor Networks and e-textile for patients' localization and monitoring	5 PP	ECG, heart rate, angle of inclination, activity index, body temperature, patient's location, battery level, alert code

Continued on next page

Table 1.2 – continued from previous page

Authors	Aim	Dataset	Acquired Data
Wu *et al.* (2010) [172]	Presenting a novel cloth electrode for ECG monitoring	1 HC	ECG
Catarino *et al.* (2012) [22]	Designing and fabricating textile integrated electrodes for ECG continuous health monitoring for disabled or elderly people	1 HC	ECG
Kuroda *et al.* (2013) [87]	Prototyping an ECG sensing e-textile vest	1 HC	ECG
Goy *et al.* (2013) [62]	Fabricating e-textiles to monitor LEVOP	5 HC	LEVOP
Postolache *et al.* (2014) [129]	Presenting a wheelchair architecture equipped with e-textiles for ECG and Skin Conductance (SKC) sensing	7 HC	ECG, SKC
Ferreira *et al.* (2016) [50]	Presenting the design and fabrication of SWS to prevent infants' SIDS	HC#	Breath pressure signal of the ribcage, pressure signal from biceps femoris muscle
Dabby *et al.* (2017) [31]	Presenting a new method for building wearable electronic and textile sensor systems directly integrated in garments to detect the heart rate	1 HC	Heart Rate
Acar *et al.*(2018) [2]	IDeveloping a single-arm ECG armband embedded with flexible graphene textiles for ECG data acquisition	1 HC	ECG
Li *et al.* (2019) [90]	Fabricating e-textiles depositing conducting materials thorough inkjet printing on conventional textiles for monitoring purposes	1 HC	ECG
Yao *et al.* (2019) [173]	Designing and fabricating multifunctional e-textiles with mechanical and functional properties comparable with typical textiles for monitoring applications	1 HC	ECG, EMG (arm), motion signals

Continued on next page

Table 1.2 – continued from previous page

Authors	Aim	Dataset	Acquired Data
Le *et al.* (2019) [89]	Comparing differences in ECG registration between silver-based textile electrodes and silver/silver-chloride gel electrodes, both integrated in a smart bra	1 HC	ECG
Fouassier *et al.* (2019) [53]	Comparing the quality of the ECG signal registered using both a 12-lead Holter and a novel smart 12-lead ECG acquisition T-shirt	30 HC	ECG
Sinha *et al.* (2020) [150]	Fabricating PEDOT:PSS coated electrodes to record EMG, ECG and EDA	4 HC^{EMG} 1 HC^{EDA} 1 HC^{ECG}	EDA, ECG, EMG (biceps, triceps, tibialis, and quadriceps)
Shathi *et al.* (2020b) [148]	Developing e-textile electrodes for the detection of high-quality biomedical signals	1 HC	ECG, pulse rate, pressure
Tang *et al.* (2020) [154]	Fabricating machine-washable e-textiles with high strain sensitivity and high thermal conduction for monitoring applications	1 HC	Motion signals, blood pulse
Arquilla *et al.* (2020) [11]	Using sewn textile electrodes for ECG monitoring	8 HC	ECG
Shathi *et al.* (2020a) [5]	Presenting a highly flexible and wearable e-textile for smart clothing and ECG detection	1 HC	ECG

Abbreviations. # number of patients not provided.

1.3.2 The Applications in the Muscular Setting

Surface Electromyography (sEMG) is a non-invasive methodology to measure muscle activity using surface electrodes placed on the skin overlying a muscle or a group of muscles [70]. This technique is widely used in rehabilitation research, sport sciences, kinesiology and ergonomics [73]. Electrodes for sEMG are mostly combined with electrode gel in order to reduce the electrode-skin impedance [151]. Nevertheless, in recent decades, e-textile sensors - fabrics which are given sensing properties of different physical nature, such as capacitive, resistive, optical and solar - are increasingly spreading for their wearable nature [20]. The researches in this field are summarized in Table 1.3.

Ozturk and Yapici [119], indeed, proposed wearable graphene textile elec-

trodes to monitor muscular activity showing their feasibility to acquire sEMG signals. They performed a benchmarking study with wet Ag/AgCl electrodes showing good agreement between the two technologies of electrodes in terms of Signal-to-Noise Ratio (SNR) and signal morphology with correlation values up to 97% for sEMG signals acquired from the biceps brachii muscle. The same authors, in line with the previous conference paper [119], presented a research article [120] in which they underlined deeply the use of graphene-coated fabrics as textile electrodes in sEMG acquisition, considering not only the biceps brachii muscle but also triceps brachii and quadriceps femoris muscles. They performed a benchmarking study between the proposed textile electrodes and commercial wet Ag/AgCl ones for each muscle in terms of the Skin-Electrode Impedance (SEI), SNR and cross correlation reaching results within the range of commercial Ag/AgCl electrodes. Results demonstrated that graphene-coated textile fabrics could represent a valid alternative to gelled Ag/AgCl electrodes and therefore they could be used to develop wearable and smart garment.

A similar work was conducted by Awan *et al.* [12] who investigated the use of a graphene-based EMG fabric sensor as a comparable alternative to commercial Ag/AgCl wet electrodes. The authors demonstrated that textile electrodes outperformed the standard Ag/AgCl electrodes in terms of SNR. Additionally, they, after tests on 8 HC, underlined graphene-based smart fabrics can potentially represent a viable alternative to non-reusable Ag/AgCl electrodes for high-quality EMG monitoring. Other authors proposed wearable devices to monitor EMG signals through textile electrodes; as first example, Nijima *et al.* [116] proposed a wearable EMG sensor for monitoring masticatory muscles with PEDOT:PSS textile electrodes with the aim to monitor daily activities such as diet, sleep bruxism, and human motor control. The same authors in a more recent work [117] used the above-mentioned prototype to monitor muscle fatigue related to the muscles of the limbs, starting from the acquisition of temporal muscles, based on the assumption that there is a strong correlation between frowning and jaw clenching muscle activity and the physical efforts made when exercising.

Choudhry *et al.* [26] designed textile-based piezoresistive sensors developed using flexible conductive threads stitched on fabric. They embedded the sensor inside a garment to measure small pressure changes exerted by human muscles. Other authors proposed multifunctional e-textiles to monitor several vital signals, EMG signals included. As described in section 1.3.1, Yao *et al.* [173] developed an integrated textile patch comprising four dry electrophysiological electrodes, a capacitive strain sensor, and a wireless heater for electrophysiological monitoring, motion tracking, and thermotherapy, respectively. Jin *et al.* [80] showed their solution demonstrated its feasibility for continuous long-term monitoring of ECG, EMG signal and motion during 1h of weight-lifting excercises without significant degradation of signal quality. As third example, Sinha *et al.* [150] showed how

PEDOT:PSS coated electrodes, integrated in a spandex t-shirt, were effectively able to record simoultaneously EMG, ECG, and EDA in dry state. The authors concluded this solution could represent a tool for continuous and simultaneous measurement of vital signals in at-risk patients. Finally, Samy *et al.* [142] employed five EMG electrodes: three were attached to subject's chin to detect its muscle movement, which can be indicative of teeth grinding (bruxism), sleep apnea and other sleep disorders, while the other two electrodes were attached to the legs, between the knee and the ankle, to record leg movement.

Table 1.3. Insights regarding literature in muscular setting: authors, aim, dataset and acquired data.

Authors	Aim	Dataset	Acquired Data
Samy *et al.* (2014) [142]	Performing sleep stage analysis with a contact-free unobtrusive system	7 HC	Respiratory rate and its variability and leg EMG from pressure images, sleep posture, stages of sleep
Niijima *et al.* (2017) [116]	Designing and fabricating an EMG-integrated sensors cap to register EMG data of the masticatory muscles for monitoring ADL	1 HC[1] 3 HC[2]	EMG (temporal muscles)
Niijima *et al.* (2018) [117]	Assessing the feasibility of estimating biceps fatigue using an e-textile headband	10 HC	EMG (temporal muscles)
Ozturk & Yapici (2019) [119]	Studying the performance of graphene textiles in muscular activity monitoring (acquisition of surface EMG signals from biceps brachii muscle), comparing the outcome with Ag/AgCl electrodes	1 HC	EMG (biceps brachii)
Awan *et al.*(2019) [12]	Presenting the fabrication of graphene-based e-textile for EMG monitoring, comparing sensing performance with commercial Ag/AgCl wet electrodes	8 HC	EMG (arm)
Yao *et al.*(2019) [173]	Designing and fabricating multifunctional e-textiles with mechanical and functional properties comparable with typical textiles for monitoring applications	1 HC	ECG, EMG (arm), motion signals

Continued on next page

Table 1.3 – continued from previous page

Authors	Aim	Dataset	Acquired Data
Jin *et al.*(2019) [80]	Fabricating a metal - elastomer - nanofibers conductive material for long-term monitoring	1 HC	ECG, EMG (bicep muscle), motion signals
Choudhry *et al.* (2020) [26]	Fabricating piezoresistive sensors – and studying their washability – to monitor breathing and muscular activity	1 HC	Breath pressure signal of the ribcage, pressure signal from biceps femoris muscle
Sinha *et al.* (2020) [150]	Fabricating PEDOT:PSS coated electrodes to record EMG, ECG and EDA	4 HC^{EMG} 1 HC^{EDA} 1 HC^{ECG}	EDA, ECG, EMG (biceps, triceps, tibialis, and quadriceps)
Ozturk & Yapici (2020) [120]	Investigating the performance of conductive graphene textiles as surface EMG electrodes, later integrated in textile electrodes as pedometer	4 HC	ssEMG

[1] experiment 1; [2] experiment 2.

1.3.3 The applications in Orthopaedics

Recently, the development and the spread of Inertial Measurement Units (IMUs) for spatio–temporal and kinematic assessment has represented an innovative progress in the field of biomechanics and wearable sensors. Indeed, wearable sensors based on IMUs are spreading in the biomedical field showing good performances [44, 141] compared to their gold standards. Moreover, considering that the working principle of IMUs is based on the measurement of inertia, IMUs can be applied anywhere without a reference [180] and integrated with textile technology [45]. These applications are particularly appreciated in the orthopaedic sector. The researches in this field are summarized in Table 1.4.

Bartalesi *et al.* [14] developed a wearable system that integrates and fuses information gathered from textile based piezoresistive sensor arrays and triaxial accelerometers, which demonstrated able to perform a real time estimation of the local curvature and the length of the spine lumbar arch. The authors performed a comparative study between their system and a stereophotogrammetric system, showing a very low error when reconstructing the lumbar arch length of a single HC. Always considering the same idea (namely, merging several technologies), Li *et al.* [91] presented a method to integrate and package a triaxial accelerometer within a textile as to create an e–textile even fully integrated within the weave structure of the fabric itself, making it invisible to the wearer. The integrated e–textile based accelerometer sensor system placed on arm and knee joints was used

to identify the activity type, such as walking or running, through the calculation of the joint bending angles. They performed a benchmarking analysis between the proposed device and the related gold standard showing a good agreement with an error lower than 1%.

Even other research groups proposed wearable systems for remote monitoring; for instance, Lorussi *et al.* [101] proposed a wearable system to remotely monitor musculoskeletal disorders. The system is composed of IMUs, e-textile sensors and a decision support system included in a dedicated app able to assist the patient in performing personalized rehabilitation exercises designed by physician/therapist, remotely and in real time (also through alerts). Raad *et al.* [131] proposed a wearable smart glove for remote monitoring of rheumatoid arthritis patients, detecting finger flexions while patients performed several activities at home. The e–textile glove used flex and force sensors, and an Arduino platform to transmit motion data to the physiotherapists through a mobile phone on which a dedicated app is installed.

Other authors proposed a complete platform for healthcare monitoring; as described even in section 1.3.1, Lopez *et al.* [104] proposed a novel healthcare IT platform is capable to monitor several physiological parameters, such as ECG, heart rate, body temperature and tracking the location of a group of patients within hospital environments through the combination of e–textiles and wireless sensors. The same authors, in another work [99], proposed a medical IT platform, based on wireless sensor networks and e–textiles, which supports indoor location-aware services as well as monitors physiological parameters, such as ECG, heart rate, body temperature.

Other researchers proposed wearable devices which are completely textile and do not integrate devices such as IMUs. In this context, Della Toffola *et al.* [157] proposed a wearable system for long term monitoring of knee kinematics: compliance with the use of knee sleeve, indeed, is monitored by using an e–textile sensor that measures the knee sleeve fabric stretch thus allowing one to infer whether the subjects under test wears the knee sleeve. Garcia Patino *et al.* [54] proposed a compact textile–based wearable platform to track trunk movements when the considered user bends forward. The smart garment developed for this purpose was prototyped with an inductive sensor formed by sewing a copper wire into an elastic fabric in a zigzag pattern. Heo *et al.* [69] proposed a flexible glove sensor - which included stretchable and flexible Polydimethylsiloxane (PDMS) films - to monitor upper extremity prosthesis functions.

Other researchers studied new arrangements of materials for biomedical applications, Jin *et al.* [80] studied a highly durable nanofiber-reinforced metal elastomer composite consisting of metal fillers, an elastomeric binder matrix, and electro spun PVDF nanofibers for enhancing both cyclic stability and conductivity, showing a good continuous long-term monitoring of ECG, EMG signal,

and motions during weightlifting exercises without significant degradation of signal quality. Li *et al.* [92] fabricated a textile–based stretchable sensor by using an electronic dyeing method; the conductive textile showed good flexibility and adaptable strain-electric response. The authors demonstrated the excellent performances for monitoring and analysis of several human activities. Tang *et al.* [154] reported the conductive, sensitive, wearable and washable vacuum pressure sensor based on Carbon Nanotubess (CNTs), e–textile with unique nanostructures growth on the non-woven fabric by using the novel and facile nano-soldering method. They proved that CNTs e–textile sensor has a good linearity, high sensitivity and low power consumption. Moreover, they showed the good repeatability, washability, durability and super-hydrophobic performance of the CNTs underling its feasibility to realize smart clothes. Yao *et al.* [173] presented mechanically and electrically robust integration of nanocomposites with textiles by laser scribing and heat press lamination showing a good washability and good electromechanical performance up to 50% strain. They underlined the potential utility of these new materials and methods in healthcare, activity tracking, rehabilitation, sports, medicine and human-machine interactions. Finally, Ye *et al.* [174] reported a scalable dip-coating strategy to construct conductive silk fibers showing its feasibility to be woven into fabrics, resulting in textiles sensitive to physical stimuli such as: force, strain and temperature.

Other authors focused on activity recognition and monitoring. Fevgas *et al.* [52], indeed, presented a platform and a methodology for rapid prototype development of e-textile applications for human activity monitoring in order to deal with human motion and gesture monitoring, posture recognition and fall detection. Vu *et al.* [168] introduced a new approach to classify human body movements, by using textile sensors, embedded into fabrics, using Artifical Intelligence (AI) in order to recognize different standard human motions (e.g. walking, jumping, running and sprinting) starting from features extracted from strain signals. The last authors proposed also another work [167] in which they presented an e–textile strain sensor integrated on a glove to monitor angles of finger motions. They also proved the feasibility of this sensor placing it onto the skin of the neck in order to record the pharynx motions when speaking, coughing and swallowing. Samy *et al.* [142] proposed an unobtrusive framework for sleep stage identification based on a high–resolution pressure–sensitive e–textile bed sheet able to acquire information related to body movement, posture and body orientation. Finally, Hayashi *et al.* [67] proposed a smart wheelchair, composed of e–textile pressure sensors placed on the seat and back support, able to monitor the patients posture on the basis of quantitative sitting-posture scores.

Table 1.4. Insights regarding orthopaedics literature: authors, aim, dataset and acquired data.

Authors	Aim	Dataset	Acquired Data
Bartalesi *et al.* (2010) [14]	Designing, developing, and testing a wearable system to perform the real time estimation of the local curvature and the length of the spine lumbar arch	1 HC	Acceleration data, mechanical deformation
Lopez *et al.* (2010a) [99]	Describing a novel healthcare IT platform for localization and monitoring within hospital environments	5 PP	ECG, heart rate, angle of inclination, activity index, body temperature, location, level of battery, alert
Lopez *et al.* (2010b) [104]	Presenting a medical IT platform platform based on Wireless Sensor Networks and e-textile for patients' localization and monitoring	5 PP	ECG, heart rate, angle of inclination, activity index, body temperature, patient's location, battery level, alert code
Fevgas *et al.* (2010) [52]	Presenting a platform and a methodology for the rapid prototype development of e-textile applications for human activity monitoring	3 HC	Acceleration data
Della Toffola *et al.* (2012) [157]	Presenting a wearable system for long-term monitoring of knee kinematics in the home and community settings	1 HC	Acceleration data, mechanical deformation
Samy *et al.* (2014) [142]	Performing sleep stage analysis with a contact-free unobtrusive system	7 HC	Respiratory rate and its variability and leg EMG from pressure images, sleep posture, stages of sleep
Hayashi *et al.* (2017) [67]	Using smart wheelchairs to monitor posture	3 HC	FS index and LL index
Li *et al.* (2017) [92]	Presenting an electronic dyeing method to fabricate wearable silver-based e-textile sensors for human motion monitoring and analysis	1 HC	Strain signals at heel, lower and upper knee
Vu & Kim (2018) [168]	Introducing a new approach to classify human body movements using textile sensors integrated into smart muscle pants	1 HC	Motion Signals

Continued on next page

Table 1.4 – continued from previous page

Authors	Aim	Dataset	Acquired Data
Lorussi *et al.* (2018) [101]	Developing a sensing platform constituted by wearable sensors for musculoskeletal rehabilitation	5 HC	Knee and scapular flexion angles
Ye *et al.* (2019) [174]	Fabricating e-textile sensors sensible to body and environmental stimuli modifying the surface of natural silks with CNTs	1 HC	Knee flexion angle, finger flexion angle
Yao *et al.*(2019) [173]	Designing and fabricating multifunctional e-textiles with mechanical and functional properties comparable with typical textiles for monitoring applications	1 HC	ECG, EMG (arm), motion signals
Jin *et al.* (2019) [80]	Fabricating a metal–elastomer–nanofibers conductive material for long-term monitoring	1 HC	ECG, EMG (bicep muscle), motion signals
Raad *et al.* (2019) [131]	Proposing a novel Smart Glove for both live and on-demand monitoring	1 HC	Motion signals (hand and finger movement)
Vu & Kim (2020) [167]	Fabricating and optimizing the performance of e-textile strain sensors	1 HC	Finger flexion angle, signal of pharynx motion
Heo *et al.* (2019) [69]	Introducing, characterizing, and experimenting novel textile strain sensors based on AgNW	1 HC	Finger flexion angles
Li *et al.* (2020) [91]	Describing a miniature accelerometer solution integrated seamlessly within the fabric of a sleeve to monitor movement	3 HC	Elbow and knee bending angle
Tang *et al.* (2020) [154]	Fabricating machine-washable e-textiles with high strain sensitivity and high thermal conduction for monitoring applications	1 HC	Motion signals, blood pulse
Garcia Patino *et al.* (2020) [54]	Designing a textile-based wearable platform to prevent low back pain	1 HC	Motion signals (Back movements)

1.3.4 The Applications in the Respiratory Tract

Respiration is a crucial vital function for humans; abnormalities in such a function may have a different origin and can lead to patient deterioration and,

ultimately, death. Previous research has extensively documented the clinical importance of respiratory rate diagnosis and how the precise and routinely monitoring is far to be achieved, on the one side for intrinsic difficulties (linked both to human and machines limitations) and on the other side for the limited use and/or the small diffusion of advanced respiratory monitoring systems [135, 115]. To reach this gap, several methods have been proposed and have been widely investigated over time [95, 166]; among these, several e-textile applications were also proposed. The researches in this field are summarized in Table 1.5.

To the best of the authors' knowledge, Huang *et al.* [75] proposed the first example in this field. Specifically, they manufactured an e-textile bed sheet (where the e-textile piezoresistive layer is enclosed between two sheets of conventional fabric layers) aimed to indirectly acquire respiratory rate data; additionally, the authors designed an IT platform capable to non-invasively and accurately process the acquired data. The analyses performed on 14 HC demonstrated the overall system was effectively capable to inconspicuously monitor patients' respiratory rate when they slept in supine position. Albeit patients' movements effectively invalidated respiratory rate monitoring, the system demonstrated a valid tool to track diseases (e.g. apnea) for which patients movements can be limited.

Similar e-textiles and IT platforms were used later from the same research group and other colleagues. On the one hand, Liu *et al.* [96] conducted new investigations to automatically monitor respiratory rate, considering either the analysis of a restricted patient area (e.g. torso) or different bed configurations (e.g. tilted bed setups); on the other hand, Samy *et al.* [142] concentrated, as already described in section 1.3.2, on new objectives, among which we can mention the sleep stage analysis. In this case, the respiratory rate (even when acquired by the e–textile bedsheet) demonstrated a different output during the different sleep stages of the patients. This finding can help to design and implement the proposed device as an unobtrusive sleep stage identification system, which would help to potentially perform early diagnoses of sleep disorders and chronic diseases.

Respiratory rate demonstrated important even in the case of infants sleeping monitoring [75]. It is not by chance if Ferreira *et al.* [50] investigated – using their custom-made chest belt and the Baby Night Watch IT platform (see also section 1.3.1) – respiratory rate variations in infants to monitor eventual SIDS events; nevertheless, it should be pointed out that – albeit the chest belt represents, for all intents and purposes, an e-textile system – respiratory rate was acquired by the authors using a triaxial accelerometer integrated in the chest belt, differently from the ECG signal.

In the same period, Ramos-Garcia *et al.* [132] designed and fabricated a Respiratory Inductive Plethysmograph (RIP) based breathing system aimed at potentially monitoring breathing rate. The proposed system was a polyester/s-

pandex t-shirt on which a stretch e-textile sensor was placed around the chest of a HC. The preliminary results indicated the proposed system – which needs further improvements to be properly used for multiple tasks – was capable to effectively monitor breathing rate of 3 HCs. Recently, Choudhry *et al.* [26] proposed a similar approach, namely they integrated on a vest a different multilayer sensor around the ribcage area of HCs. The preliminary results indicated the system was capable to recognize changes in sensor resistance while breathing and that the acquired signal was coherent with average adult breaths count. Finally, Lian *et al.* [93] proposed a multifunctional e–textile material – whose layers were composed of high-density AgNWs and a sensing fabric, respectively – which was used to fabricate a face mask, though which they showed the feasibility to indirectly evaluate variations in breathing rate. This prototype could show potentials applications also for healthcare monitoring (e.g. cardiac and respiratory illnesses linked to particulate matter 2.5 penetration in human body), albeit – to the best of the authors' knowledge – the authors did not consider this particular case as the main application for the multifunctional e–textile.

1.3.5 Other Themes

The previous subsections have dealt with the main themes on which the applications and developments of e–textile technologies have focused. However, there are applications of e–textile on less common themes, which confirm the wide development of these technologies in the last decade and testify the variety of purposes to which textile technologies can be applied. In this paragraph we have collected works that offer applications on 'other themes' different from those described in detail in the previous subsections, widening the horizon of biomedical applications of e–textile technologies. The researches presented in this subsection are summarized in Table 1.6.

Golpravar and Yapici focused their work on the use of e–textiles in the field of Electroocoulography (EOG), proposing, for the first time, the use of graphene-coated fabric electrodes for EOG acquisition. In [56] they performed a comparative study between conventional Ag/AgCl electrodes and their e–textile electrodes demonstrating high degree of flexibility, elasticity and the possibility of incorporating the novel electrodes into various types of personal clothing. The following year, the same authors presented two research articles [58, 57] in which they designed a devoted unit for textile-based EOG that can achieve on-board noise removal and signal amplification. Moreover, they have developed and implemented a controlled automatic blink detection algorithm, able to detect voluntary blinks in real-time. The performances of the device in recording EOG signal during specific eye movement patterns and in detecting voluntary blinks have been explored in their works resulting in good agreement with the reference

Table 1.5. Insights regarding literature in respiratory field: authors, aim, dataset and acquired data.

Authors	Aim	Dataset	Acquired Data
Huang *et al.* (2013) [75]	Presenting an e-textile bedsheet to measure human respiratory rate	14 HC	Respiratory rate
Samy *et al.* (2014) [142]	Performing sleep stage analysis with a contact-free unobtrusive system	7 HC	Respiratory rate and its variability and leg EMG from pressure images, sleep posture, stages of sleep
Liu *et al.* (2014) [96]	Presenting an unobtrusive on-bed respiration system	12 HC	Respiratory rate
Ramos-Garcia *et al.* (2016) [132]	Using a coverstitched stretch sensor in a commercial shirt to monitor respiration	3 HC	Breathing patterns
Ferreira *et al.* (2016) [50]	Presenting the design and fabrication of SWS to prevent infants' SIDS	HC#	Body temperature, respiratory rate, ECG
Choundry *et al.* (2020) [26]	Fabricating piezoresistive sensors – and studying their washability – to monitor breathing and muscular activity	1 HC	Breath pressure signal of the ribcage, pressure signal from biceps femoris muscle
Lian *et al.* (2020) [93]	Fabricating a multifunctional e-textile for multiple applications (such as diagnostics and environmental)	1 HC	Breath pressure signal

EOG systems based on Ag/AgCl electrodes.

EDA, also known as Galvanic Skin Response (GSR), is another bioelectrical signal, usually recorded with common Ag/AgCl electrodes, which has been one of the subject of study and applications of textile-based electrodes and devices. Sinha *et al.* [150] employed the same PEDOT:PSS based electrodes used for ECG and EMG recording even to collect EDA signal from fingers and wrist. To this aim, they developed a sensing shirt able to simultaneously record the three biosignals, finding potential applications in continuous health monitoring as well as physiotherapy. Similarly, Postolache *et al.* [129] developed e–textile electrodes for measuring skin conductance using the same materials employed for ECG recording (textile made of fibers coated with conductive polymer and silver). E–textile electrodes were attached to the wheelchair armrests in order to monitor physiological stress parameters of the wheelchair user in unobtrusive way. Haddad *et al.* [63] used a different approach to develop EDA electrodes;

specifically, they integrated Ag/AgCl uniformly coated yarns within three different textile substrates (100% cotton, 100% nylon, and 100% polyester). The e–textile electrodes were used to record EDA on the distal phalanx of the fingers, and their performances were compared with the standard rigid Ag/AgCl electrodes, resulting in higher stability for e–textile electrodes when changes in skin temperature occurred. Jennifer Healey [68] proposed a different application of GSR measurement, developing a 'GSR sock' by integrating two fabric electrodes from a commercial heart rate monitor strap into a standard sock. The electrodes were placed to make contact with the ball and heel foot of a HC. The experimental testing showed that the sock prototype provided a meaningful measure of GSR activity that can be used unobtrusively in daily monitoring.
Chen *et al.* [25] applied their expertise in flexible electronics and polymers to develop a fiber-shaped e-textile strain sensor using polyurethane fibers, AgNWs and Styrene–Butadiene–Styrene (SBS) via knitting and simple dip-coating processes. Due to the textile-based structures and hierarchical fibers, the e–textile exhibited good capability of detecting multiple deformation, including tensile strain and pressure, which enables a wide range of biomedical purposes. In particular, the authors proposed different applications in health monitoring such as pulse beating detection, phonation detection, scoliosis correction, and Restless Legs Syndrome (RLS) diagnosing.
Another important biomedical application, which is particularly suited with wearable and textile-based electronic, is the measure of skin temperature. This is an important parameter for a variety of health monitoring applications, where changes in temperature can indicate changes in health. Embedding temperature sensors within textiles provides an easy method for directly measuring body temperature in defined areas. As first example, Lopez *et al.* [99, 104] embedded a thermometer in the Wearable Data Acquisition Device to include the body temperature as a further parameter provided by the proposed healthcare monitoring system. Ferreira *et al.* [50] used an infrared thermopile sensor embedded in the wearable chest belt, to measure the body temperature of infants, adding this parameter to the other signals registered by the device and previously discussed in the other subsections. Moving to more specific textile-based sensors, Lugoda *et al.* [102] developed a temperature sensing yarn, using a micro thermistor covered with packing fibers and a warp knitted tube. The temperature sensing yarns were then used to create a series of temperature sensing garments: armbands, a glove, and a sock. The performances of the temperature sensing wearable devices were investigated and, from the outcomes of the conducted analyses, the authors found some limitations in measuring skin temperature due to the deformation of the yarn structure and also depending on the fit of the garment.

Jiang *et al.* [79] also proposed a wearable sensing device with embedded temperature and humidity sensors, the latter used as sweat sensor. However, the

authors focused on the use of a textile based Near Field Communication (NFC) antenna, which is able to power the system and transmit sensors data. The measurement results have shown that the textile NFC antennas can still perform properly under bending up to 150°, with a maximum range of 6 cm to access sensor data. This innovation figures to be a very attractive field of development towards self-powered wearable devices, to overcome the limitations of power supplies, very critical challenges for the e–textile field.

Lactate and sodium are other commonly analysed markers in sweat, directly measured on body and, thus, very suitable for wearable textile application. Sweat lactate is a biochemical indicator of anaerobic metabolism in patients with circulatory failure, while sweat sodium is an excellent marker for potential electrolyte imbalance during exercise. Zhao *et al.* [179] presented a thread-based wearable electrochemical biosensor with ZnO-NW-decorated sensing electrodes, for on-body, simultaneous detection of lactate and sodium ion in sweat during perspiration. The biosensor and its signal readout and transmission circuits were fully integrated into a wearable sweat headband, which can wireless communicate with a smartphone for data transmission. Real-time on-body sweat collection and analysis were performed on a HC during intense exercise, confirming the accuracy and stability of biosensor in real use.

A very interesting application of textile electronics was presented by Mason *et al.* [108]. The authors investigated the response of a smart fabric, with integrated conductive pathways and strain gauges, at microwave frequencies region for both biomedical sensing and signal transmission purposes. In terms of sensing, this early work showed that it is possible to detect dielectric change, thus meaning that it may be possible to incorporate complex dielectric sensing capability into garments which could be used to identify patient's health indicators via analysis of bodily temperature, ECG and EMG, sweat rate and its composition to infer bodily fluid parameters such as blood glucose or alcohol level, or to monitor the performance of drugs for chronic patients. This novel sensor was even patented owing to the great potentialities shown in biomedical applications.

Finally, Rong Liu *et al.* [97] presented a peculiar application of e–textile, developing intelligent pants for monitoring incontinence status. The smart garment was developed incorporating conductive yarns in fabrics, using advanced circular seamless knitting technology. The presence of urine causes the variation of the measured electrical resistance of the conductive pathways, allowing to sense, monitor, and alert wearers and care providers on urinary incontinence status.

Table 1.6. Insights regarding e–textile literature in other fields: authors, aim, dataset and data.

Authors	Aim	Dataset	Acquired Data
Bartalesi *et al.* (2010) [14]	Designing, developing, and testing a wearable system to perform the real time estimation of the local curvature and the length of the spine lumbar arch	1 HC	Acceleration data, mechanical deformation
Lopez *et al.* (2010a) [99]	Describing a novel healthcare IT platform for localization and monitoring within hospital environments	5 PP	ECG, heart rate, angle of inclination, activity index, body temperature, location, level of battery, alert
Lopez *et al.* (2010b) [104]	Presenting a medical IT platform platform based on Wireless Sensor Networks and e-textile for patients' localization and monitoring	5 PP	ECG, heart rate, angle of inclination, activity index, body temperature, patient's location, battery level, alert code
Healey *et al.* (2011) [68]	Presenting and validating performances of a novel e-textile sock for measuring GSR	1 HC	Foot GSR
Liu *et al.* (2012) [97]	Manufacturing intelligent incontinence pants made of conductive yarns to monitor the incontinence status	HC#	Volume of leaked urine
Della Toffola *et al.* (2012) [157]	Presenting a wearable system for long-term monitoring of knee kinematics in the home and community settings	1 HC	Acceleration data, mechanical deformation
Samy *et al.* (2014) [142]	Performing sleep stage analysis with a contact-free unobtrusive system	7 HC	Respiratory rate and its variability and leg EMG from pressure images, sleep posture, stages of sleep
Postolache *et al.* (2014) [129]	Presenting a wheelchair architecture equipped with e-textiles for ECG and SKC sensing	7 HC	ECG, SKC
Liu *et al.* (2014) [96]	Presenting an unobtrusive on-bed respiration system	12 HC	Respiratory rate
Ferreira *et al.* (2016) [50]	Presenting the design and fabrication of SWS to prevent infants' SIDS	HC#	Breath pressure signal of the ribcage, pressure signal from biceps femoris muscle

Continued on next page

Table 1.6 – continued from previous page

Authors	Aim	Dataset	Acquired Data
Golparvar *et al.* (2017) [56]	Acquiring EOG signals with graphene textile electrodes comparing the outcome with conventional Ag/AgCl electrodes	1 HC	EOG
Li *et al.* (2017) [92]	Presenting an electronic dyeing method to fabricate wearable silver-based e-textile sensors for human motion monitoring and analysis	1 HC	Strain signals at heel, lower and upper knee
Mason *et al.* (2017) [108]	Evaluating the performance of a flexible sensor with an embedded e-textile cloth for sensing applications	1 HC	Biomedical microwave sensing
Golparvar *et al.* (2018b) [57]	Characterization of graphene-coated electroconductive textile electrodes for EOG acquisition	4 HC 4 PP	Monitoring EOG-related pathologies
Lugoda *et al.* (2018) [102]	Fabricating temperature sensing yarns to manufacture temperature sensing garments	5 HC	Skin temperature
Golparvar & Yapici (2017) [58]	Acquiring EOG signals with graphene textile electrodes comparing the outcome with conventional Ag/AgCl electrodes	1 HC	EOG
Chen *et al.* (2018) [25]	Fabricating a multifunctional e-textile for multidetection of strain, pressure, and force maps	1 HC	Resistance signals
Haddad *et al.* (2018) [63]	Designing and integrating Ag/AgCl e–textile electrodes to monitor EDA comparing the outcome with standard electrodes	1 HC	EDA stimulus responses
Vu & Kim (2020) [167]	Fabricating and optimizing the performance of e-textile strain sensors	1 HC	Finger flexion angle, signal of pharynx motion
Jiang *et al.* (2020) [79]	Integrating textile NFC antennas with temperature and humidity sensors to enable battery-free wireless sensing for monitoring purposes	1 HC	Temperature and humidity

Continued on next page

Table 1.6 – continued from previous page

Authors	Aim	Dataset	Acquired Data
Sinha *et al.* (2019) [150]	Fabricating PEDOT:PSS coated electrodes to record EMG, ECG and EDA	4 HC^{EMG} 1 HC^{EDA} 1 HC^{ECG}	EDA, ECG, EMG (biceps, triceps, tibialis, and quadriceps
Zhao et al. (2020) [179]	Presenting a thread-based wearable nanobiosensor to detect lactate and sodium concentrations during perspiration	1 HC	Sodium and lactate concentration in human sweat

Abbreviations. # number of patients not provided.

1.3.6 Conclusions

The proposed review of literature showed the development of e–textile applications in the medical field in the last decade. In recent years, several fields of medicine have been analysed: cardiology, physiatry and orthopaedics, respiratory tract but also sparse studies on other themes were found. The studies differed in purposes but with one major limitation emerging from this review: most studies focused on development and testing on a healthy subject the new device, and only few studies considered a dataset consisting of more than tens of HC. Therefore, researchers should consider validating their novel devices on a larger cohort of subjects (healthy and pathological) for further studies. This improvement would also enable to conduct studies with AI techniques on more populated dataset since using machine learning on poor dataset would not generate reliable results.

Chapter 2

Development of Smart T-Shirt for Remote Health Monitoring

The first e–textile device developed during the research activity was a smart shirt, named SWEET Shirt. The smart e–textile device was designed to provide a system for the remote health monitoring of patients, in every condition and environment. It can be configured as an excellent solution for de-hospitalized chronic patients who need to constantly monitor their health status. The proposed system combines all the elements for the development of a telemedicine infrastructure: the wearable device, a mobile application for gathering data, a dedicated cloud based service for data storage and a user interface for processing and presenting data to the clinician. The first section of this Chapter presents the design and development of the wearable system, including the mobile application and the signal processing algorithms. The second section is dedicated to the experimental validation analysis carried out on healthy and pathological subjects in order to verify the reliability of the system in comparison with gold-standard methods used in clinical practice.

2.1 Wearable System

The SWEET Shirt is a wearable sensing device that allows for the acquisition of ECG, brachial biceps EMG and trunk acceleration signals. It can be integrated within a complete system for remote healthcare purposes, as illustrated by the schematic shown in Figure 2.1.

The wearable sensor unit allows the bio-signals acquisition when connected to the analogue front-end located in the electronic unit. This unit also contains

a microcontroller and allows data transmission through an integrated Bluetooth Low Energy (BLE) module. A custom-made Android mobile application has been developed to receive and visualize real-time signals on a smartphone, and to upload data on a dedicated web server afterwards. This server presents a restricted area that is exclusively accessible (following prior authentication) by authorised and appointed healthcare professionals, who can download, analyse and process the data using the custom-made MATLAB desktop software.

In the following sections the functional modules of the system are individually presented.

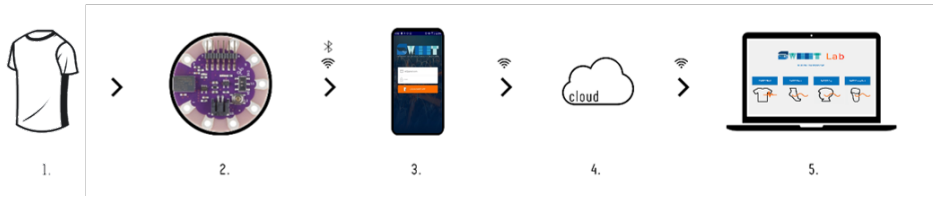

Figure 2.1. System Architecture: (**1**) SWEET Shirt–Textile Unit; (**2**) SWEET Shirt–Control Unit; (**3**) SWEET App; (**4**) Web Server; (**5**) SWEET Lab.

2.1.1 Wearable Sensing Unit

The wearable sensing unit is made up of a commercial elastic t-shirt in which e-textile electrodes are integrated. A knit conductive fabric with a resistance of less than 0.03 Ω per cm in any direction across the textile was used to produce the electrodes. This fabric (Adafruit Inc. www.adafruit.com – product ID: 1167) is plated with real silver, which gives it highly conductive properties and has been used in several applications for biosignal acquisition [60, 163, 156, 155]. Two 4-by-2 cm electrodes were integrated within the garment as sensing elements for electrocardiography, two 2-by-2 cm electrodes placed on each shirt sleeve for sEMG acquisition and a 2-by-2 cm electrode integrated within the upper part of the chest as a ground electrode for all the biosignals. A conductive ribbon (5 mm in width, Adafruit Inc. product ID: 1244) was then used to connect electrodes to the output connectors of the wearable unit, represented by snap buttons placed in a pocket on the chest of the shirt. The conductive ribbon is made of woven conductive stainless-steel fibres, with a resistance of less than 0.1 Ω per cm. Conductive traces sewed on the shirt have been covered by non-conductive fabric to avoid contact with skin. Figure 2.2 shows the wearable sensing unit, with the complete unit and the main details highlighted.

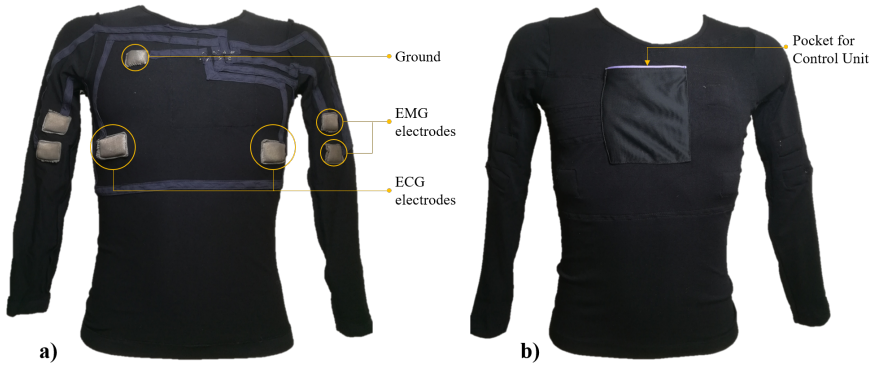

Figure 2.2. SWEET shirt sensing unit: (**a**) internal view with textile electrodes and connections, (**b**) external view.

2.1.2 Electronic Unit

The electronic unit is a compact module containing all the electric and electronic elements that allow for the acquisition, digitisation and wireless transmission of the signals.

A custom-made analogue front-end for ECG and EMG measurement was developed, in order to opportunely face the higher impedance caused by the fabric electrodes. The analogue front-end for ECG measurement comprises four principal stages: an instrumentational amplifier INA 118 from Texas Instruments, a high-pass passive filter with a cut-off frequency of 0.05 Hz, an isolation stage designed with an OpAmp LM358 in voltage follower configuration, and a low-pass active filter with a cut-off frequency of 40 Hz. The first filter is a first order high-pass CR passive filter, while the last stage is represented by a first-order active filter comprising an OpAmp LM324 in non-inverting configuration with a RC feedback.

In terms of the EMG analogue front-end, three principal stages were designed, with the first two similar to those used for the ECG analogue front-end but with the high-pass cut-off frequency set to 15 Hz. The last stage is a precision rectifier circuit with the integration of a low-pass filter. The rectifier circuit comprises an OpAmp LM324, two diodes and a resistor on the feedback connection. This form of configuration is also known as super-diode configuration. A capacitor was added in parallel to the resistor to ensure this stage acts as a first-order low-pass filter. The various components were chosen to set the filter cut-off frequency at 30 Hz. The introduction of this rectifying stage was important as we are interested in the EMG envelope signal for performing the subsequent processing

operations. Generally, an EMG signal is sampled and then rectified in the digital domain, however, in this case it is rectified in the analog domain in order to use a lower sampling frequency. The digitisation of EMG signals requires high sampling frequency, around 800-1000 Hz, since the highest spectral components are around 400-500 Hz. Otherwise, EMG envelope requires lower sampling rate as its main spectral information is at low frequencies. The use of lower sampling rate facilitates the real-time transmission of the signal. Moreover, using this configuration, the mobile application can provide the user with real time EMG envelope signals, without the use of a processing stage, that would increases the complexity of the system and potentially introduce delays.

The electronic board FLORA 9-DOF (Adafruit Inc.), which mounts the tri-axial inertial module iNEMO LSM9DS0, was integrated within the electronic unit to acquire accelerometric signals, while a LilyPad Simblee™ BLE Board (Sparkfun Inc.) was used as system control unit. This unit provides the digitisation of ECG and sEMG signals, and it is connected to Flora accelerometer through the serial Inter-Integrated Circuit (I2C) bus. LilyPad Simblee board was selected because it integrates Simblee™ Bluetooth® Smart Module, allowing data transmission via BLE. BLE technology presents a perfect trade-off between energy consumption, latency, piconet size, and throughput [59]. The choice to use BLE technology can also be regarded as a means of increasing the battery life of the device as much as possible. Battery life is a central issue in the development of portable devices and, in this type of application, it is mostly influenced by the data transmission operations. Indeed, BLE is one of the most saving data-saving transmission protocols, while other solutions have been proposed based on reducing the amount of data to be sent, using a compression method that does not degrade the signal quality [13, 128].

The control unit features were implemented through employing an ARM® Cortex M0 microcontroller that can be programmed using the Arduino IDE. The control unit was programmed to digitise ECG and sEMG analogue signals, and to receive digital data from the accelerometer. Here, ECG signal is digitised with a sample rate of 200 Hz, while sEMG and accelerometric signals are acquired using a sample period of 15ms (66.7 Hz). All data are collected in 20-bytes-sized packets and are sent in real-time, via BLE, to the smartphone launching the SWEET App. The packet transfer rate was set to 66.7 Hz, which was experimentally identified as the maximum rate supported by BLE transmission without data loss. Hence, each packet contains one sample from sEMG and triaxial acceleration signals, and three successive ECG samples, in accordance with their sampling rates.

Despite the fact that the sampling rates chosen for ECG and sEMG signals were lower than those usually used, they were in line with the time resolution required by the target clinical applications. ECG digital processing was focused on hearth rate analysis, which can be accurately done also with lower sampling

rate [105], than the frequencies required for signal morphology analysis. With regard to sEMG, the envelope signal was extracted in the analog domain such that it can be safely sampled with the chosen rate.

All the modules that make up the electronic unit are powered by a 1200 mAh/3.7 V lithium battery, placed on the back of the same unit, which is enclosed in a 3D-printed plastic case (10cm x 7.5cm x 2cm). On the top part of the case, eight snap buttons were integrated to allow for connection to the wearable sensing unit, thus providing the input signals for the analogue front ends. Figure 2.3 shows the internal electronic board and the complete unit.

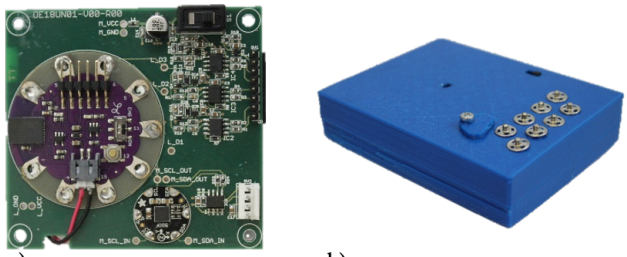

a) b)

Figure 2.3. SWEET Shirt Electronic Unit: (**a**) internal electronic unit, (**b**) complete unit, external view.

2.1.3 Mobile Application

SWEET App is a custom-made application for mobile devices requiring an operating system of Android 6.0 or higher and BLE technology. The application allows the smartphone to communicate and receive data coming from the electronic unit, via the BLE protocol. When the application is started, it is possible to associate and connect the wearable device using its Media Access Control (MAC) address. Following this, the measurement session can start, with the data transferred from the electronic unit to the mobile device, which allows for real-time signal plotting. At the end of the session, the data will be automatically saved in a ".csv" file, which is stored locally and can be uploaded at any time to a dedicated web server. Figure 2.4 shows the main frames of the app.

2.1.4 Signal Processing Algorithm

Data from web server can be accessed and downloaded only by authorised healthcare professionals. The custom-made MATLAB GUI software, SWEET Lab, can be used to plot and post-process signals in order to achieve a huge set

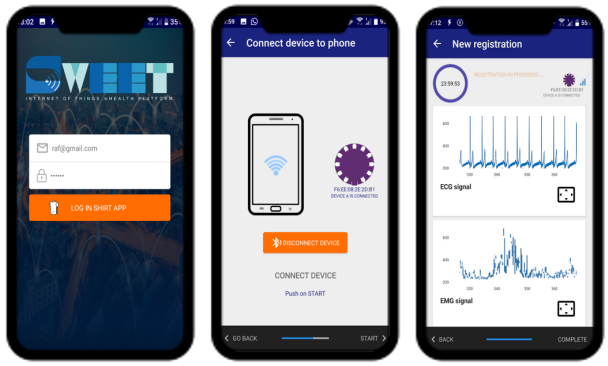

Figure 2.4. SWEET App main frames: (**a**) login, (**b**) unit connection and (**c**) real time signal visualization.

of synthetic parameters of clinical interest. The algorithms used to process ECG, sEMG and accelerometric signals coming from the smart shirt are here briefly discussed.

The first step in ECG signal processing involves the detection of QRS complexes using Okada algorithm [118], for the assessment of the tachogram and the discrete series of RR intervals. The subsequent analysis is divided into several frameworks, the first of which relates to the Heart Rate (HR) analysis, with the instantaneous HR assessed as the mean over four successive beats. From this series, the minimum, the maximum, the medium and the median HRs can be extracted and tachycardia (HR>110 bpm) and bradycardia (HR<60bpm) events subsequently searched and listed.

The second framework is dedicated to the Heart Rate Variability (HRV) analysis in terms of the time, frequency and time-frequency domains. Here, the beats are first classified in terms of normal, ectopic, Premature Ventricular Contraction (PVC) and artifact based on their timing before the RR series is edited to exclude any artifacts and any beat-to-beat intervals that are too short or too long. The new RR series is then processed in time domain to extract the statistical and geometrical measures, as listed in Table 2.1[46].
HRV is also assessed in frequency domain, by analysing how the Power Spectral Density (PSD) is distributed as a function of frequency. The PSD presents three main components in terms of Very Low Frequency (VLF), Low Frequency (LF) and High Frequency (HF). The frequency peaks and the absolute and the relative power values of each component are computed along with the LFHF ratio [106]. Three different methods are provided by the software to compute the PSD,

namely, the Welch Periodogram [171], Burg Periodogram [18] and Lomb-Scargle Periodogram [98] methods. The same analyses are conducted on the windowed periodogram of the RR series to obtain a time-frequency domain analysis of HRV.

Table 2.1. HRV time domain variables

Statistical Measures	
Variable	**Description**
Standard Deviation of Normal-to-Normal beats (SDNN) (ms)	Standard Deviation of normal-to-normal intervals (NN). SDNN reflects all cycles responsible for HR variation in time, thus representing the total variability.
SDANN (ms)	Standard Deviation of the average NN intervals calculated over 5 minutes. SDNN is therefore a measure of changes in HR due to cycles longer than 5 minutes.
SDNNi (ms)	Mean of SDs of NN intervals, calculated over 5 minutes.
RMSSD (ms)	Square root of the mean of the squares of the successive differences between adjacent NN intervals.
NN50	Number of pairs of successive NNs that differ by more than 50 ms.
pNN50 (%)	Proportion of NN50 divided by total number of NN intervals.
Geometrical Measures	
Variable	**Description**
HRV Ti	Area of the histogram distribution of RR intervals, normalized to the maximum value of the histogram.
TINN	Base width of the RR intervals histogram.

The third framework in the ECG processing relates Heart Rate Turbulence (HRT) analysis. This form of analysis represents a non-invasive method that explains the response of the heart to ventricular arrythmias [30] and is a good predictor of mortality following acute myocardial infarction [144]. Two numerical parameters are assessed by the software to describe HRT: Turbulence Onset (TO) to describe the initial acceleration of HR after a PVC, and Turbulence Slope (TS) to reflect the subsequent deceleration of the sinus rhythm [30].

The fourth framework provides a nonlinear analysis of ECG signals using four

different approaches: sample entropy, Detrended Fluctuation Analysis (DFA), Poincarè plot and Fractal Dimension Analysis (FDA). Here, sample entropy presents a nonlinear method for determining the complexity of a RR series, which is computed in terms of various values of k and is used for HRV analysis [6]. Meanwhile, DFA is used to quantify the fractal properties of brief intervals of the tachogram signal [76], while a Poincaré plot is a plot of RR intervals versus the previous RR intervals used to quantify self-similarity. Two numerical parameters are assessed in Poincarè plot analysis: SD2 (the magnitude of the major axis of the ellipse fitting the data; represents the short-term variability) and SD1 (the magnitude of the minor axis of the ellipse; represents the long-term variability). Finally, FDA provides the measurement of the fractal dimension of the RR series assessed using a Higuchi algorithm [72]. Fractal dimension is a useful indicator in cardiology since it assumes different values for different heart disease [3].

The sEMG signals are processed using two different methods. The first one allows for the detection of muscle activation and deactivation. For this purpose a dual threshold algorithm is applied to the sEMG envelope. When the signal passes one of the thresholds for a given period of time, the muscle is considered activated or deactivated. The quantitative assessment of the muscle pattern is provided by means of the following parameters: start and stop time of the muscle activations, activation time, area between the curve and the threshold, temporal position of the maximum activation and number of activations registered.

The second framework of analysis of sEMG is based on the Gaussian decomposition of the signal, which is expressed as a sum of non-normalized Gaussian functions with different amplitudes and standard deviations. The parameters of the component functions are estimated using the maximum likelihood method. The decomposition of the linear envelope into Gaussian curves allows the assessment of the effective intensity of muscular activation, identifying the Gaussian function with the greatest area included in the active phase of the muscle.

From the accelerometric signal acquired by the sensor placed on the chest, it is possible to clinically estimate the physical activity and mobility of a patient, important information especially in the field of rehabilitation medicine. The assessment is made by a series of parameters obtained from the processing of the accelerometric signal. The recording is divided into epochs lasting one minute and, for each of them, a comparison takes place between the values assumed by the modulus of acceleration and a threshold, chosen to be 200 mg (with g=gravity acceleration), a value that guarantees a better discrimination between different physical activities performed. This processing produces the following metrics which are important to estimate the level of physical activity: number of threshold crossings, time above threshold, integrated area between the signal and the threshold, variance of the signal and number of epochs analysed. The linear combination of this set of parameters can provide an estimate of the MET

(metabolic equivalent of task), which is the objective measure of the ratio of the rate at which a person expends energy, relative to the mass of that person, while performing some specific physical activity compared to a reference.

2.2 Validation Analysis

The performances of the smart shirt in acquiring ECG signal were validated through a benchmarking analysis with a gold standard system. Three different type of analysis were conducted in order to address any possible non-conformity in the measurement and/or processing phases managed by the proposed prototype. Firstly, the RR intervals identified by the SWEET Shirt were compared with those obtained via a reference device. Secondly, the similarity between the ECG signals obtained via the different devices was assessed. Finally, comparative analysis was carried out to validate a specific subset of parameters derived from the SWEET Lab software signal processing.

2.2.1 Experimental Setup

A three-channel digital Holter recorder (Oxford Medilog FD5, Schiller, Doral, FL, United States of America) was used as the reference for the ECG signal measurement. The device incorporates seven electrodes and operates with a sampling rate of 8000 Hz. One healthy subject, aged 25, was equipped with the clinical Holter device along with the wearable device, SWEET Shirt, for the ECG measurement (Figure 2.5). Here, the Holter's electrodes were placed on the subject's thorax (Figure 2.5a, b) in order to avoid any overlapping with the SWEET Shirt e-textile electrodes and to ensure the two ECG waveform were as similar as possible by means of visual analysis. The ECG acquisition time was set to 2 h.

2.2.2 Digital Processing and Analysis

ECG signals from both measurement units were loaded in the MATLAB environment for pre-processing and analysis operations, with both signals passed through a notch digital filter to remove any 50 Hz interference. The R peaks in the ECG signal from SWEET Shirt were identified using Okada algorithm, while those in the Holter ECG were automatically detected via its own software and could be loaded in the MATLAB environment. The first analysis was carried out to compare the RR intervals by means of Passing–Bablok (PB) regression. To achieve interval-to-interval correspondence, six RR values from the Holter series

Figure 2.5. ECG electrodes configuration used for signal acquisition.

were removed since they corresponded to a region of artefacts in the SWEET ECG signal. Following this, comparative analysis was performed using the MATLAB function for PB regression (PB function).

ECG waves for each beat were subsequently isolated to allow for a beat-to-beat morphology comparison. The cut-off point was chosen as the midpoint between two subsequent R peaks in order to cover the complete signal. We chose R peaks as fiducial points since no significant differences were found among the RR locations in the first analysis (see the results section). A set of a total of 6968 corresponding beats were obtained for the analysis. The waveforms were then resampled on a normalised axis, with a common number of samples in order to allow for correlation analysis among the corresponding beats. The number of samples was chosen to equal the maximum number of samples found in a non-normalised beat. A resampling operation allows for avoiding any signal distortion in the normalising time axis. We also decided to individually analyse the three principal constituent waves, namely, the P-wave, the QRS complex and the T-wave. Two cut-off points were set in the normalised time axis to divide the three single waves, which were selected to be the two stationary points between the three local maxima representing the single waves, as calculated based on the average beat waveform from the SWEET Shirt recording (Figure 2.6). The complete beat and the single waveforms were rearranged in eight matrices (four for each device recording), with each column containing the signal corresponding to an occurred beat. Correlation analysis for the waveforms was carried out using the MATLAB function, 'corr', which computes the linear correlation between each pair of columns in the input matrices. The diagonal elements of the output matrix hence represent the linear correlations between the corresponding waveforms recorded by the devices under examination. The 'corr' function also returns a matrix of p-values for testing the hypothesis of no correlation *versus* the alternative hypothesis of a non-zero correlation.

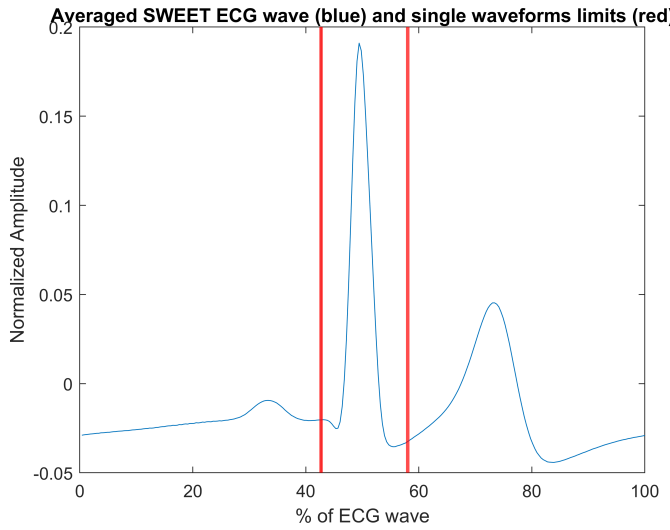

Figure 2.6. Average beat waveform from SWEET shirt and cut points (red vertical lines) used to isolate single waves.

Moreover, a subset of parameters deriving from the processing software was compared to those offered by the commercial Holter software, in order to validate signal processing algorithms. To this end, a further 2-h ECG recording was measured on a 68-year-old volunteer experiencing a pathological disorder (cardiopathic), with the same experimental setup as used previously. The two records were then windowed in terms of 24 five-minute segments, which were individually processed, carrying out a set of 24 measures for each record and for each parameter. ECG signals were windowed both to enlarge the dataset for the comparison, and because five minutes is the recommended duration for short-term ECG analysis [46]. Since Holter software only provides HRV measures in time and frequency domains, validation analysis was carried out on a subset of two representative parameters, one for each HRV field, which were computed by both systems, that is, the SDNN for time domain, and the LFHF ratio for frequency domain. The agreement between measures was assessed using Root Mean Square Error (RMSE), PB regression and Bland–Altman (BA) analysis.

PB regression is a method proposed in 1983 for testing the agreement of two sets of measurement achieved by different systems [124]. The novelties taken by this method, with respect to the standard linear regression are that it is based on nonparametric model, it is not sensitive towards outliers, and it assumes

imprecision in both measurement methods and that errors in both methods have the same distribution, not necessarily normal. As quantitative outcomes, this method returns slope (proportional systematic error) and intercept (constant systematic error) of the fitting linear model. The quantitative-based rules to accept the agreement between systems are whether the Confidence Intervals (CI) of slope and intercept contain respectively 1 and 0 [124].

BA analysis is a graphical method based on the plots of the differences between two measurements against their averages, and it is the most popular method used to measure agreement between two measurement systems [177]. If the differences are randomly distributed around the zero-value axis, no proportional nor systematic error is underlined by the analysis. Quantitative assessment is given through the bias, as the mean of the differences, and the Limits of Agreement (LoA) assessed as the bias ± 1.96 times standard deviation of the differences [7, 16]. If the differences between methods do not have a normal and/or symmetric distribution, LoA are considered to be between the 2.5% and 97.5% percentiles. Significant statistical errors are said to be present if the confidence interval does not contain zero value. Bland and Altman proposed to accept the agreement between the methods under test if this interval contains zero value [7].

2.2.3 Results

RR Intervals Comparison

RR series were compared using PB regression. Here, the PB regression involved searching for a linear relationship between the measures from the two systems and returns slope and offset of the fitting linear model. The systems could be considered as equivalent if the confidence intervals of slope and offset contained 1 and 0, respectively. Table 2.2 shows the results of the PB regression for the RR intervals.

Signal Waveform Comparison

ECG waveforms were compared using Pearson's linear correlation analysis. Figure 2.7 shows the distribution of Pearson's correlation coefficients for the complete ECG waveform, P-wave, QRS complex and T-wave. High values of correlation have been pointed out for ECG waveform (mean value $\pm$ standard deviation: (0.94 ± 0.07), for QRS complex (0.96 ± 0.04) and T-wave (0.96 ± 0.09), while lower values were returned in P-wave analysis (-0.19 ± 0.36).
The quality of correlation between each couple of beats was assessed using the following rule: (i) high correlation if $|r| >= 0.7$, (ii) moderate correlation if $0.3 <= |r| < 0.7$ and (iii) low correlation when $|r| < 0.3$. Table 2.3 shows a

Table 2.2. Summary statistics and results of Passing–Bablok regression analysis for RR interval series.

Statistics		**Mean±std**
RR intervals from SWEET Shirt (ms)		1032 ± 77
RR intervals from Holter MEdilog Darwin		1032 ± 77
Passing–Bablok Regression	**Mean**	**Confidence interval**
Slope	1.00	1.00 to 1.00
Offset (ms)	0	0 to 0

summary of the qualitative assessment of correlation, in terms of percentage of beats, indicating high, moderate or low correlation.
Almost all ECG beats recorded by the prototypical device exhibited a high correlation with the corresponding waveforms obtained via the standard instrument, with a p-value excluding the hypothesis of null correlation between them. Specifically, the QRS complex and T-wave were the most comparable components, while the P-waves mainly exhibited moderate or low correlation values.

Table 2.3. Qualitative assessment of correlation for ECG waveforms.

	Quality of Correlation		
% of the entire set	High	Moderate	Low
P wave	5.97***	49.13**	44.90
QRS complex	99.92***	0.04**	0.04
T wave	98.87***	0.82**	0.31
ECG waveform	98.82***	0.88**	0.30

[1] ns $p > 0.05$, * $p < 0.05$, ** $p < 0.01$, *** $p < 0.001$, **** $p < 0.0001$.

Signal Processing Algorithms Validation

The first approach to the analysis of the parameters generated by the signal processing algorithms involved assessing the RMSEs among the different sets of measures. Table 2.4 shows values of RMSE and the principal descriptive statistics of the datasets, which were divided according to subject.

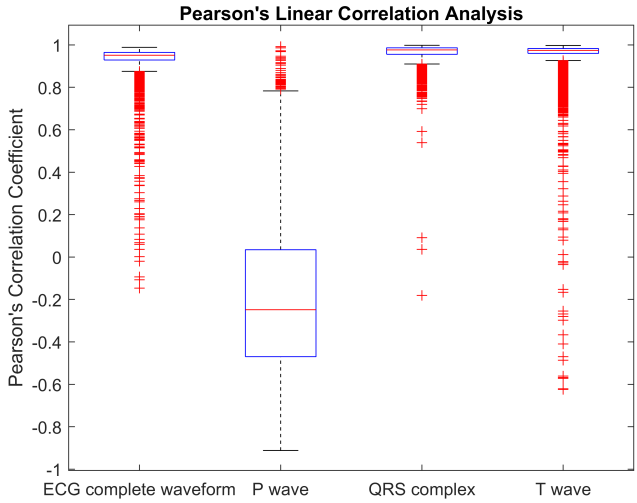

Figure 2.7. Boxplot of Pearson's correlation coefficient for complete and single ECG waveforms.

In the first section of Table 2.4, results from non-pathological volunteer session are reported. In this case the RMSE values were extremely low for both parameters: 0.3% of the mean value for SDNN and 3.6% of the mean value for LFHF ratio. However, different results were obtained with the pathological subject, with the RMSE values greater in terms of both parameters: SDNN presented a RMSE of almost 20% of the mean value, while LFHF ratio RMSE was higher than 50% of the mean.

The analysis of agreement was then further investigated by means of PB regression and BA analysis, with the results presented in Table 2.5.
For each of the analysed parameters, slope and offset from PB regression are provided, along with their 95% CI. Across all the results, slope values were close to 1 and their CIs always include 1. Similarly, the offset values were close to 0 in all analyses, with CIs always including 0 values. In terms of the pathological subject results, CIs were larger than the corresponding CIs in the measurements derived from the recording involving the healthy volunteer.

BA analysis results included some bias with the 95% CI and the LoA. In terms of the results from non-pathological volunteer, the bias values were very close to 0, while both bias CIs and LoA exhibited a low width and always included a 0 value. However, in terms of the results for the pathological subject, the bias

Table 2.4. Main statistics and RMSE assessed for the HRV variables under test.

Non-Pathological Subject			
	Holter (mean±std)	**SWEET (mean±std)**	**RMSE**
SDNN (ms)	63 ± 11	63 ± 11	0.184
LFHF Ratio (adim)	1.5 ± 0.8	1.5 ± 0.9	0.0561
Pathological Subject			
	Holter (mean±std)	**SWEET (mean±std)**	**RMSE**
SDNN (ms)	21 ± 6	20 ± 6	4.41
LFHF Ratio (adim)	4 ± 4	3 ± 3	1.97

Table 2.5. Results of Passing–Bablok regression and Bland–Altman analysis for HRV measures.

		Non-Pathological Subject	
		SDNN	**LFHF Ratio**
PB Regression	**Slope**	1.00	1.00
	Slope CI	0.993 to 1.01	0.974 to 1.04
	Offset	0	-0.00740
	Offset CI	-0.454 to 0.430	-0.0506 to 0.0273
BA Analysis	**Bias**	0.00870	0.00539
	Bias CI	-0.0713 to 0.0887	-0.0189 to 0.0297
	LoA	-0.360 to 0.377	-0.107 to 0.117
		Pathological Subject	
PB Regression	**Slope**	0.932	0.919
	Slope CI	0.597 to 1.39	0.618 to 1.39
	Offset	0.692	-0.409
	Offset CI	-8.86 to 7.02	-1.50 to 0.358
BA Analysis	**Bias**	1.10	0.684
	Bias CI	-0.711 to 2.92	-0.101 to 1.47
	LoA	-7.44 to 9.65	-3.01 to 4.38

values for SDNN and LFHF ratio were higher, with a wider LoA including 0. BA plots are presented in Figure 2.8a and Figure 2.8b. While the differences between the methods were greater in terms of both parameters assessed using the pathological subject, they exhibited a random distribution, meaning no systematic or proportional error could be confirmed from this analysis.

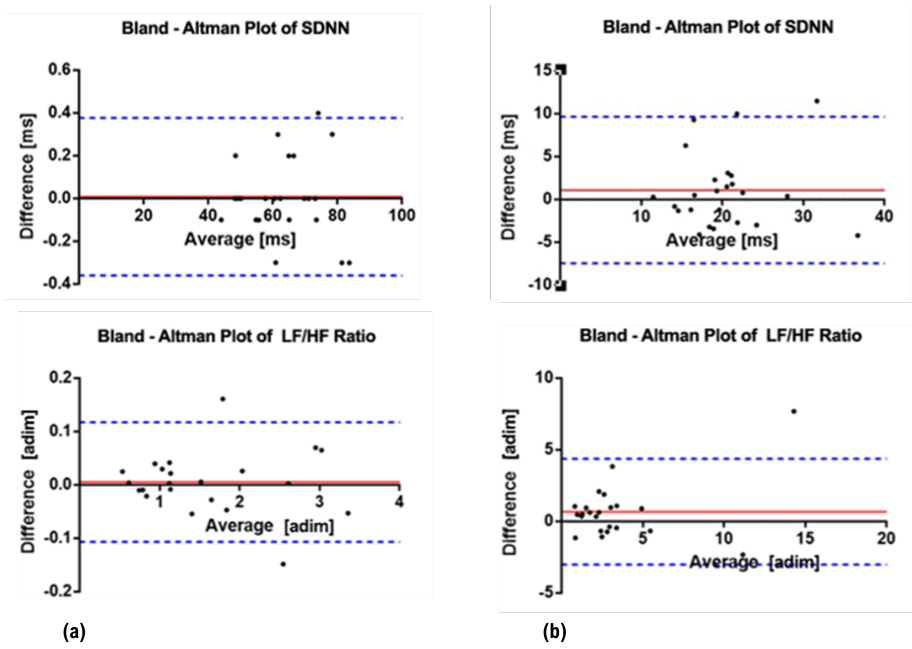

Figure 2.8. Bland–Altman plots of the parameters for: (a) non-pathological volunteer; (b) pathological subject. Red lines represent bias, blue dashed lines represent LoA.

2.2.4 Discussion

In the first analysis, the RR intervals detected by the two systems under investigation were compared by PB regression. Results shown in Table 2.2 confirm that systems can be considered equivalent in the identification of R peaks along ECG signal as beat reference points.
Signal waveforms were then compared by means of Pearson's correlation analysis. This assessment demonstrated that good agreement existed between the signals, particularly in terms of the QRS complex and T-wave, while less correspondence was found in the comparison of the P-waves (see Figure 2.7 and Table 2.3). Figure 2.9 shows the averaged ECG waveforms recorded by the two systems. Here, P-waves are less visible in the Holter signal than in SWEET Shirt recording. This was due to the non-standard electrode placement used for the Holter system (see Figure 2.5), which was chosen to avoid the overlapping with the textile electrodes enclosed in the shirt. Therefore, the lower agreement level with the P-waves can be attributed to the different electrode placements used, which is

almost mandatory in a simultaneous recording. It can be therefore affirmed that the prototypical shirt has the capacity to clearly record an ECG signal that is comparable with those acquired by commonly used clinical portable devices. In the end, the performances of the developed software for signal processing was analysed. As shown in Figure 2.8a, Table 2.4 and Table 2.5 very good results have been achieved in the analysis of parameters assessed on non-pathological subject. The RMSE for both parameters under examination was extremely low, as were the biases assessed via the BA analysis. Meanwhile, PB analysis revealed that there was a regression line very close to the identity line, underlining a strict correspondence between the measurements from the two devices. However, lower agreement was found in the analysis involving the pathological subject. Here, RMSE and bias values were higher (Table 2.4), and PB CIs were wider (Table 2.5), albeit that they still involved values that allowed for concluding that there was some agreement between the two methods. However, BA plots (see 2.8b) did not exhibit any prevalent trend in the distribution of the differences, thus suggesting that no systematic or proportional differences existed between the measurement systems.

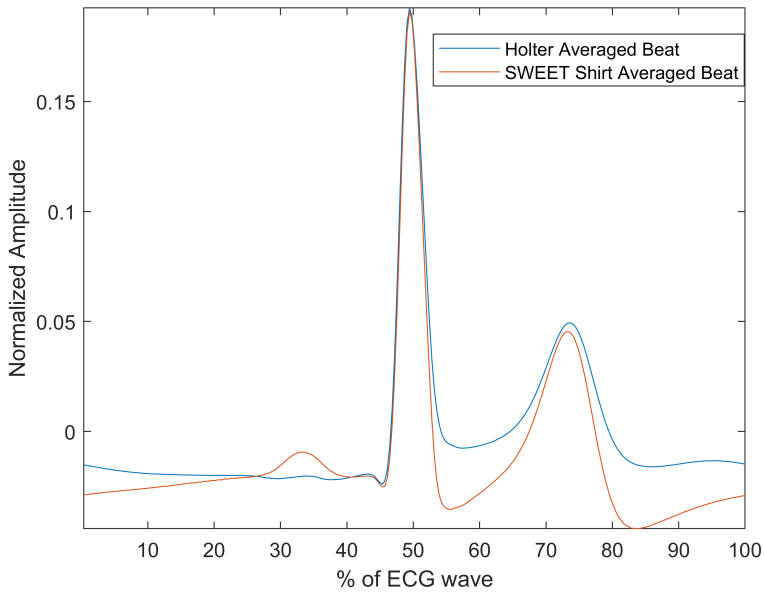

Figure 2.9. Comparison of averaged ECG beat waveforms from Holter device (blue) and sensorised shirt (red).

Based on these results, the lower agreement level in the parameters related to the pathological subject can be attributed to the greater presence of artefacts in the SWEET Shirt record, which was likely due to the weak adherence of the textile electrodes on the patient's skin or the higher number of movements made by the subject during the recording session. ECG signal from SWEET Shirt was clearly visible in 94.66% of the registration time, while the signal from the Holter recorder did not present any artefact. The presence of artefact regions will affect any signal processing results since the artefacts must be replaced by a specific number of normative RR intervals to ensure the continuity of the RR series. In this case, the results were further affected by the fact that they were averaged using a reduced window of 5 min.

Chapter 3

Development of Smart Socks for Remote Health Monitoring

Gait is a complex motor function that, involving the central nervous system and the musculoskeletal system, requires the activation and coordination of numerous muscles and joints. Consequently, a deficit in either system can alter the motor pattern. Technological advances have enabled the quantitative analysis of gait with the possibility of: formulating a prognosis, making a diagnosis but also evaluating the rehabilitation outcome of therapeutic interventions. However, the current technologies used for gait assessment are expensive, typically require the supervision of healthcare professionals and should therefore be used in clinical settings. Specific clinical trials sometimes do not reflect the true variability of the subject's gait, which may instead occur in response to contextual variables and changing environments encountered in daily life. In addition, a further factor to be considered, which may affect gait, is the performance of a test under the supervision of a healthcare professional, which therefore induces the subject to make a greater effort and modify the actual motor pattern accordingly. As a result of these considerations, several researchers support the potential value of remote monitoring of free-living walking behaviour at home or in the community [38, 153].

In this scenario the second e-textile system developed during the research activity was based on smart socks named SWEET Socks. The system is able to collect the angular velocities of lower limbs, using IMUs, and the plantar pressures, by means of textile sensors. The device can be considered a wearable and portable system for the assessment of both postural and gait tasks, exploiting the recent advances in the field of the e-textile, electronic and signal processing. In particular, the system is intended to provide the assessment of spatio-temporal

gait parameters by processing the angular velocities signals while the pressure signals are used to assess the Center Of Pressure (COP) displacements during static postural tests. The details of the prototype design and development are presented below followed by its experimental validation. The wearable smart socks are integrated in a complete system for remote health monitoring, presented in the schematic diagram in Figure 3.1.

Figure 3.1. System Architecture: (**1**) SWEET Sock–Textile Unit; (**2**) SWEET Sock—Control Unit; (**3**) SWEET App; (**4**) Web Server; (**5**) SWEET Lab.

3.1 Wearable System

The wearable sensor unit allows the acquisition of bio-signals when connected to the analogue front-end located in the electronic unit. This unit also contains a microcontroller and allows data transmission through an integrated BLE module. A custom-made Android mobile application has been developed to receive and visualize real-time signals on a smartphone, and to upload data on a dedicated web server afterwards. This is a restricted area that is accessible after prior authentication, exclusively by authorized and appointed health professionals, who can download, analyze, and process data using the custom-made MATLAB desktop software.

In the following sections, the functional modules of the system are individually presented.

3.1.1 Wearable Sensing Unit

The wearable sensing unit consists of a commercial sports sock in which three pressure sensors, in e-textile technology, have been integrated as sensing elements in three strategic points of the foot arch. The number and placement of sensors were based on anatomical considerations: in standing position, the main force transmitted onto the foot originates at the bones of the lower leg. At the ankle, this force is divided into three smaller forces in the style of a tripod. Within the foot, one of these three forces is directly transmitted onto the calcaneus, the

second one onto the first metatarsal, and the third one is distributed across the second to fifth metatarsal [74]. Therefore, three pressure sensors per foot were used: one under the heel (HEEL), one under the first metatarsal bone (MTB1), and one under the fifth metatarsal bone (MTB5) (Figure 3.2c). Besides the experimental device presented in [74], also the commercial smart socks Sensoria are designed with the same number and placement of the pressure sensors. The performances of the latter in static postural assessment have been also investigated, with good results, in comparison with a stabilometric platform [34]. The use of the minimum number of sensors needed for the analysis reduces the complexity of textile design and can improve the comfort and wearability for users. Sensors have been realized by using 2-by-4 cm sheets of EeonTex fabric (EeonTex Eeonyx, Pinole USA), a conductive and non-woven microfiber with piezoresistive functionality (surface resistivity 2000 Ω/sq), offering a reduction of the electrical resistance to the application of force. Their characterization was carried out with load tests using a controlled mechanical clamp with decreasing/increasing loads [33]. The three conductive sensors have been covered by non-conductive fabric to prevent degradation by contact with the skin and are thin enough to provide postural monitoring at natural in-shoe conditions, without distortion of plantar pressure. A conductive ribbon (5 mm tick), with a resistance of less than 0.1 Ω per cm, has been used to connect sensors to the output connectors of the wearable unit. Compared to the conductive wires available on the market, the ribbon has a lower resistance (0.1 vs. 0.9 Ω per cm) and is more robust as it does not break due to stretch. The design of conductive pathways provides a placement of all connectors of the data acquisition system, represented by snap buttons, on the lateral part of the sock, which essentially improves the system usability. The textile connections have been sewn on the side of the sock avoiding, when possible, the passage under the sole of the feet, where they could be deteriorated. Connection lengths have also been minimized by studying the shortest path in order to reduce noise and interference. Figure 3.2 shows the complete device with its sartorial design.

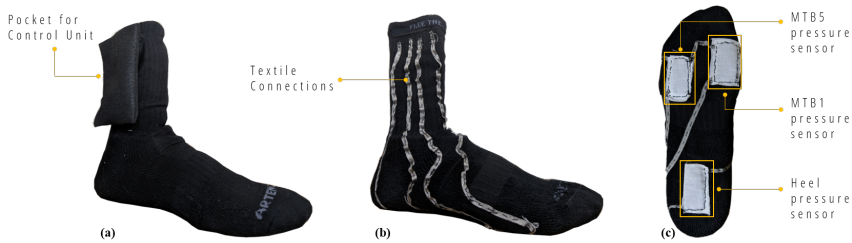

Figure 3.2. SWEET Sock sensing unit: (**a**) external view; (**b**) internal view of textile connections; (**c**) textile pressure sensors.

3.1.2 Electronic Unit

The electronic unit is a compact module containing all the electric and electronic elements to allow acquisition, digitisation, storage, and wireless transmission of the signals.

A conditioning circuit, for each conductive sensor, has been realized in order to read a voltage signal proportional to the applied force. This circuit is realized by means of a voltage divider consisting of two resistors: one of which is of known value and the other represented by the e-textile sensor. The known resistance value is fixed to 18 kΩ, around which the conductive sensor resistance ranges, to reach the condition of maximal sensitivity.

The IMU FLORA 9-DOF (Adafruit Inc.: New York City, New York, USA) has been integrated in the electronic unit to acquire gyroscopic signal. It consists of a small electronic board mounting LSM9DS1 module, a system-in-package featuring a 3D digital linear acceleration sensor, a 3D digital angular velocity sensor, and a 3D digital magnetic sensor.

A LilyPad Simblee™ BLE Board (Sparkfun Inc.: Niwot, Colorado, USA) has been used as the microcontroller. It provides the digitisation of pressure signals, and it is connected to Flora IMU through the I2C serial bus interface. LilyPad Simblee also allows to send data via BLE protocol (or Bluetooth 4.0), using Simblee™ Bluetooth® Smart Module integrated on the shield. BLE technology represents a perfect trade-off between energy consumption, latency, piconet size, and throughput. Its control features are implemented exploiting the ARM® Cortex M0 microcontroller that can be programmed using the Arduino IDE. The control unit is programmed to sample pressure analogue signals with a sample period of 15 ms (66.7 Hz), and to receive digital data from the gyroscope with the same rate. Data are collected in 16-bytes-sized packets (2 bytes for each information: Packet, Time, x-y-z axes of the gyroscope, MTB1, MTB5, and HEEL pressure data) and real-time sent, via BLE, to the smartphone using SWEET App. Other

signals deriving from IMUs (signals from accelerometer and magnetometer) are not recorded by the device because they do not provide any essential information for the planned assessments. An algorithm based only on angular velocity signals was implemented to evaluate all spatio-temporal metrics, because accelerometer signals are affected by gravity and are sensitive to sensor location [112]. When using accelerometers, it is important that they are placed in the same location each time as the signal is affected by how far from the center of rotation they are. The advantage of using a shank mounted gyroscope compared to accelerometers is that, as long as the gyroscope is recording data in the correct plane, it does not matter where on the shank the sensor is placed [41, 133]. This reduction in the amount of acquired and sent data allows to improve signals sampling and sending rate.
All modules making up the electronic unit are powered by a 190 mAh/3.7 V lithium battery, placed on the back of the same unit. The electronic unit is housed in a 3D-printed plastic case (73 mm × 52 mm × 21 mm). On the top part of the case, 4 snap buttons allow the connection to the wearable sensing unit, in order to provide the input signals for the analogue front ends. In Figure 3.3 the electronic unit, with its main details, is shown.

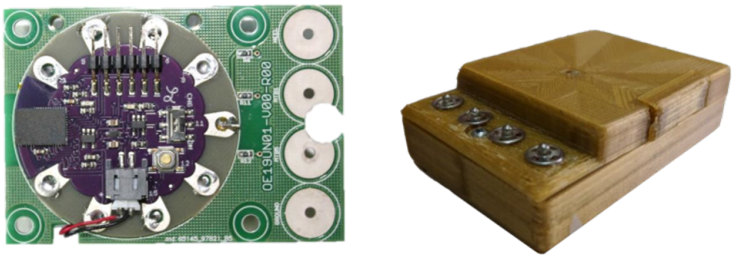

(a) (b)

Figure 3.3. SWEET Sock Electronic Unit: (**a**) internal electronic unit; (**b**) complete unit external view.

3.1.3 Mobile Application

A custom-made Java language application for mobile devices requiring Android 6.0 or higher operating system and BLE technology was developed. The application allows the smartphone to communicate and receive data coming from the electronic unit, via BLE protocol. When the application is started it is possible to associate and connect the wearable device, using its MAC address. Then, the measurement session can start, data are transferred from the electronic unit to the mobile device, which allows signals real time plotting. At the end of

the session data are automatically saved in a ".csv" file, which is stored locally and can be uploaded at any time to a dedicated web server. In Figure 3.4 the main frames of the app are shown.

3.1.4 Signal Processing Algorithms

A custom-made MATLAB GUI software has been developed to allow signal visualization and digital processing. Health professionals have the possibility to download data from the server and analyze them using the tools offered by this software. Pressure and gyroscope signals gathered by the hardware are individually processed to respectively perform posturographic assessment and spatio-temporal gait analysis. The two types of signal were not integrated because they are used in the analysis of two separate phases: pressure signals for static postural assessment while angular velocities in dynamic walking tasks analysis.
A gyroscope-based algorithm for gait analysis has been developed. The angular velocity signals on the sagittal plane are selected and low-pass filtered with 4th-order Butterworth filter (cut-off frequency 5 Hz) to reduce noise. Mid-swing, heel-strike, and toe-off events are then identified on the filtered signals for both feet, using a threshold-based algorithm [138]. The starting point of the algorithm is the identification of the time events corresponding to the mid-swing, identified as the local maximum peaks of the signal. In the next step, local minimum peaks prior and after the mid-swing point are selected as, respectively, toe-off and heel-strike time events. Starting from these gait events times, all temporal parameters of gait analysis are calculated. Algorithms exploiting angular velocity signals, were proven to be more repeatable than acceleration-based algorithm

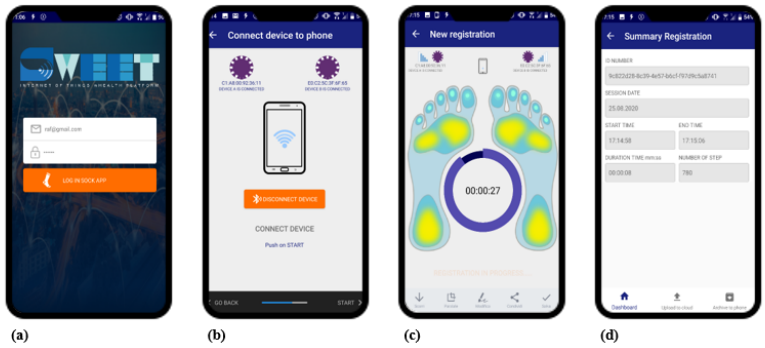

Figure 3.4. SWEET App main frames: (**a**) login; (**b**) unit connection; (**c**) signal recording; (**d**) results summary.

in detecting gait events [121]. Moreover, considering IMUs positioned on the shanks, algorithms using 'peak identification' showed the best performance in the detection of heel-strike and toe-off [159, 65]. In Table 3.1, the list of temporal parameters is provided with a description clearly outlining the methods used to calculate them. Spatial parameters are assessed using a single pendulum model described in [41], where the distance from the foot to the top vertex of the rotation is modeled as equal to the height of the subject multiplied by a scaling factor. Equation (3.1) shows how the stride length is calculated:

$$StrideLength(m) = S \times H \times 2(1 - \cos\theta) \tag{3.1}$$

S represents the scaling factor chosen equal to 0.52 [41], H represents subject height (m) and θ is the angular displacement in the sagittal plane during the stride (rad), assessed by integration of the gyroscope signal.

Plantar pressure signals collected by the smart socks are used to perform sway analysis, as a systematic assessment of the readiness and stability of the human body to achieve and maintain equilibrium. This analysis starts with the estimation of the COP, whose displacement during stand task is a meaningful parameter for a quantitative evaluation of the ability to maintain equilibrium. At each instant, COP coordinates in the Medio-Lateral (ML) (X_{COP}) and Antero-Posterior (AP) (Y_{COP}) directions have been calculated by processing raw pressure data according to the following Equation (3.2),

$$\begin{aligned} X_{COP} &= \frac{\sum_{i=1}^{N} X_i P_i}{\sum_{i=1}^{N} P_i} \\ Y_{COP} &= \frac{\sum_{i=1}^{N} Y_i P_i}{\sum_{i=1}^{N} P_i} \end{aligned} \tag{3.2}$$

where N denotes the total number of sensors, and X and Y are the sensor coordinate inside the whole foot shape area and P the pressure value. The resulting signals express COP displacement along time in the ML and AP directions, with respect to a reference point located in the middle between the feet. The monodimensional representations of these signals constitute the ML and AP stabilograms, while the combined bidimensional plot is referred to as statokinesigram, representing the ground projection of the COP during the stand task.
Signals are filtered with a low-pass 4th-order Butterworth digital filter with a cut-off frequency of 5 Hz [130], and then analysed in time domain to calculate a set of parameters describing the stability of the subject during the task (Table 3.2) [134, 4, 34].
Stabilometric signals are also analyzed in frequency domain. The MATLAB periodogram algorithm is used to estimate PSD, modified using the Hamming win-

Table 3.1. Spatio-temporal gait parameters.

Temporal Measures	
Variable	**Description**
Gait Cycle Time (s)	Defined as the time between two successive heel strikes of the same foot.
Stance Time (s)	The amount of time a foot is in contact with the ground within a single gait cycle. It is the time between the heel-strike and the successive toe-off of the same foot.
Stance Phase (%)	Stance time expressed in percentage of the Gait Cycle Time (GCT).
Swing Time (s)	Duration of the swing phase, in which the foot is not in contact with the ground. It is calculated as the time between the toe-off and the successive heel strike of the same foot.
Swing Phase (%)	Swing time expressed in percentage of the GCT.
Single Support (%)	Part of the GCT in which a single foot is in contact with the ground. It is the time between the toe-off of the opposite foot and the successive heel-strike of the opposite foot, expressed in percentage of the GCT.
Double Support (%)	Part of the GCT in which both feet are in contact with the ground. It is the time between the heel-strike of a foot and the successive toe-off of the opposite foot, expressed in percentage of the GCT.
Cadence (steps/min)	Number of steps per minute.
Spatial Measures	
Variable	**Description**
Stride Length (m)	Distance covered during GCT.
Stride Velocity (m/s)	Defined as the ratio between Stride Length and GCT.

dow. Frequency assessment is provided by means of a set of measures describing the distribution of PSD, such as peak and centroidal frequencies, band powers, and others. All the parameters assessed are listed in Table 3.2. The description clarifies the methods used to evaluate both spatial and frequency domain metrics starting from stabilometric signals and ground projection of the COP trajectory.

Table 3.2. Static postural assessment parameters.

Time Domain Measures	
Variable	**Description**
Mean COP coordinates (cm)	ML and AP mean COP displacements during time.
Mean Distance (cm)	Mean distance of COP trajectory from the center of the trajectory itself.
COP Trajectory Range (cm)	Maximum distance between 2 points of COP trajectory in ML and AP directions.
Root Mean Square (RMS) (cm)	RMS of COP trajectory. It is provided also for single ML and AP directions.
Angle form AP axis (deg)	Mean angle formed by the segments composing COP trajectory and AP direction.
Sway Path (cm)	Total length of COP trajectory, computed as the sum of distances between successive points of the trajectory.
Mean Velocity (cm/s)	Mean velocity of COP trajectory, computed as the ratio between sway path length and duration of the test.
95% Ellipse Area (cm^2)	Area of 95% confidence ellipse encompassing the COP trajectory in transverse plane.
95% Ellipse Angle (deg)	95% confidence ellipse inclination with respect to the ML direction.
Frequency Domain Measures	
Variable	**Description**
Peak Frequency (Hz)	Peak frequency for ML and AP power spectrum.
Median Frequency (Hz)	Frequency below which the 50th percentile of total power is present.
80% Frequency (Hz)	Frequency below which the 80th percentile of total power is present.
Centroidal Frequency (Hz)	Spectral centroid of power spectrum. It indicates where the center of mass of the spectrum is located.
Band Power (cm^2)	Power comprised in low [0.1–0.2 Hz], mid [0.2–0.3 Hz], and high [0.3–1 Hz] frequency bands, expressed as absolute and percentage values.

3.2 Validation Analysis

The proposed system was validated through a benchmarking study with a reference system.

In [10], a first validation analysis was performed by comparing the raw accelerometric and plantar pressure signals acquired by the prototype with those recorded by reference systems. Following the results obtained, a further goal was to validate the performance of the device by exploring the results of gait assessment, in order to identify any non-conformities in the measurement and/or processing phases managed by the new prototype. Spatio-temporal gait parameters calculated by SWEET Sock were compared with those measured by the optoelectronic stereophotogrammetric system. The comparison has been carried out by means of statistical methods. This section describes the methods used for data acquisition and analysis.

3.2.1 Stereophotogrammetric System for Gait Analysis

The reference system chosen for the validation analysis is SMART-DX 700 by BTS Bioengineering, an optoelectronic stereophotogrammetric system used for movement analysis. Stereophotogrammetry is usually considered a 'gold standard' in gait analysis when used appropriately. The system is made of 6 infrared digital cameras, with a sensor resolution of 1.5 megapixel, an acquisition frequency from 250 fps (at maximum resolution) to 1000 fps and an accuracy lower than 0.1 mm. The recognition of body segments during movement is achieved through the use of twenty-two retro-reflective passive markers (diameter 14 mm), which are attached to subject's skin at specific landmarks. Video data are processed on a PC workstation running SMART Clinic software, able to store and compute a set of parameters concerning kinematic (spatio-temporal parameters, joint angles) and dynamic (forces exchanged).

3.2.2 Experimental Setup

One-hundred-and-eight records were acquired on three HCs: two males (aged 27 and 26) and one female (aged 25). Participants were free of neurological, muscular, and skeletal comorbidities affecting mobility and gait. Each subject wore the sensorised socks connected to the electronic unit and was equipped with the markers of the stereophotogrammetric system, in order to perform simultaneous recording of the walking tasks with the two systems under test (Figure 3.5). The markers were attached to subject's skin according to the protocol described by Davis *et al.* [35].
The trials involved free walking tests on a 11 m walkway in the movement analysis laboratory of University Hospital 'Ruggi D'Aragona' of Salerno (Italy). This walking trial is the standard clinical protocol used in the laboratory, and it is also used in gait analysis for scientific purposes [64, 47]. Each subject was instructed to perform eight independent trials respectively at preferred, slow and fast self-

selected walking speed. After that, the use of a metronome was introduced to force subjects walking at fixed normal, slow and high speed. Metronome rate was set at 100%, 67%, and 133% of the average cadence previously assessed for each subject over 5 free walking tests using the accelerometers-based gait analysis system Opal by APDM. Subjects performed four walking trials at each speed imposed by metronome. The trials were performed at different walking speed in order to obtain a dataset covering a wider range of values. The sample size would be better increased including additional participants, however the prototypical nature of the device, along with problems due to the COVID-19 pandemic, made it difficult to involve a larger cohort of subjects. Future developments will certainly include more subjects in order to take into account the gait variability between subjects.
In order to validate the proposed e–textile wearable system, the gait analysis parameters obtained from this device have been compared with those obtained by the reference system. Starting from gyroscope signals measured by SWEET Sock, spatio-temporal gait parameters were computed by the custom-made MATLAB algorithms shown in the previous paragraph (Subsection 3.1.4). The corresponding parameters assessed by the reference system were retrieved from the reports generated by SMART CLINIC software.
The following spatio-temporal parameters were considered for the benchmarking analysis; GCT (s), Cadence (step/min), Stance Time (s), Swing Time (s), and Step Length (m).

3.2.3 Statistical Analysis

The agreement between measurements computed by the two systems–SWEET Sock and SMART-DX 700–was investigated by means of two-tailed paired t-test, PB regression, and BA analysis. The paired t-test has been performed for all the parameters selected for the analysis, in its parametric or nonparametric form (Wilcoxon matched pairs signed-rank test) in according to D'Agostino–Pearson omnibus normality test result. With the paired t-test, the null hypothesis of no difference between the two systems in mean values of each spatio-temporal parameter was tested. A two-tailed test was used and the nominal alpha level was set to 0.05 [15]. In combination with the t-test, the linear correlation between each pair of measurements has been assessed, using Pearson's correlation coefficient (r). The agreement was further investigated using PB regression and BA plots (see Subsection 2.2.2), with the aim to find out any proportional or constant systematic error between the two methods of measurement.
Statistical analyses were performed using R software (ver. 4.0.3).

Figure 3.5. Subject equipped with both systems: SWEET Sock and reflective markers.

3.2.4 Results

The analysis of agreement between the two methods of measurement was firstly tested performing a paired t-test on all the parameters considered for the analysis. For each parameter, the values deriving from all the trials performed were considered, with no separation between subjects or walking speeds adopted. Table 3.3 shows mean and standard deviation values of each analysed parameter dataset for each system of measure. The results of the two tailed paired t-test, with a confidence interval of 95%, are reported using a symbol in accordance with the following convention: ns p-value > 0.05, * p-value < 0.05, ** p-value < 0.01, *** p-value < 0.001, **** p-value < 0.0001. The hypothesis of no difference between systems was tested, so lower p-values suggest rejecting the accordance of systems. In the same table Pearson's r values are reported.
The BA analysis produces the plots shown in Figures 3.6a–3.10a. They provide a qualitative assessment of the distribution of the differences between methods. The descriptive numeric values deriving from the analysis are reported in Table 3.4. The bias represents the mean of the differences between the measures computed by the systems, it is provided with the limits of its 95% CI. In the plots, biases are reported as continue red lines, while the red dashed lines represent the

corresponding confidence intervals. The LoA reported in table are also shown in the graphical representations as black dashed lines. They are assessed as the 2.5 and 97.5 percentiles of differences, as they do not have a symmetric gaussian distribution.
The last analysis on data was performed using PB regression. In addition to the previous analyses, this analysis can reveal the presence of a trend between the measures of the two systems, thus indicating a proportional error in the tested method according to the slope of the fitting regression line. Figures 3.6b–3.10b show the scatter plot of the dataset for each parameter, with the PB regression line in black. The shaded area around the regression line represents its CI, while the red dashed line corresponds to the reference identity line, to which the regression line should be tend in a scenario of perfect agreement. In the PB plots, Pearson's correlation coefficient (r) is also shown because high values of r justify the choice to perform a linear regression analysis. The quantitative outcomes of PB analysis are reported in Table 3.5: slope and intercept of the regression line are listed for each parameter, along with the corresponding 95% CI limits.

Table 3.3. Paired-T test.

Variable	SWEET (mean±std)	BTS (mean±std)	p-value Summary [1]	Pearson's r
GCT (s)	1.1 ± 0.3	1.1 ± 0.3	*ns*	0.992
Cadence (step/min)	109 ± 22	109 ± 22	0.013*	0.996
Stance Time (s)	0.6 ± 0.2	0.7 ± 0.2	<0.0001****	0.994
Swing Time (s)	0.52 ± 0.07	0.45 ± 0.08	<0.0001****	0.969
Step Length (m)	0.73 ± 0.08	0.7 ± 0.1	<0.0001****	0.283

[1] ns $p > 0.05$, * $p < 0.05$, ** $p < 0.01$, *** $p < 0.001$, **** $p < 0.0001$.

Table 3.4. Bland–Altman analysis.

Variable	Bias		Limits of Agreement
	Value	Bias CI	CI
GCT	8.70×10^{-5}	-0.00650 to 0.00633	-0.0582 to 0.0471
Cadence (step/min)	−0.353	-0.736 to 0.0300	-3.83 to 3.26
Stance Time (s)	−0.0671	-0.0716 to -0.0626	-0.108 to -0.00890
Swing Time (s)	0.0731	0.0695 to 0.0767	0.0365 to 0.0977
Step Length (m)	0.0557	0.0326 to 0.0788	-0.133 to 0.255

Table 3.5. Passing–Bablok regression analysis.

Variable	Slope		Intercept	
	Value	Slope CI	Value	Intercept CI
GCT	1.00	0.988 to 1.02	−0.001 55	-0.0179 to 0.0176
Cadence (step/min)	0.989	0.972 to 1.00	0.737	-0.950 to 2.38
Stance Time (s)	1.06	1.03 to 1.08	−0.109	-0.126 to -0.0429
Swing Time (s)	0.904	0.869 to 0.941	0.116	0.0999 to 0.132
Step Length (m)	0.695	0.521 to 0.945	0.249	0.0759 to 0.363

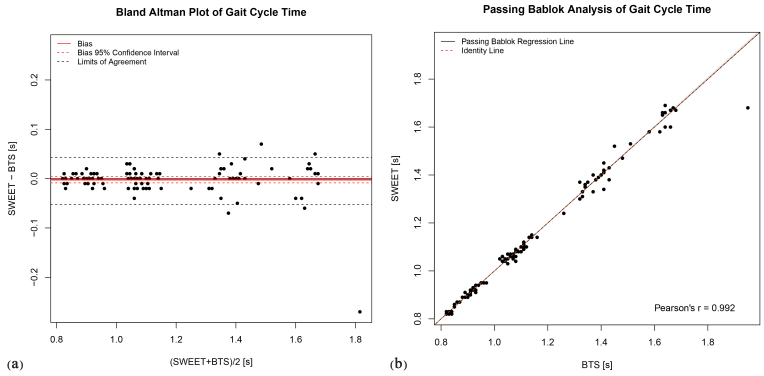

Figure 3.6. Gait Cycle Time: (**a**) Bland–Altman plot; (**b**) Passing–Bablok regression analysis.

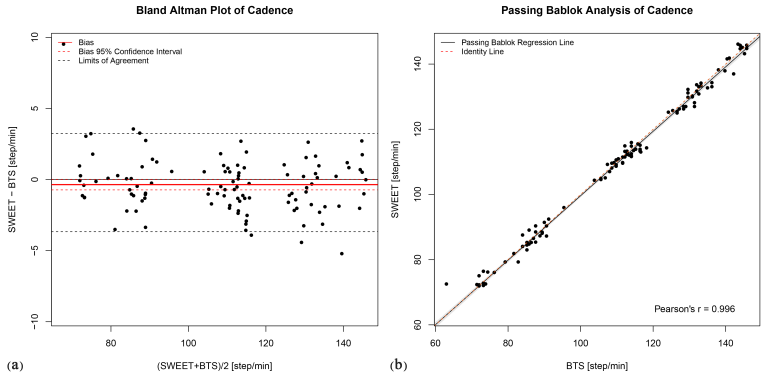

Figure 3.7. Cadence: (**a**) Bland–Altman plot; (**b**) Passing–Bablok regression analysis.

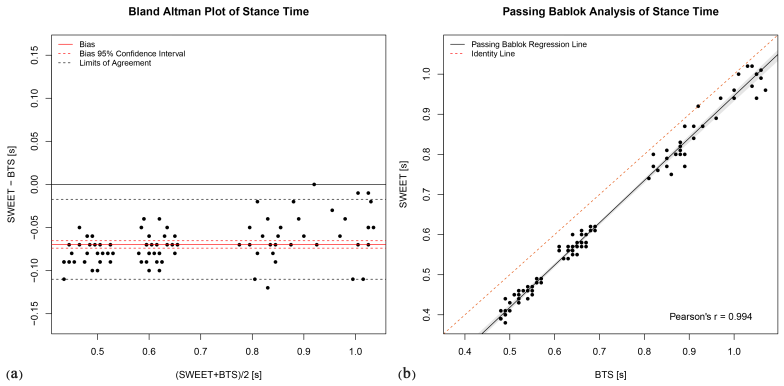

Figure 3.8. Stance Time: (**a**) Bland–Altman plot; (**b**) Passing–Bablok regression analysis.

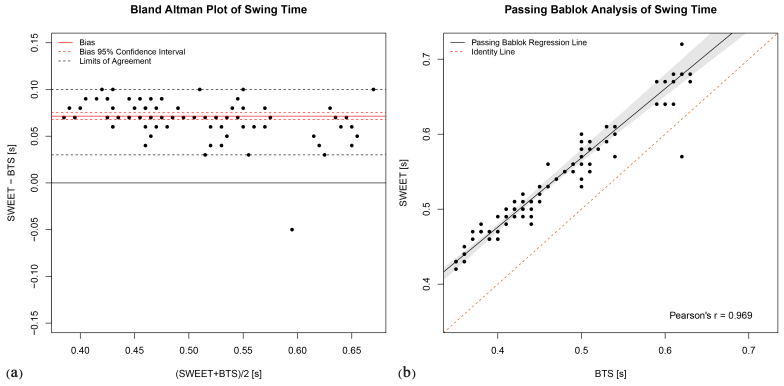

Figure 3.9. Swing Time: (**a**) Bland–Altman plot; (**b**) Passing–Bablok regression analysis.

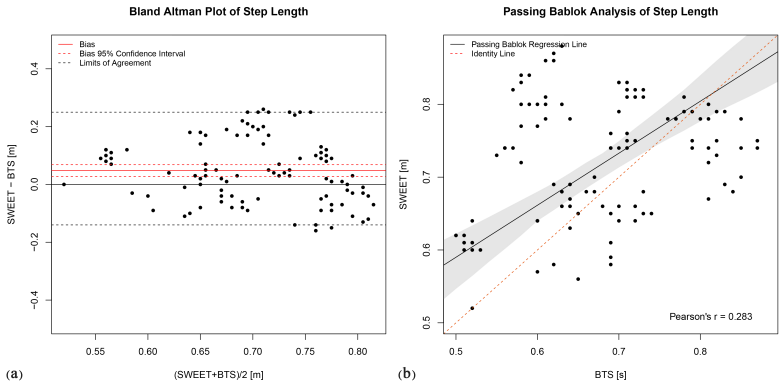

Figure 3.10. Step length: (**a**) Bland–Altman plot; (**b**) Passing–Bablok regression analysis.

3.2.5 Discussion

In the assessment of the mean GCT, significant agreement has been pointed out by the statistical analysis. The paired t-test leads to a non-significant p-value ($p > 0.05$), suggesting to accept the hypothesis of no difference between systems. The bias value in the BA analysis is null (0.00 from Table 3.4) and the LoA are very low (in the order of few hundredths of a second). The evidenced error value is consistent with the literature. The bias is lower than the mean differences found in the evaluation of the GCT between IMU and gold standard methods in other works [17, 55, 83]. The Pearson's correlation coefficient is very high (0.992), supporting the concept of a linear dependence between the measures, explored by means of PB analysis. The regression line obtained with this method coincides with the identity line (slope = 1.00, intercept = 0.00), confirming the significant agreement between the two methods in assessing GCT.

Concerning the measure of cadence, a deeper discussion is required. The T-test result suggests to refuse the hypothesis of absence of difference between the methods, but with low significance ($0.05 < p$-value < 0.01). The bias pointed out by BA analysis is very low (-0.35, about 0.3% of the average value of cadence), with its 95% CI containing the zero value and limited to few units of steps per minute (-0.74 to 0.03). The bias value obtained is consistent with the results proposed by Bugané *et al.* [17] and Hartmann *et al.* [66], although their methods were based on the use of just one IMU.PB regression is legitimated by a high value of Pearson's r (0.996): its slope is very close to 1 (0.99 with CI of 0.97–1.00), the intercept is different from 0 (0.74) but its CI contains this value (-0.95 to 2.38). Starting from these results and analysing the BA Plot in Figure 3.7a,

it can be observed that the SWEET system slightly underestimates the value of cadence compared to BTS system. Further exploring data, the cause of the non-perfect agreement was identified in the different range of steps analysed by the two systems. The reference system SMART-DX 700 by BTS performs gait analysis on a limited range of steps, contained in the central 3 or 4 strides of the walking trial, as they are completely included in the field of view of the cameras. The detected volume cannot be extended because it is limited by the configuration of the system which considers the limited volume of the laboratory. Instead, SWEET Sock system elaborates the entire signal coming from the IMUs, removing only the first and the last steps performed to start and stop walking. The analysis of the punctual values of cadence assessed in each single step of the walking trial by SWEET Sock system clarify that in the first and last part of walking a lower step cadence is adopted. Figure 3.11 shows, for each step of the walking trial, the average of the differences between the punctual cadence assessed by SWEET and the mean step cadence suggested by BTS system. It can be observed that in the first and last part of walking the difference is higher in absolute value, while in the middle steps it is reduced. It can therefore be said that a better agreement would probably have been obtained if the two systems had analysed the same range of steps. This was not performed for two reasons: firstly, because in SMART-DX 700 the steps to be considered in the analysis have to be chosen manually, whereas the signal processing of SWEET Sock is fully automatic, and secondly, because it was chosen not to modify the analysis methods of the SWEET system, which can provide more accurate results by taking the entire walking process into account.
For the same purpose, it would have been interesting to consider the raw data from the stereophotogrammetric system to obtain the point cadence by analysing the tracks of the heel markers alone. However, it was not possible to access the raw data for these experimental sessions, but future studies will take this into consideration.

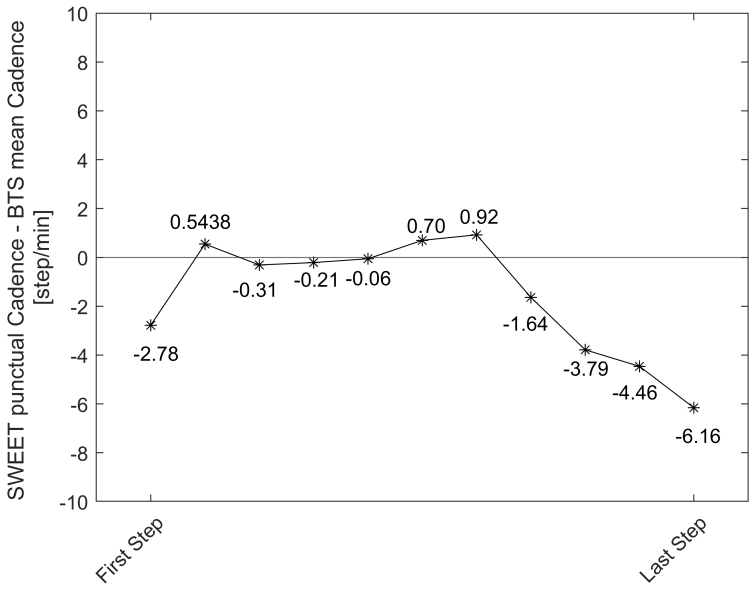

Figure 3.11. Mean difference between the punctual cadence assessed by SWEET and the mean step cadence suggested by BTS system for each step of the walking trial.

Stance and swing phase durations are complementary parameters, because they are the two parts composing the GCT. GCT is defined as the time between two successive initial contacts of the same foot. Stance phase duration is the time between the initial contact and the successive terminal contact of the same foot, while swing time goes from the terminal contact to the subsequent initial contact. The complementarity of these parameters is perfectly reflected in the results of the statistical analyses. The t-test identified a significant statistical difference between the systems(p-values < 0.0001), even if a linear correlation exists in both stance and swing phase durations, as shown by Pearson's r values, respectively 0.994 and 0.969. The BA plots clearly show that SWEET system underestimates Stance time compared to BTS system (bias $= -0.07$), and therefore overestimates of the same quantity the Swing time (bias $= 0.07$). Also in this case, the results are in line with the literature where several authors, using a different number of IMUs, different experimental settings and different reference systems, have shown a significant error in the evaluation of the stance and swing phases duration [55, 39, 83]. The BA plots also highlight heteroscedasticity in Stance measures with larger variance at higher values (i.e. lower walking speed). This behaviour

support the hypothesis that faster movement is more consistent [107, 114]. When heteroscedasticity is assessed, a $log-transformation$ of the data could be useful to eliminate a proportional bias. However, in this case the systematic error is predominant, reducing the need to correct heteroscedasticity. PB results confirm the presence of a systematic error in the measures: intercepts' CIs are symmetric for the two variables and do not contain zero value (stance CIs = −0.13 to −0.09, swing CIs = 0.10 to 0.13). It also points out a proportional error proven by the fact that the slopes of the two regression lines are different from 1 (the CIs are respectively from 1.03 to 1.08 and, symmetrically, from 0.87 to 0.94). Therefore, the difference between the methods of measures is made of a constant part and a proportional part which grows when the value of the parameter is increased. The error is to be probably addressed to the wrong detection of the initial and terminal contact of the foot with the ground, made by SWEET system through the analysis of the filtered gyroscope signal in accordance to the rules illustrated by Doheny *et al.* in [41]. Although the GCT shows very good agreement, it does not mean that the initial contacts are well identified in the signal, because they could be all translated in time of the same quantity, still resulting in good output values. To understand the error a further analysis is required on the mutual position of initial and terminal contacts identified on gyroscope signals. One aspect to be taken into account is that reported by Catalfamo *et al.*, who pointed out that the detection of gait events is affected by the choice of the filter cut-off frequency [21].

The last parameter is the step length, which has been selected to investigate the performances of SWEET system in the assessment of spatial measures. Results of the statistical analysis are not very encouraging. T-test points out a significant statistical difference between the measures of the systems ($p < 0.0001$), that is confirmed by BA analysis. Actually, even if the CI of bias includes the zero, it is quite wide (−0.13 to 0.25 m) for the precision required in this spatial metric. Moreover, the reduced value of Pearson's coefficient shows that no linear correlation exists between the measures ($r = 0.283$), so it does not make sense to perform the PB regression analysis. Actually PB regression line in Figure 3.10b does not fit accurately the points, which are distributed with no detectable trend. These results allow to affirm that there is not agreement between the systems in the assessment of the step length. Tunca *et al.* [162] demonstrated good agreement with a reference system in the evaluation of the spatial metric stride length, using a system based on two IMUs placed on the feet. Similarly, the meta-analysis conducted by Petraglia *et al.* [127] indicated no statistically significant difference between IMUs-based systems and gold standard measurements for step length, although higher variance was found in this parameter with respect to the other temporal metrics.
The cause of the error could be probably found in the processing of the gyroscope

signal that lead to the assessment of the spatial parameters. The error in the detection of gait events, demonstrated by the results on the temporal parameters of stance and swing, consequently leads to an error in the evaluation of the spatial parameter obtained from a direct integration of the angular velocity signal recorded during a step. Direct integration methods also require the implementation of countermeasures for drift compensation [23], not applied at this stage of development. Moreover, the algorithm adopted, proposed in [41], is based on modeling the movement of the shank as a single pendulum, thus deriving the spatial parameters from the calculation of the angle covered by the foot during the swing phase and using geometrical consideration. A further analysis is required to understand if this model is too simplistic to represent leg swing during gait or if other aspects (device positioning, signal filtering, etc.) cause errors in the measure of spatial parameters in SWEET Sock system. The first purpose is to try maintaining a gyroscope-based algorithm for gait assessment, by considering other more specific models proposed in literature regarding the movement of the shank during the swing phase. An example is the double segment gait model involving both shank and thigh proposed by Aminian *et al.* in [158]. Doing so the use of other sensor data, such as linear accelerations, can be avoided, while retaining the advantages of the gyroscope explored in the description of the electronic unit, and avoiding reconfiguration of the entire system.

A deep work based on the exploration of the scientific literature was performed to find out and analyse other results from gait analysis systems based on similar measuring principles. Some works exist regarding validation analysis of wearable systems for gait analysis based on processing of kinematic signals. These studies address comparative analyses with clinical instruments, such as instrumented treadmill [170], force platform [125] or pressure sensitive walkway (GAITRite®) [111, 37, 112, 159, 39, 55, 160, 78, 66, 19, 100, 145, 71]. To the best of our knowledge, few works present similar experimental setting. In three scientific researches the stereophotogrammetric system was used as reference system: Köse *et al.* [88] used BTS SmartD (10 cameras), Kluge *et al.* [83] used Simi Reality Motion System (8 cameras) and Esser *et al.* [49] used Qualisys OMCS. Among these, only the method proposed by Kluge *et al.* [83] requires two IMUs on the lower limbs, although the positions is slightly different with respect to the presented smart device. Results from the analysed works show a common trend: temporal parameters present a better agreement than spatial metrics. Among temporal parameters, step time and GCT show the best agreement, while stance and swing phases measurements are moderately correlated with reference measures. Results presented in this article are in accordance with this trend, confirming the poor performances of IMU-based systems in assessing gait spatial metrics. Only in [112] spatial metrics show a good agreement level, that could be caused by the different placement of IMUs, placed on both feet

rather than on shanks. Results from the works in [112, 170] demonstrated that foot placement allow a better measurement of spatial gait parameters. This positioning was not chosen in this research work because it may worsen the comfort and wearability of the system for users and preclude its in-shoes use.

Comfort Assessment

In addition to the validation of technical performance, the wearability and comfort assessment was carried out in order to evaluate the acceptance of the system by final users and to identify possible areas of improvement in terms of design. To carry out this conformity assessment, an already validated methodology was used, specifically the Comfort Rating Scales (CRSs).
The wearability evaluation of a device is a multidimensional analysis: wearable devices affect the wearer in different ways. Among the effects to be taken into consideration, there are those related to comfort. When wearing something, the level of comfort can be affected by several aspects, such as device size and weight, how it affects movement, and pain.
The design of the sock has been implemented in order to achieve the greatest comfort for the user. The integrated pressure sensors are made of textile material, therefore are flexible and imperceptible on the skin. The electronic unit has also been designed to be as comfortable as possible for the user: it is lightweight and it can be connected to the textile sock without the need to use bands. In fact, the use of the latter could cause discomfort to the user due to the presence of a narrow element tied to the limb.
In addition to physical factors, comfort may be affected by psychological responses such as embarrassment or anxiety. Consequently, Knight and Baber proposed that comfort should be measured across a number of dimensions and for such task they developed the CRSs [84].
The CRSs provide a quick and easy-to-use tool to assess the comfort of wearable devices, which attempt to gain a comprehensive assessment of the comfort status of the wearer of any item of technology by measuring comfort across the six dimensions described in Table 3.6.
In rating perceptions of comfort, the scorer simply marks on the scale his or her level of agreement, from low (0) to high (20), with the statements made in the "description" column of Table 3.6. According to Knight and Baber, this range was considered large enough to elicit a range of responses that could be used for detailed analysis [84].
The three participants involved in the study were invited to fill in the CRSs to provide a judgment on their comfort. Table 3.6 shows the scores assigned, for each field, by the subjects involved in the study.
Although the evaluation was carried out on only three people, it provides a pre-

liminary measure of the comfort of the prototype device. Knight *et al.* [85] have proposed five Wearability Levels (WLs), determined by proportioning the scales into equal parts (Table 3.7). The mean score of Emotion dimension is in the WL2 suggesting that users show little embarrassment in wearing the system. All the other dimensions were rated in the WL1 proving a high wearability and comfort of the device. However, to better identify the WL of the device and how to improve it, future analysis will aim to make a significant assessment of comfort, testing the device on a wider cohort of subjects.

Table 3.6. Comfort rating scales.

Title	Description	Subject 1	Subject 2	Subject 3	Mean
Emotion	I am worried about how I look when I wear this device. I feel tense or on edge because I am wearing the device.	7	4	7	6.0
Attachment	I can feel the device on my body. I can feel the device moving.	3	3	5	3.7
Harm	The device is causing me some harm. The device is painful to wear.	0	0	0	0.0
Perceived change	Wearing the device makes me feel physically different. I feel strange wearing the device.	5	0	0	1.7
Movement	The device affects the way I move. The device inhibits or restricts my movement.	5	2	1	2.7
Anxiety	I do not feel secure wearing the device.	0	0	0	0.0

Table 3.7. Wearability Level.

Wearability Level	CRS Score	Outcome
WL1	0–4	System is wearable
WL2	5–8	System is wearable, but changes may be necessary, further investigation is needed
WL3	9–12	System is wearable, but changes are advised, uncomfortable
WL4	13–16	System is not wearable, fatiguing, very uncomfortable
WL5	17–20	System is not wearable, extremely stressful, and potentially harmful

Chapter 4

Development of a Smart Ankle – Foot Orthosis

4.1 Background

A further device in e-textile technology developed during the research activity is a sensorised Ankle-Foot Orthosis (AFO). The AFO is an orthopaedic aid used for the management of patients suffering from drop foot. The drop foot syndrome is a common problem with varied aetiology, generally caused by total or partial paralysis of the muscles innervated by the peroneal nerve, the tibialis anterior muscle and the peroneal group. The disorder is characterised by the lack of voluntary control of ankle dorsiflexion and subtalar eversion. As a result, the deambulation of patients is characterised by steppage gait, i.e., during the ground contact phase, the toes initiate contact, followed by the lateral crest of the foot and, finally, the heel. 'Foot-slap' and toe-dragging are the main complications of patients with weakness of the dorsiflexor muscles. 'Foot-slap' is the uncontrolled and rapid striking of the foot on the ground that produces the characteristic heel sound; 'toe-drag' is the dragging of the forefoot during walking due to inadequate elevation from the ground during the swing phase of the gait cycle. Thus, the gait is asymmetrical, inharmonious and unstable, with high risk of falling and stumbling.

Treatments for foot drop vary depending on the specific causes. Treatments such as braces and orthoses [8, 29], functional electrical stimulation [103, 126, 86] and surgery [175] have been shown to be effective for foot drop. In order to monitor patients suffering from this syndrome, quantitative feedback acquired during the use of an AFO could be useful and interesting. For this reason, a sensorised orthosis has been developed that can detect angular velocity signals of

the ankle joint, surface electromyographic activity of the agonist and antagonist muscles of the calf, and plantar pressure signals. These signals can be very interesting in the monitoring of the performances of patient, as they can be used to perform a complete postural and gait analysis, enriched with information about the muscular activation patterns.

The wearable sensor unit allows the bio-signals acquisition when connected to the analogue front-end located in the electronic unit. This unit also contains a microcontroller and allows data transmission through an integrated BLE module. The following sections present the design and development of this novel device.

4.2 Wearable Device

The wearable device is made up of three elements: an orthopaedic insole, an L-shaped AFO and the e-textile sensing unit. The first two elements are produced by means of 3D printing technology, and are used as supporting elements on which the textile sensors are embedded. In the following sections the single elements constituting the device are described.

4.2.1 Orthopaedic Insole

A typical workflow for the design and 3D printing of insoles was used to realise the foot orthosis. In particular, the process started with the use of Sensor Medica Freemed baropodometric platform (Sensor Medica srl, Guidonia Montecelio, Roma), an instrument that allows static and dynamic plantar pressure mapping. For the intended purpose, both static and dynamic acquisitions were carried out. In the static trial the subject stands in orthostatic position on the platform, while in dynamic trials the subject performs several steps over the platform.

The pressure maps obtained from static and dynamic trials were then imported into the easyCAD Insole^{TM} (Sensor Medica srl, Guidonia Montecelio, Roma), a 3D CAD modelling software, which allows the creation of the model of the orthopaedic insole. The software prompts the user to select a template based on the patient's foot size, and a plantar orthosis is automatically generated to harmonically redistribute pressures over the foot plantar arch.

At the end of the design, an STL model describing the upper surface of the foot orthosis was exported from easyCAD, and a smoothing operation was performed using the MeshMixer software (Autodesk Inc.)
The 3D model of the orthosis was then imported into Simplify3D slicing software to prepare the GCode file to be fed into the 3D printer, based on Fused Deposition Modelling technology. At the end of the printing process, the plantar

orthosis shown in Figure 4.1 was finally obtained, to be used as support for the development of the sensorised devices.

Figure 4.1. Orthopedic Insole Prototype.

4.2.2 Ankle-Foot Orthosis

The AFO used as support was produced through the Selective Laser Sintering (SLS) 3D printing. The supporting element has an L-shape with a rigid sole and a posterior leaf covering the calf.

The first step in the creation of the AFO orthosis was the import of the STL file from the 3D scan of the limb of the patient into the Cube software. The 3D model was then post-processed to remove portions not of interest. Within the main working interface, smoothing operations were performed on the mesh and the ankle joint was modified to reach the standard position (90 degrees). Then, the surface of the orthosis, described as a mesh, was created. On the new surface, the cut lines of the areas to be opened on the orthosis were created. In addition, the surface was also subjected to the 'Thickening' tool to give the brace the desired thickness.

To enable the brace to be printed correctly, it was necessary to divide the 3D model into two sub-parts, since the 3D printing volume was too small to contain the entire AFO. The two sub-parts were then exported as two separate STL files. Both files were imported into the Sinterit Studio software (Sinterit sp. z o.o., Kraków, Poland) to generate the Sinterit Lisa Pro SLS printer control gcode. After importing the two STL files, they were positioned within the printing volume, and the print process was pre-screened and, finally, launched. Once the

printing process was complete and the material reached a core temperature of less than 60 degrees Celsius, the compacted block of material is removed from the 3D printer and placed on the workstation for the mechanical removal of the non-sintered material.

The two parts generated by the printer are joined to obtain the final orthosis shown in Figure 4.2.

Figure 4.2. Ankle-Foot Orthosis Prototype.

4.2.3 Wearable Sensing Units

The first wearable sensing unit consists of a felt insole in which three pressure sensors, in e-textile technology, have been integrated as sensing elements at three strategic points of the arch of the foot. The number and positioning of the sensors is based on the similar considerations made for the smart socks. Three pressure sensors per foot were therefore used: one under the heel, one under the first metatarsal bone and one under the fifth metatarsal bone. The decision to integrate the sensors on an insole came from the idea of creating a modular structure in which the insole can be removed from the orthosis and, if necessary, be washed.

The sensors were manufactured using EeonTex fabric sheets. The difference with respect to the above described smart socks is that, in this case, it was decided to abandon the rectangular configuration of the sensor in favour of a circular shape with a diameter of 1 cm. This choice allows for a limited and specific detection area at the identified anatomical points of the plantar arch. The three pressure sensors were covered with felt patches to prevent degradation of the sensor in contact with the skin. The sensors were connected to the output

connectors using conductive tape, with a thickness of 5 mm and a resistance of less than 0.1Ω per cm. The connectors were realised using metal clips, sewn directly to the four free edges of the conductive tape and positioned at the top of the insole, which extends to the back of the heel. Specifically, before being applied to the insole, the clips were sewn with conductive thread onto a conductive textile backing plated with real silver that gives it highly conductive properties. The length of the connections was minimised by studying the shortest path to reduce noise and interference. Figure 4.3 shows the complete device with its sartorial details. The textile sensing felt insole was fixed on the supporting orthopaedic insole, which in turn was placed on the sole of the AFO.

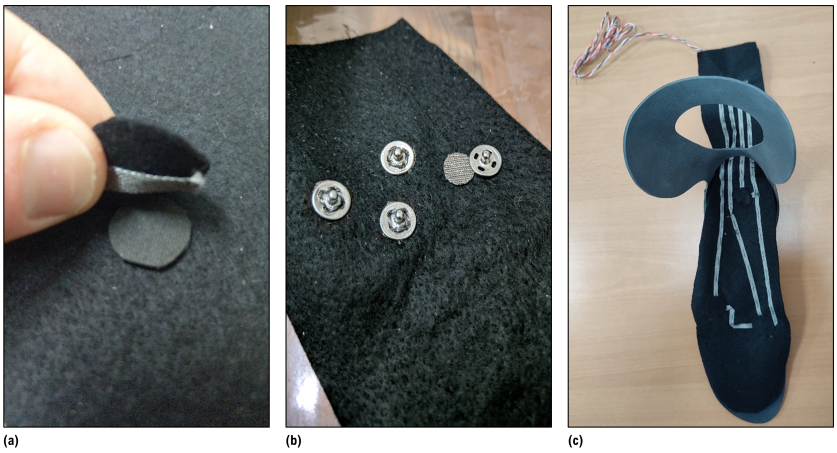

Figure 4.3. AFO wearable sensing unit: (a) circular Eeontex fabric sensor, in direct contact with the conductive tape and covered with a non-conductive fabric patch; (b) four conductive metal clips, sewn onto conductive textile backing, allowing the textile part to be connected to the electronics unit; (c) textile sensorized insole integrated in printed AFO.

Another textile unit was developed for the acquisition of sEMG signals. To this end, four circular textile electrodes, with a diameter of 1cm, were integrated inside an elastic textile band. The band is worn on the calf, just below the knee, to acquire signals from two muscles of interest: tibialis anterior and gastrocnemius lateralis. Since the leg is not a perfect cylinder, the band is designed and manufactured in a trapezoidal shape, so that the upper part is wider than the lower part. It is equipped with internal channels to arrange the connections, in order to avoid their contact with the skin. Figure 4.4 shows the complete device with its custom-made design.

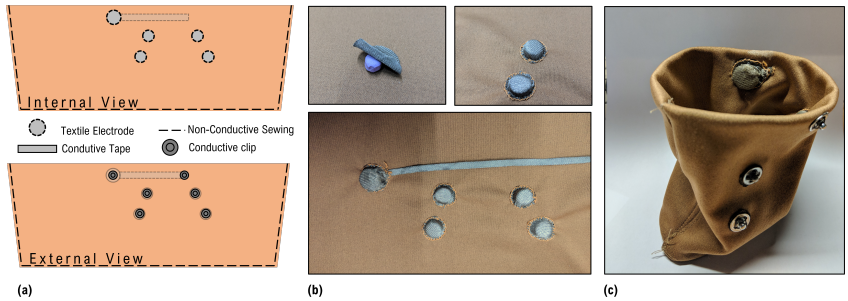

Figure 4.4. sEMG textile elastic band: (a) schematic diagram of the band seen internally (upper part) and externally (lower part); (b) textile electrodes placed on a rubber shim to promote adhesion to the skin; (c) final version of the band with integrated sensors.

The textile electrodes were placed on the elastic band according to SENIAM recommendations (SENIAM), 3 cm apart so that they could be directly connected to the MyoWare acquisition board. A single reference electrode, with a larger diameter (1.5cm), was placed on the tibial tuberosity. The electrodes were made of conductive fabric (www.adafruit.com - product ID: 1167) fixed on a soft thick backing to force electrode-to-cute contact. Six metal clips for the connection of two acquisition boards were fixed on the outside part of the band with conductive thread.

The two separate textile units are both opportunely connected to the central electronic unit, which allows for the acquisition and transmission of the biomedical signals.

4.3 Electronic Unit

The electronic unit contains all electrical and electronic elements to enable the acquisition and wireless transmission of signals. The central core contains the microcontroller and the IMU, moreover two electronic boards for the acquisition of the sEMG signals were used, directly connected to the textile sensing band.

In particular, the sEMG signals are gathered by MyoWare™ Muscle Sensor boards (AT-04-001), by SparkFun Electronics® (6333 Dry Creek Parkway, Niwot, Colorado). This module offers a very high input impedance value ($110G\Omega$) to overcome the problem of high skin-electrode contact impedance. The MyoWare board acts by measuring the electrical activity of a muscle. The output signal ranges $0 - VsVolts$, where Vs indicates the voltage of the power supply. It

presents two female clips in order to connect to electrodes. In the development of the wearable device these connectors are used to directly connect the MyoWare boards to the elastic textile band, thus avoiding the use of further connections. The boards contain a conditioning circuit for sEMG, so that the output is the amplified, rectified and integrated signal (sEMG envelope) that can be directly connected to the microcontroller Analogue-to-Digital Converter (ADC) input.

The IMU FLORA 9-DOF (Adafruit Inc.: New York City, New York, USA) has been integrated into the electronic core to acquire gyroscopic signals. It consists of a small electronic board mounting LSM9DS1 module, a system-in-package featuring a 3D digital linear accelerometer, a 3D digital gyroscope, and a 3D digital magnetometer.

The STM32WB55 Nucleo board (STMicroelectronics, Geneva, Switzerland) was used as the control unit for the system, and is placed in the electronic core. It provides for digitisation of the analog sEMG and pressure signals and is connected to the inertial unit FLORA via the I2C serial bus. The Nucleus board also allows data to be sent via the BLE 5.0 protocol.

The functionality of the control unit was implemented using the STM32-WB55RGV6[1] microcontroller programmed using the STM32CubeIDE 1.7.0 integrated development environment. The control unit is programmed to digitise the analog sEMG and pressure signals and to receive digital data from the IMU. Data are collected in 20-bytes packets and sent in real time via BLE to the smartphone using a dedicated smartphone application. Each packet contains the following bytes: 2 bytes for the packet sequence number, 2 bytes for the time stamp, 2 bytes for each pressure signal (6bytes), 2 bytes for each sEMG signal (4bytes) and 2 bytes for each angular velocity signal axis (6bytes).

The MyoWare boards are connected to the textile band and to the central electronic core, which is plugged on the other textile unit. Figure 4.5 shows the electronic schematic between the textile unit and the electronic unit.

4.4 Discussion

The realized device is capable of acquiring all the signals for which it was designed. The system is clearly a prototypical solution that needs to be engineered in order to be actually used. In any case, the aim has been primarily to start a study process to design a device that can effectively meet the needs of many pathological subjects, given the widespread prevalence of the drop foot deficit. Secondly, the aim was to demonstrate the feasibility of wearable solutions based on e-textile technology in different areas of medicine for different applications.

[1] https://www.st.com/en/microcontrollers-microprocessors/stm32wb55rg.html

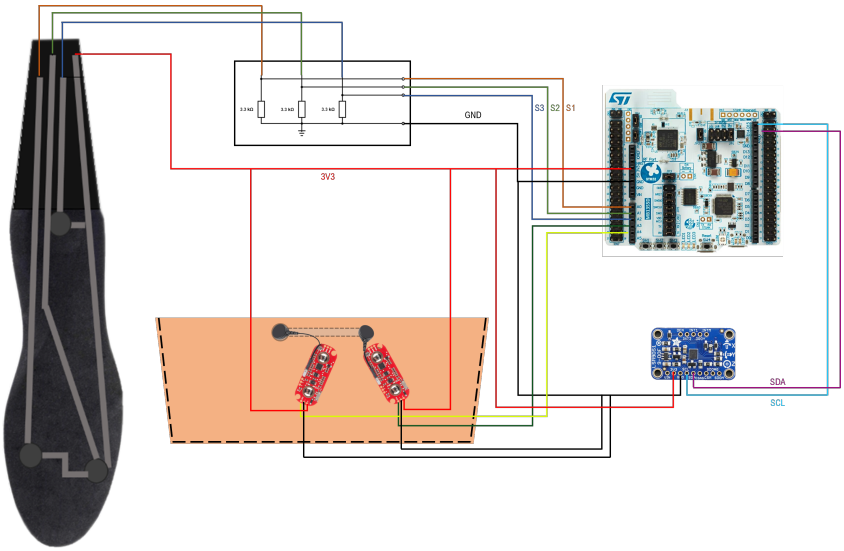

Figure 4.5. Electronic schematic of the system.

In this sense, it can be affirmed that the produced devices successfully cover different needs presented by the healthcare market and, with an appropriate engineering phase, can aim to be relevant solutions for remote patient management and monitoring.

Chapter 5

Performance Validation of a Commercial Garment for Remote Patients Monitoring

This chapter presents Sensoria Smart socks, a novel e-textile based portable system for gait analysis, and analyse its performance in detecting the major temporal gait metrics. The results provided by the system are validated in comparison with those of the IMU–based gait analysis system OPAL Mobility Lab by APDM (APDM Inc., Portland, OR, USA).

Sensoria is an American leading company in the sector of smart and electronic garments. The current aim of the Company is to move to the healthcare sector, exploiting their expertise to develop smart garments for health applications. The study presented in this Chapter was conducted on request of the Company, with the aim of supporting the developers team in validating the methods and algorithms associated with the system, before its marketing, in order to provide the user robust gait analysis results.

This experimentation is perfectly in line with the focus of this thesis work because it allowed the use of a wearable, industrially manufactured, compact and miniaturised e-textile device, fully integrated in a remote telemonitoring chain. The focus on the market of textile devices for health, which is currently in an embryonic phase but with ample growth prospects, is crucial in order follow, and hopefully anticipate, technological progresses, while maintaining a specialised profile in the sector.

5.1 Sensoria Smart Socks

Sensoria Smart Socks are wearable sensing devices, produced by Sensoria Health Inc. (Redmond, WA, USA) (https://www.sensoriahealth.com/), that enable the calculation of spatio-temporal gait analysis metrics exploiting the two typologies of embedded sensors: IMU worn at ankle height and textile pressure sensors placed under the foot plantar arch. The wearable device is integrated into a complete system for remote health monitoring, including also a dedicated mobile application and a web service for data storage, as illustrated in the schematic diagram in Figure 5.1.

Figure 5.1. Sensoria system architecture: 1. Smart socks; 2. mobile application; 3. web service.

The wearable textile unit allows for signals acquisition when connected to the electronic unit. The electronic core can transfer data to any mobile device and to a cloud-based Health Insurance Portability and Account-ability Act (HIPAA)–compliant storage system. This is a reserved area, accessible after authentication. The user can download raw and filtered signals and the parameters obtained from the digital processing. In the following sections, the functional modules of the system are presented.

5.1.1 Wearable Device

Sensoria socks are equipped with 3 textile sensors positioned at 3 specific points of the plantar arch: first and fifth metatarsal bones and calcaneus (heel) (Figure 5.2c). These sensors are connected to a docking socket, on the lateral part of the sock, by means of conductive traces that follow a zig-zag pattern to increase elasticity.

At the lateral superior end of the sock, there is the socket where the Sensoria electronic Core is connected, which integrates an IMU and a microcontroller for transmitting the acquired data via Bluetooth (Figure 5.2b).

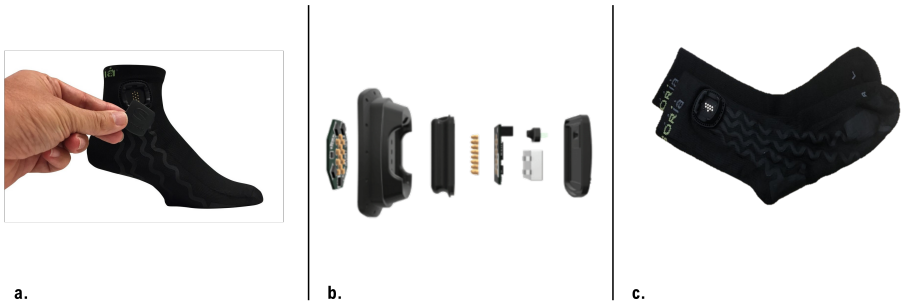

Figure 5.2. Sensoria Smart socks: a. Complete Device; b. Electronic Sensoria Core; c. Wearable E-textile Units.

5.1.2 Mobile Application

Sensoria Workbench is an application for mobile devices requiring the Android 8.0 operating system. The application is a tool for connecting and acquiring raw data from Sensoria devices (powered by Sensoria Core). Login credentials are required when starting the application. Once logged in, a page is displayed with the Sensoria Gears available for the account. A Sensoria Gear is a particular Sensoria device (e.g. Sensoria Socks, Sensoria Mat, etc.) provided by Sensoria that can be used to collect and stream data to Sensoria Workbench App. To proceed you must select the device you want to use (Figure 5.4a). Once you have selected the desired gear, you must connect the cores (Figure 5.4b). For all Gears except "Lab", the number of Cores to be connected is fixed and the application will proceed automatically. To connect a Core, simply click on it in the list of available devices found nearby or bring your smartphone close to it.

On the 'Footwear Pair' screen, you can read some useful information about the Core: raw and/or processed data on acceleration, angular velocity and orientation (Figure 5.4d). The bar at the top also specifies the position of the Core (right/left in the specific case of sensorised socks).

You can access the settings for the specific Core by clicking on the gear icon and in this section you can edit all the sampling parameters. The first page contains the general app settings and applies to all Cores (Figure 5.4e). The data logging settings allow you to change the type of data that is logged and sent to the Cloud. It is also possible to send events that occur during data recording (e.g. a step taken) to the Cloud. The second page contains the settings specific to the Core currently in use (Figure 5.4f). It is possible to make the desired changes but also to restore the default settings. Restoring the Core settings will only restore the settings for that specific Core and not for other Cores or general

settings.

On the main 'Footwear Pair' page, a 'Record' button allows for starting the acquisition. The same button stops the recording when required (Figure 5.4g). Once the test session has been recorded, you can upload it to the dedicated Cloud portal and then download it (Figure 5.4h). The portal can be accessed with the credentials used to access the mobile application (Figure 5.3a). Once logged in, click on the "Sessions" section on the main page and click on the ".csv" file generated for the specific session (Figure 5.3c). Six files are generated for each acquisition session: two files, one for each core, containing raw data from IMU and pressure sensors; two files, one for each core, containing the filtered data; one file with aggregated results about COP and one file containing the results of gait analysis. The latter is the one considered in this analysis, as it contains the gait parameters calculated after the experimental walking trials. Figure 5.4 shows the main structures of the application.

5.2 Methods

5.2.1 Mobility Lab System

The performances of Sensoria Smart Socks in evaluating gait analysis temporal metrics were validated through a benchmarking analysis with the IMU–based system for clinical gait analysis Mobility Lab. The Mobility Lab system by APDM consists of: a set of wireless, body-worn IMUs, called Opal™ sensors, measuring 43.7 x 39.7 x 13.7 mm (LxWxH), each with a docking station; an Access Point for wireless data transmission (with a sampling rate of 128Hz) and synchronisation of the independent sensors; Mobility Lab software to manage the acquisitions and processing of the recorded data. IMU-based systems are nowadays widely used for body movement measurements as they offer accuracy along with ease of use [43, 51, 32, 10]. Their use is both clinically and scientifically relevant, in various fields such as orthopaedics [61] or ergonomics [42, 43], but it is also widely used to assess the pathological impact of neurological diseases [48, 27]. The accuracy of IMUs in measuring spatio-temporal gait parameters has been demonstrated by comparing the performance of these systems with gold standard 3D motion capture [9, 136, 162]. The system used in this study was also validated with other types of systems, such as a pressure sensor walkway, demonstrating good accuracy in both temporal and spatial gait metrics [145, 112].

The WALK test protocol was used in this study, one of the plugins offered by APDM Mobility Lab, which required the use of three IMUs: one on the low back (just below L5 level) and two on the dorsal surface of the feet.

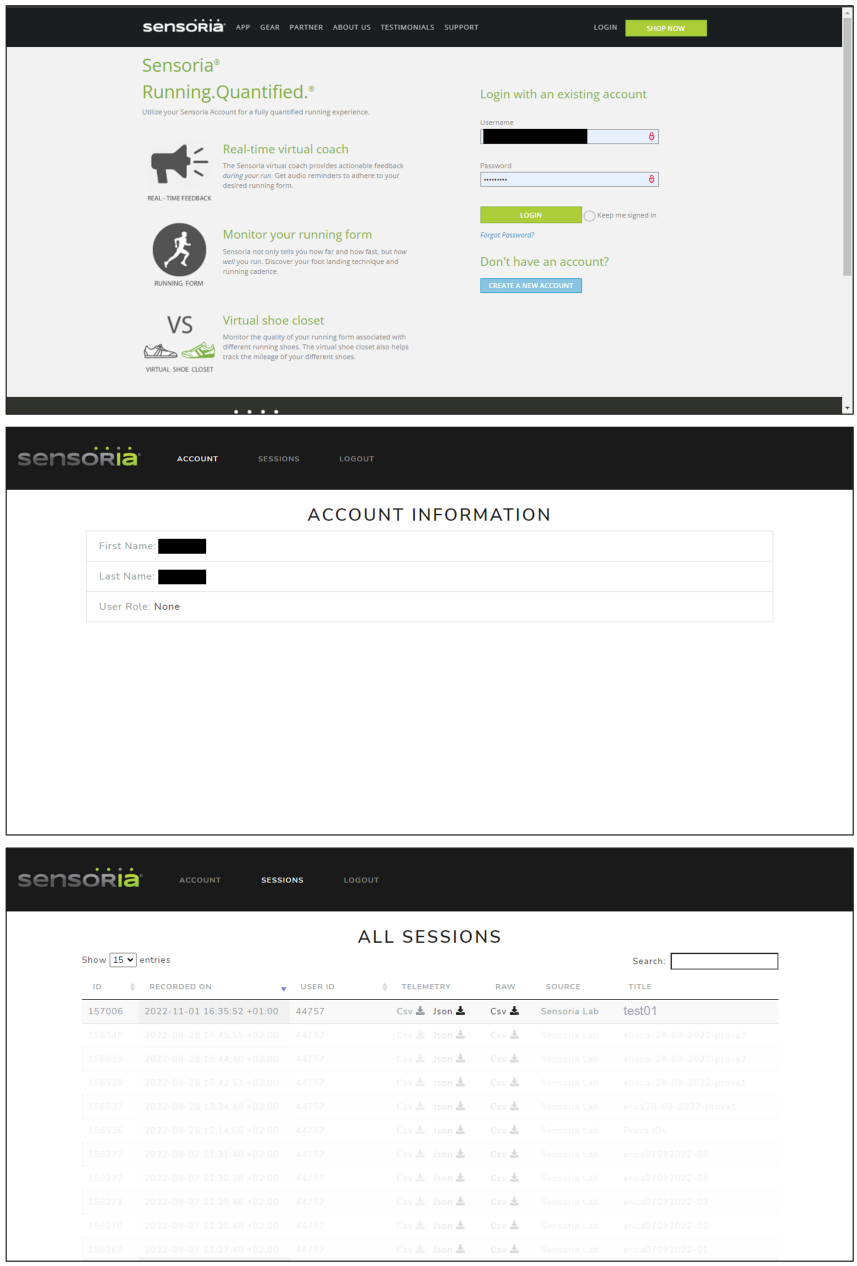

Figure 5.3. Sensoria Portal main frames: (a) login page; (b) account information page; (c) sessions page.

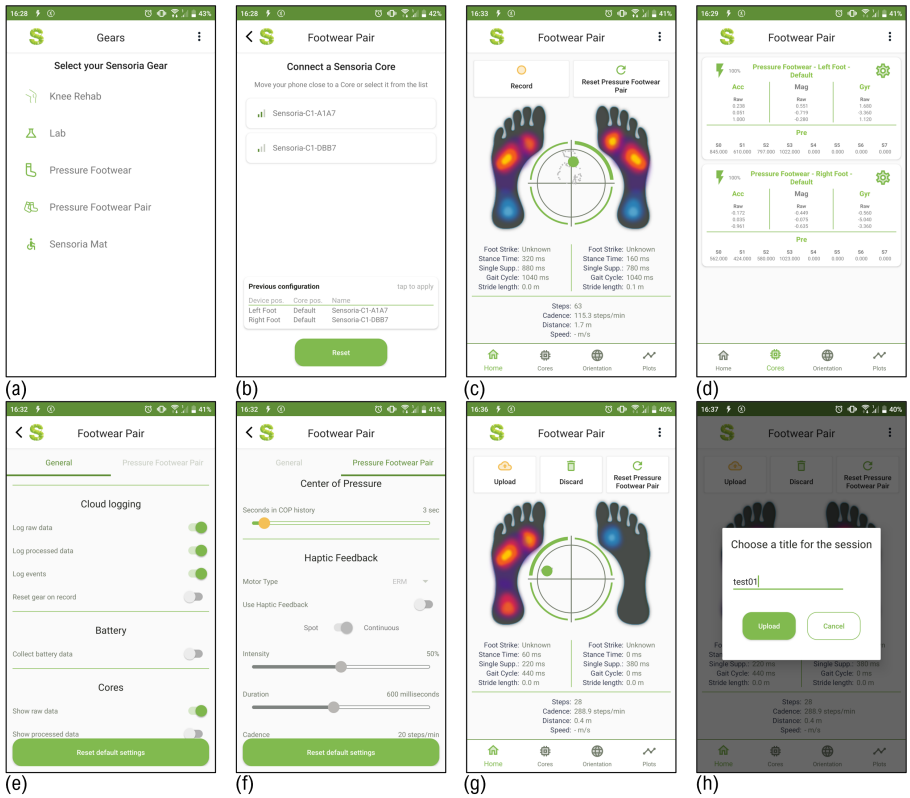

Figure 5.4. Sensoria App main frames: (a) device selection; (b) cores connection; (c) opening screen; (d) raw data screen; (e) general app settings; (f) core specific settings; (g) stop recording; (h) file uploading.

5.2.2 Experimental Procedure

Twelve healthy subjects (9 females, 3 males) were enrolled in this study. Each subject wore the sensing Sensoria Smart socks and three OPAL Inertial Measurement Units (two on the feet and one in lumbar position), in order to perform simultaneous recording of the walking. Figure 5.5 shows a subject wearing the Opals and Sensoria socks simultaneously while performing the walking trial. The trial consisted of walking 10 metres, turn around a pivot and walk back to the starting point at preferred speed. Five walking trials for each subject were used for the benchmarking analysis. The focus was on the following set of temporal parameters, which have clinical relevance in the gait analysis:

- GCT (s): the duration of a full gait cycle, measured from the foot initial contact to the next initial contact of the same foot;
- Stance (%GCT): the percentage of the GCT in which the foot is on the ground;
- Cadence (steps/min): the number of steps per minute.

The study was conducted at the Sensoria Laboratory, in Naples.

The agreement between measurements computed by the two systems–Sensoria Sock and Opal system–was investigated by means of PB regression and BA analysis, with the aim to find out any proportional or constant systematic error between the two methods of measurement. An in-depth description of these statistical analyses is provided in the section 2.2.2. Statistical analyses were performed using R version 4.0.3 (R Foundation, Vienna, Austria).

Figure 5.5. Subject equipped with both systems: Sensoria Smart socks and Opals sensors.

5.3 Results

The plots shown in Figures 5.6a–5.7a–5.8–5.9a represent the BA analysis results. Table 5.1 reports the quantitative results deriving from the analysis. The bias represents the mean of the differences between the measures computed

by the systems, it is provided with the 95% CI. The red lines in the BA plots represent bias values, while the corresponding CIs is reported in red dashed lines. The LoA reported in Table 5.1 are also shown in the graphical representations as black dashed lines. The LoA are assessed as the bias ± 1.96 times standard deviation of the differences [7, 16], as they have a symmetric gaussian distribution.

The PB regression can reveal the presence of a trend between the measures of the two systems, thus indicating a proportional error in the tested method according to the slope of the fitting regression line. PB analysis is preceded by the evaluation of Pearson's correlation coefficient: if this parameter is very far from $pm1$ the correlation between measures is very weak and the PB regression does not make sense. This situation is registered for the stance phase parameter, which presents Pearson's coefficients equal to 0.0824 and 0.591 for left and right foot respectively. For this parameter the PB regression was not performed.

Figures 5.6b– 5.7b–5.9b show the scatter plot of the dataset for each parameter, with the PB regression line in black. The shaded area around the regression line represents its CI, while the red dashed line corresponds to the reference identity line. In the PB plots, Pearson's correlation coefficient (r) is also shown. The quantitative outcomes of PB analysis are reported in Table 5.2: slope and intercept of the regression line are listed for each parameter, along with the corresponding 95% CI limits.

Table 5.1. Results of Bland–Altman analysis.

	Gait Cycle Time		**Stance Phase**		**Cadence**
	Left	**Right**	**Left**	**Right**	
Bias	0.00930	0.000251	-8.60	-8.79	-0.530
Lower Bound Bias CI	-0.00140	-0.00919	-9.54	-9.51	-1.22
Upper Bound Bias CI	0.0201	0.00969	-7.67	-8.06	0.160
Lower Bound LoA	-0.0583	-0.0591	-14.5	-13.4	-4.87
Upper Bound LoA	0.0770	0.0596	-2.71	-4.22	3.81

Table 5.2. Results of Passing–Bablok regression analysis.

	GCT		Stance Phase		Cadence
	Left	**Right**	**Left**	**Right**	
Pearson's r	0.967	0.973	0.0824	0.591	0.974
Slope	1.00	0.966	-	-	0.964
Lower Bound Slope CI	0.923	0.886	-	-	0.887
Upper Bound Slope CI	1.11	1.04	-	-	1.01
Intercept	0.00217	0.0423	-	-	3.34
Lower Bound Intercept CI	-0.121	-0.0401	-	-	-1.49
Upper Bound Intercept CI	0.101	0.135	-	-	10.8

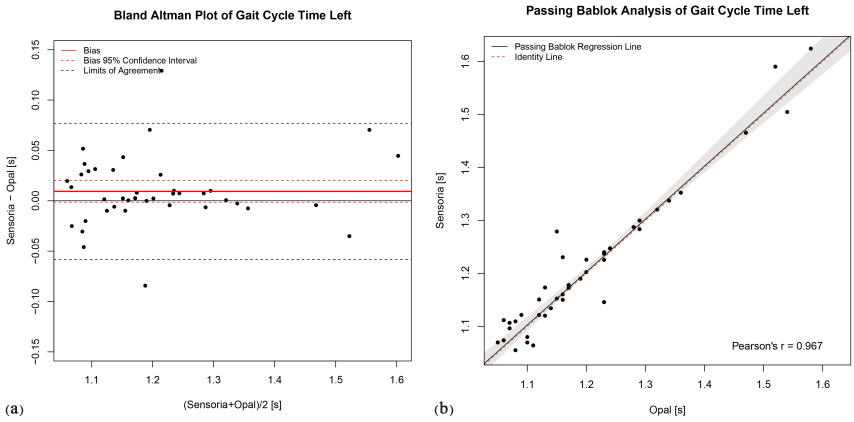

Figure 5.6. Gait Cycle Time Left: (**a**) Bland–Altman plot; (**b**) Passing–Bablok regression analysis.

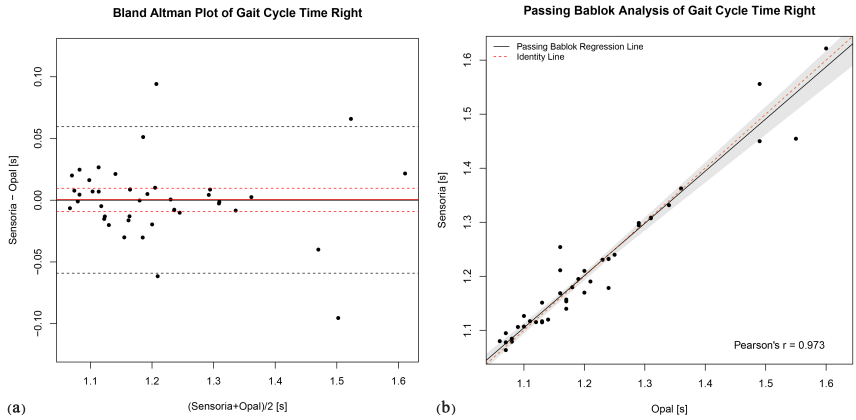

Figure 5.7. Gait Cycle Time Right: (**a**) Bland–Altman plot; (**b**) Passing–Bablok regression analysis.

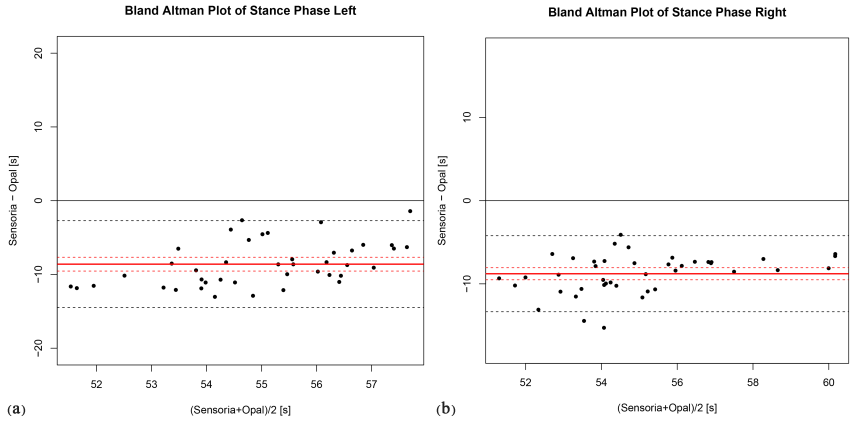

Figure 5.8. Stance Phase: (**a**) Bland–Altman plot for left limb; (**b**) Bland–Altman plot for right limb.

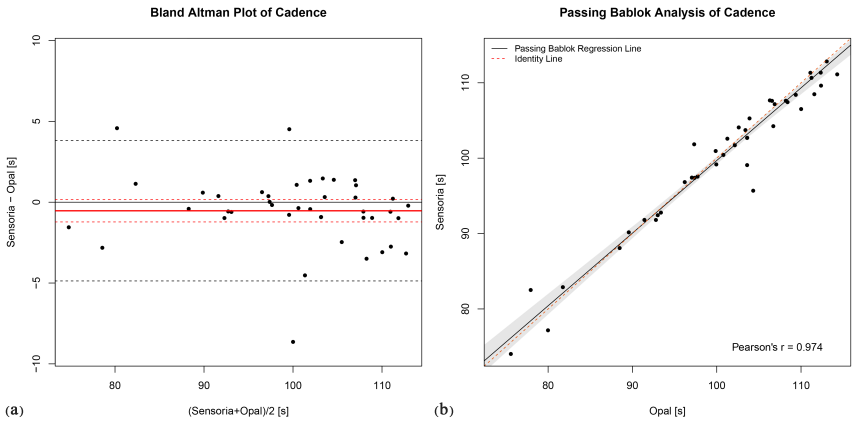

Figure 5.9. Cadence: (**a**) Bland–Altman plot; (**b**) Passing–Bablok regression analysis.

5.4 Discussion and Conclusion

In this preliminary study the performances of the wearable Sensoria Smart socks in evaluating the major temporal gait metrics were investigated. Results underline a general agreement in measuring GCT on both feet (left foot bias = 0.00935s, right foot bias = 0.000251s) and mean Cadence (bias = -0.530steps/min). The CIs of biases include the zero value for these metrics, indicating that the differences randomly occur and are not systematic. The Pearson's correlation coefficients are very high (0.967 for GCT Left, 0.973 for GCT Right and 0.974 for mean Cadence), supporting the concept of a linear dependence between the measures, explored by means of PB analysis. The PB regression lines are very close to the identity line with slope's CIs and intercept's CIs respectively containing 1 and 0 values. These preliminary results point out a relevant agreement between the two systems in assessing gait cycle time and cadence.

The BA plots for Stance Phase metric, assessed for the two limbs, show significant differences between the measures provided by the two systems: Sensoria Smart socks underestimate the foot stance phase with respect to the reference system OPAL Mobility Lab. The bias value for left limb is -8.60% and its CI does not include zero. The bias value for right limb is -8.79% and its CI does not include zero. The Pearson's correlation coefficients are very low (left foot r = 0.0824, right foot r = 0.591) underlining the absence of linear relationship between measures. Following these results, the PB analysis on the Stance Phase

parameter was not performed.

There are not many studies in the literature concerning the study of the performance of Sensoria Smart Socks devices. Yeung *et al.* [176] proposed a validation of the system against the GAITRite for motion analysis. In this study, they found higher differences in Cadence measurement than in our analysis. It is difficult to compare the results as the authors used an earlier version of the device, based on a different positioning of the cores and therefore different processing algorithms. Furthermore, they did not analyse other more specific temporal parameters, such as Gait Cycle Time or Stance and Swing phases.

The agreement in GCT values and the simultaneous disagreement of stance phase demonstrate discrepancies between the two systems in the detection of intermediate gait events (initial and terminal contact). In conclusion, Smart socks performance in the detection of GCT and cadence are satisfactory, however improvements are needed in order to assess more specific gait metrics. In future studies, the aim is to test the socks on a larger population and in the assessment of other temporal and spatial gait metrics.

Chapter 6

Conclusions

In this thesis work, the realisation and validation of different remote clinical monitoring devices using e-textile technology was presented.

The design and development of wearable systems to detect and quantify physical signals generated by the human body offers an opportunity for the diagnosis, treatment and monitoring of different pathologies. This field of research has been the subject of interest in recent decades, as shown by the increasing research and development efforts in this area. The analysis of electrophysiological signals (such as ECG, EMG, etc.) represents an important tool for health monitoring. However, the technologies used to detect such signals are based on the use of electrodes attached to the body by means of adhesive tape, mechanical clamps or straps. In order to provide innovative tools for sensing and monitoring electrophysiological activity and physiological parameters, the interest and study of wearable sensors with characteristics of light weight, high flexibility, biocompatibility and extensibility has arisen. The rapid development of new sensing materials, manufacturing processes and electrical sensing techniques has contributed to considerable progress in the realisation of wearable sensors. However, for actual applications of wearable sensors in human activity monitoring and personal health care, some challenges remain. These include, for instance, the need to design and customise sensors and electrodes to detect physiological signals at different locations on the human body, offering acceptable sensitivity and signal quality for the required clinical application.

These aspects represent challenges for the development of new devices, taking advantage of the rapid development of technology. The involvement of large companies, such as Apple or Google, has encouraged the focus of research activities in this field with the goal of developing and deploying wearable products ready for various applications. Healthcare remains one of the most interesting markets; the benefits provided by wearable technologies can potentially establish

significant cost reductions for healthcare systems. However, to date, wearable technologies that use the full potential of textile electronics are not yet available in healthcare.
Based on these considerations, the purpose of this thesis was to propose and evaluate the performance of wearable devices in e-textile technology, applied to the biomedical field, for detecting different physiological signals.

The first focus provided is about a sensing shirt for the measurement and analysis of ECG, EMG and acceleration signals, based on textile sensors. The innovative features of the system rely in the multi-parametric approach in health monitoring and in the wide set of tools offered for digital signal processing. In the development of the sensing unit, sensors, electrodes, and bus structures are all integrated in the textile garment, making it possible to perform normal daily activities while the clinical status is monitored by a specialist, without any discomfort. The system includes a custom-based app for real time visualization of the acquired signals and a software desktop for off-line plotting and digital signal processing, in order to show the feasibility of telemedicine system for remote monitoring.
The validation analysis regarding ECG measurement and digital processing have led to encouraging results, indicating that reliable measures can be obtained using the prototypical wearable device. The research study also pointed out one of the limitation of the textile electrodes: the adherence with the skin must be increased to reduce motion artifacts arousing in the signal.

The second focus provided is about sensing socks for the measurement and analysis of plantar pressure and acceleration signals of the lower limbs, based on textile sensors. The system presents the same telemedicine chain as the previous application but it provides posturographic assessment and gait analysis.
The sensing unit is a textile sock in which textile sensors and connections are integrated, allowing the use during daily activities, without any discomfort.
The validation analysis against an optoelectronic stereophotogrammetric system for gait analysis, shows that the agreement is not confirmed for all the spatio-temporal gait parameters analyzed. However, based on the findings, the novel system offers reliable measures of gait cycle time and cadence while some issues were found in the validation of the other temporal and spatial parameters.
Comfort of this device was also evaluated, using the CRS scale, as this aspect appears to be non-negligible in the design and implementation of a wearable device for use in the outdoor environment.

A further achievement concerns the embedding of textile sensors in an AFO for posturographic assessment, gait analysis, and muscle activity detection.
This application shows that the concepts previously discussed can be used to create customized systems which can be applied to different clinical settings.

Finally, in order to analyze the textile device market, the performance of

Sensoria smart socks was observed and validated. Again, the results show a less than perfect agreement with reference systems, underscoring the need for further development to obtain more reliable systems for clinical evaluations.
The proposed devices should not only be considered for use on patients but can also be used in other areas of medicine. A valid field of interest is occupational ergonomics, related to the prevention of work–related musculoskeletal disorders (WRMSDs) in workers. The use of comfortable wearable devices during working hours could help monitor postural and dynamic variables in activities most associated with exposure to biomechanical overload (i.e., frequent material handling, pushing and pulling, awkward postures, prolonged standing, and significant sideways twisting).

The advantages of wearability and portability, combined in a minimally invasive device, together with the future opportunity of integration into Internet of Things (IoT) networks open new perspectives to increase the effectiveness of prevention and safety strategies in healthcare.

Bibliography

[1] A Abed, C Cochrane, F Boussu, O Cherkaoui, and R Elmoznine. Design and development of a piezo-resistive sensor based on PEDOT: PSS applied to Sisal's natural fiber for monitoring of 3D warp Interlock fabric. *IOP Conference Series: Materials Science and Engineering*, 827(1):012019, April 2020.

[2] Gizem Acar, Ozberk Ozturk, and Murat Kaya Yapici. Wearable graphene nanotextile embedded smart armband for cardiac monitoring. In *2018 IEEE SENSORS*, pages 1–4, 2018.

[3] Rajendra Acharya U., P. Subbanna Bhat, N. Kannathal, Ashok Rao, and Choo Min Lim. Analysis of cardiac health using fractal dimension and wavelet transformation. *ITBM-RBM*, 26(2):133–139, April 2005.

[4] V. Agostini, E. Aiello, D. Fortunato, M. Knaflitz, and L. Gastaldi. A wearable device to assess postural sway. In *2019 IEEE 23rd International Symposium on Consumer Technologies (ISCT)*, pages 197–200, June 2019. ISSN: 2159-1423.

[5] Mahmuda Akter Shathi, Chen Minzhi, Nazakat Ali Khoso, Hridam Deb, Arsalan Ahmed, and Wang Sai Sai. All organic graphene oxide and poly (3, 4-ethylene dioxythiophene) - poly (styrene sulfonate) coated knitted textile fabrics for wearable electrocardiography (ecg) monitoring. *Synthetic Metals*, 263:116329, 2020.

[6] Haitham M. Al-Angari and Alan V. Sahakian. Use of Sample Entropy Approach to Study Heart Rate Variability in Obstructive Sleep Apnea Syndrome. *IEEE Transactions on Biomedical Engineering*, 54(10):1900–1904, October 2007.

[7] Douglas G Altman and J Martin Bland. Measurement in medicine: the analysis of method comparison studies. *Journal of the Royal Statistical Society: Series D (The Statistician)*, 32(3):307–317, 1983.

[8] Federica Amitrano, Armando Coccia, Gaetano Pagano, Lucia Dileo, Ernesto Losavio, Giuseppe Tombolini, and Giovanni D'Addio. The Impact of Ankle-Foot Orthoses on Spatio-Temporal Gait Parameters in Drop-Foot Patients. In *2022 IEEE International Symposium on Medical Measurements and Applications (MeMeA)*, pages 1–6, Messina, Italy, June 2022. IEEE.

[9] Federica Amitrano, Armando Coccia, Carlo Ricciardi, Leandro Donisi, Giuseppe Cesarelli, Edda Maria Capodaglio, and Giovanni D'Addio. Design and Validation of an E-Textile-Based Wearable Sock for Remote Gait and Postural Assessment. *Sensors*, 20(22):6691, November 2020.

[10] Federica Amitrano, Leandro Donisi, Armando Coccia, Arcangelo Biancardi, Gaetano Pagano, and Giovanni D'Addio. Experimental Development and Validation of an E-Textile Sock Prototype. In *2020 IEEE International Symposium on Medical Measurements and Applications (MeMeA)*, pages 1–5, Bari, Italy, June 2020. IEEE.

[11] Katya Arquilla, Andrea K. Webb, and Allison P. Anderson. Textile electrocardiogram (ecg) electrodes for wearable health monitoring. *Sensors*, 20(4), 2020.

[12] Fatima Awan, Yilin He, Linh Le, Le-Lan Tran, Huy-Dung Han, and Loan Pham Nguyen. Electromyography acquisition system using graphene-based e-textiles. In *2019 International Symposium on Electrical and Electronics Engineering (ISEE)*, pages 59–62, 2019.

[13] Eulalia Balestrieri, Pasquale Daponte, Luca De Vito, Francesco Picariello, Sergio Rapuano, and Ioan Tudosa. A Wi-Fi IoT prototype for ECG monitoring exploiting a novel Compressed Sensing method. *ACTA IMEKO*, 9(2):38, June 2020.

[14] R. Bartalesi, F. Lorussi, D. De Rossi, M. Tesconi, and A. Tognetti. Wearable monitoring of lumbar spine curvature by inertial and e-textile sensory fusion. In *2010 Annual International Conference of the IEEE Engineering in Medicine and Biology*, pages 6373–6376, 2010.

[15] R. Clifford Blair and Stephen Cole. Two-Sided Equivalence Testing Of The Difference Between Two Means. *Journal of Modern Applied Statistical Methods*, 1(1), May 2002.

[16] J. M. Bland and D. G. Altman. Measuring agreement in method comparison studies. *Statistical Methods in Medical Research*, 8(2):135–160, June 1999.

[17] F. Bugané, M.G. Benedetti, G. Casadio, S. Attala, F. Biagi, M. Manca, and A. Leardini. Estimation of spatial-temporal gait parameters in level walking based on a single accelerometer: Validation on normal subjects by standard gait analysis. *Computer Methods and Programs in Biomedicine*, 108(1):129–137, October 2012.

[18] John Parker Burg. Absolute Power Density Spectra. In C. Ray Smith and W. T. Grandy, editors, *Maximum-Entropy and Bayesian Methods in Inverse Problems*, pages 273–286. Springer Netherlands, Dordrecht, 1985.

[19] Seonjeong Byun, Ji Won Han, Tae Hui Kim, and Ki Woong Kim. Test-Retest Reliability and Concurrent Validity of a Single Tri-Axial Accelerometer-Based Gait Analysis in Older Adults with Normal Cognition. *PLOS ONE*, 11(7):e0158956, July 2016.

[20] Lina M Castano and Alison B Flatau. Smart fabric sensors and e-textile technologies: a review. *Smart Materials and Structures*, 23(5):053001, apr 2014.

[21] Paola Catalfamo, Salim Ghoussayni, and David Ewins. Gait Event Detection on Level Ground and Incline Walking Using a Rate Gyroscope. *Sensors*, 10(6):5683–5702, June 2010.

[22] André Catarino, Helder Carvalho, Maria J. Dias, Tiago Pereira, Octavian Postolache, and Pedro S. Girão. Continuous health monitoring using e-textile integrated biosensors. In *2012 International Conference and Exposition on Electrical and Power Engineering*, pages 605–609, 2012.

[23] Andrea Cereatti, Diana Trojaniello, and Ugo Della Croce. Accurately measuring human movement using magneto-inertial sensors: techniques and challenges. In *2015 IEEE International Symposium on Inertial Sensors and Systems (ISISS) Proceedings*, pages 1–4, Hapuna Beach, HI, USA, March 2015. IEEE.

[24] Guorui Chen, Xiao Xiao, Xun Zhao, Trinny Tat, Michael Bick, and Jun Chen. Electronic Textiles for Wearable Point-of-Care Systems. *Chemical Reviews*, 122(3):3259–3291, February 2022.

[25] Song Chen, Shuqi Liu, Pingping Wang, Haizhou Liu, and Lan Liu. Highly stretchable fiber-shaped e-textiles for strain/pressure sensing, full-range human motions detection, health monitoring, and 2d force mapping. *Journal of Materials Science*, 53(4):2995–3005, 2018.

[26] Nauman Ali Choudhry, Abher Rasheed, Sheraz Ahmad, Lyndon Arnold, and Lijing Wang. Design, development and characterization of textile stitch-based piezoresistive sensors for wearable monitoring. *IEEE Sensors Journal*, 20(18):10485–10494, 2020.

[27] Armando Coccia, Federica Amitrano, Pietro Balbi, Leandro Donisi, Arcangelo Biancardi, and Giovanni D'Addio. Analysis of Test-Retest Repeatability of Gait Analysis Parameters in Hereditary Spastic Paraplegia. In *2021 IEEE International Symposium on Medical Measurements and Applications (MeMeA)*, pages 1–6, Lausanne, Switzerland, June 2021. IEEE.

[28] Armando Coccia, Federica Amitrano, Leandro Donisi, Giuseppe Cesarelli, Gaetano Pagano, Mario Cesarelli, and Giovanni D'Addio. Design and validation of an e-textile-based wearable system for remote health monitoring. *ACTA IMEKO*, 10(2):220–229, 2021.

[29] Armando Coccia, Federica Amitrano, Gaetano Pagano, Lucia Dileo, Vito Marsico, Giuseppe Tombolini, and Giovanni D'Addio. Biomechanical modelling for quantitative assessment of gait kinematics in drop foot patients with ankle foot orthosis. In *2022 IEEE International Symposium on Medical Measurements and Applications (MeMeA)*, pages 1–6, Messina, Italy, June 2022. IEEE.

[30] Iwona Cygankiewicz and Wojciech Zaręba. Heart rate turbulence - an overview of methods and applications. *Cardiology Journal*, 13(5):359–368, 2006.

[31] Nadine Dabby, Aleksandar Aleksov, Eric Lewallen, Sasha Oster, Racquel Fygenson, Braxton Lathrop, Michael Bynum, Mezhgan Samady, Steven Klein, and Steven Girouard. A scalable process for manufacturing integrated, washable smart garments applied to heart rate monitoring. In *Proceedings of the 2017 ACM International Symposium on Wearable Computers*, ISWC '17, page 38–41, New York, NY, USA, 2017. Association for Computing Machinery.

[32] G. D'Addio, L. Donisi, G. Pagano, G. Improta, A. Biancardi, and M. Cesarelli. Agreement between Opal and G-Walk Wearable Inertial Systems in Gait Analysis on Normal and Pathological Subjects. In *2019 41st Annual International Conference of the IEEE Engineering in Medicine and Biology Society (EMBC)*, pages 3286–3289, Berlin, Germany, July 2019. IEEE.

[33] G. D'Addio, S. Evangelista, L. Donisi, A. Biancardi, E. Andreozzi, G. Pagano, P. Arpaia, and M. Cesarelli. Development of a Prototype E-Textile Sock. In *2019 41st Annual International Conference of the IEEE Engineering in Medicine and Biology Society (EMBC)*, pages 17498–1752, Berlin, Germany, July 2019. IEEE.

[34] G. D'Addio, L. Iuppariello, G. Pagano, A. Biancardi, B. Lanzillo, N. Pappone, and M. Cesarelli. New posturographic assessment by means of novel e-textile and wireless socks device. In *2016 IEEE International Symposium on Medical Measurements and Applications (MeMeA)*, pages 1–5, Benevento, Italy, May 2016. IEEE.

[35] Roy B. Davis, Sylvia Õunpuu, Dennis Tyburski, and James R. Gage. A gait analysis data collection and reduction technique. *Human Movement Science*, 10(5):575–587, October 1991.

[36] Séverine de Mulatier, Mohamed Nasreldin, Roger Delattre, Marc Ramuz, and Thierry Djenizian. Electronic Circuits Integration in Textiles for Data Processing in Wearable Technologies. *Advanced Materials Technologies*, 3(10):1700320, October 2018.

[37] Roel De Ridder, Julien Lebleu, Tine Willems, Cedric De Blaiser, Christine Detrembleur, and Philip Roosen. Concurrent Validity of a Commercial Wireless Trunk Triaxial Accelerometer System for Gait Analysis. *Journal of Sport Rehabilitation*, 28(6):jsr.2018–0295, August 2019.

[38] Silvia Del Din, Alan Godfrey, Brook Galna, Sue Lord, and Lynn Rochester. Free-living gait characteristics in ageing and Parkinson's disease: impact of environment and ambulatory bout length. *Journal of NeuroEngineering and Rehabilitation*, 13(1):46, May 2016.

[39] Silvia Del Din, Alan Godfrey, and Lynn Rochester. Validation of an Accelerometer to Quantify a Comprehensive Battery of Gait Characteristics in Healthy Older Adults and Parkinson's Disease: Toward Clinical and at Home Use. *IEEE Journal of Biomedical and Health Informatics*, 20(3):838–847, May 2016.

[40] D. DeRossi and A. Lymberis. Guest Editorial New Generation of Smart Wearable Health Systems and Applications. *IEEE Transactions on Information Technology in Biomedicine*, 9(3):293–294, September 2005.

[41] Emer P. Doheny, Timothy G. Foran, and Barry R. Greene. A single gyroscope method for spatial gait analysis. *Annual International Conference of the IEEE Engineering in Medicine and Biology Society. IEEE Engineering in Medicine and Biology Society. Annual International Conference*, 2010:1300–1303, 2010.

[42] Leandro Donisi, Federica Amitrano, Armando Coccia, Luca Mercogliano, Giuseppe Cesarelli, and Giovanni D'Addio. Influence of the Backpack on School Children's Gait: A Statistical and Machine Learning Approach. In Tomaz Jarm, Aleksandra Cvetkoska, Samo Mahnič-Kalamiza, and Damijan Miklavcic, editors, *8th European Medical and Biological Engineering*

Conference, volume 80, pages 682–688. Springer International Publishing, Cham, 2021.

[43] Leandro Donisi, Giuseppe Cesarelli, Armando Coccia, Monica Panigazzi, Edda Maria Capodaglio, and Giovanni D'Addio. Work-Related Risk Assessment According to the Revised NIOSH Lifting Equation: A Preliminary Study Using a Wearable Inertial Sensor and Machine Learning. *Sensors*, 21(8):2593, April 2021.

[44] Leandro Donisi, Gaetano Pagano, Giuseppe Cesarelli, Armando Coccia, Federica Amitrano, and Giovanni D'Addio. Benchmarking between two wearable inertial systems for gait analysis based on a different sensor placement using several statistical approaches. *Measurement*, 173:108642, 2021.

[45] G. D'Addio, S. Evangelista, L. Donisi, A. Biancardi, E. Andreozzi, G. Pagano, P. Arpaia, and M. Cesarelli. Development of a prototype e-textile sock*. In *2019 41st Annual International Conference of the IEEE Engineering in Medicine and Biology Society (EMBC)*, pages 17498–1752, 2019.

[46] Task Force of the European Society of Cardiology the North A Electrophysiology. Heart Rate Variability: Standards of Measurement, Physiological Interpretation, and Clinical Use. *Circulation*, 93(5):1043–1065, March 1996.

[47] Moataz Eltoukhy, Christopher Kuenze, Jeonghoon Oh, Marco Jacopetti, Savannah Wooten, and Joseph Signorile. Microsoft Kinect can distinguish differences in over-ground gait between older persons with and without Parkinson's disease. *Medical Engineering & Physics*, 44:1–7, June 2017.

[48] Patrick Esser, Helen Dawes, Johnny Collett, Max G. Feltham, and Ken Howells. Assessment of spatio-temporal gait parameters using inertial measurement units in neurological populations. *Gait & Posture*, 34(4):558–560, October 2011.

[49] Patrick Esser, Helen Dawes, Johnny Collett, Max G. Feltham, and Ken Howells. Validity and inter-rater reliability of inertial gait measurements in Parkinson's disease: A pilot study. *Journal of Neuroscience Methods*, 205(1):177–181, March 2012.

[50] André G. Ferreira, Duarte Fernandes, Sérgio Branco, João L. Monteiro, Jorge Cabral, André P. Catarino, and Ana M. Rocha. A smart wearable system for sudden infant death syndrome monitoring. In *2016 IEEE International Conference on Industrial Technology (ICIT)*, pages 1920–1925, 2016.

[51] François Feuvrier, Benoît Sijobert, Christine Azevedo, Karolina Griffiths, Sandrine Alonso, Arnaud Dupeyron, Isabelle Laffont, and Jérôme Froger. Inertial measurement unit compared to an optical motion capturing system in post-stroke individuals with foot-drop syndrome. *Annals of Physical and Rehabilitation Medicine*, 63(3):195–201, May 2020.

[52] A. Fevgas, P. Tsompanopoulou, and S. Lalis. Rapid prototype development for studying human activity. In Panagiotis D. Bamidis and Nicolas Pallikarakis, editors, *XII Mediterranean Conference on Medical and Biological Engineering and Computing 2010*, pages 643–646, Berlin, Heidelberg, 2010. Springer Berlin Heidelberg.

[53] David Fouassier, Xavier Roy, Anne Blanchard, and Jean-Sébastien Hulot. Assessment of signal quality measured with a smart 12-lead ecg acquisition t-shirt. *Annals of Noninvasive Electrocardiology*, 25(1):e12682, 2020.

[54] Astrid García Patiño, Mahta Khoshnam, and Carlo Menon. Wearable device to monitor back movements using an inductive textile sensor. *Sensors*, 20(3), 2020.

[55] Alan Godfrey, Silvia Del Din, Gillian Barry, John C. Mathers, and Lynn Rochester. Within trial validation and reliability of a single tri-axial accelerometer for gait assessment. In *2014 36th Annual International Conference of the IEEE Engineering in Medicine and Biology Society*, pages 5892–5895, Chicago, IL, August 2014. IEEE.

[56] Ata Jedari Golparvar and Murat Kaya Yapici. Wearable graphene textile-enabled eog sensing. In *2017 IEEE SENSORS*, pages 1–3, 2017.

[57] Ata Jedari Golparvar and Murat Kaya Yapici. Electrooculography by wearable graphene textiles. *IEEE Sensors Journal*, 18(21):8971–8978, 2018.

[58] Ata Jedari Golparvar and Murat Kaya Yapici. Graphene-coated wearable textiles for eog-based human-computer interaction. In *2018 IEEE 15th International Conference on Wearable and Implantable Body Sensor Networks (BSN)*, pages 189–192, 2018.

[59] Carles Gomez, Joaquim Oller, and Josep Paradells. Overview and Evaluation of Bluetooth Low Energy: An Emerging Low-Power Wireless Technology. *Sensors*, 12(9):11734–11753, August 2012.

[60] Laura Gonzales, Katherine Walker, Kevin Keller, Daniel Beckman, Henry Goodell, Grace Wright, Christian Rhone, Andrew Emery, and Rachana Gupta. Textile sensor system for electrocardiogram monitoring. In *2015 IEEE Virtual Conference on Applications of Commercial Sensors (VCACS)*, pages 1–4, Raleigh, NC, USA, March 2015. IEEE.

[61] Uri Gottlieb, Tharani Balasukumaran, Jay R. Hoffman, and Shmuel Springer. Agreement of Gait Events Detection during Treadmill Backward Walking by Kinematic Data and Inertial Motion Units. *Sensors*, 20(21):6331, November 2020.

[62] Carla Belen Goy, Juan Martin Dominguez, MA Gómez López, Rossana Elena Madrid, and MC Herrera. Electrical characterization of conductive textile materials and its evaluation as electrodes for venous occlusion plethysmography. *Journal of medical engineering & technology*, 37(6):359–367, 2013.

[63] Peter A. Haddad, Amir Servati, Saeid Soltanian, Frank Ko, and Peyman Servati. Breathable dry silver/silver chloride electronic textile electrodes for electrodermal activity monitoring. *Biosensors*, 8(3), 2018.

[64] Magdalena Hagner-Derengowska, Krystian Kałużny, Anna Kałużna, Walery Zukow, Kamil Leis, Małgorzata Domagalska-Szopa, Bartosz Kochański, and Jacek Budzyński. Effect of a training program of overground walking on BTS gait parameters in elderly women during single and dual cognitive tasks. *International Journal of Rehabilitation Research*, 43(4):355–360, December 2020.

[65] Nooshin Haji Ghassemi, Julius Hannink, Christine Martindale, Heiko Gaßner, Meinard Müller, Jochen Klucken, and Björn Eskofier. Segmentation of Gait Sequences in Sensor-Based Movement Analysis: A Comparison of Methods in Parkinson's Disease. *Sensors*, 18(2):145, January 2018.

[66] Antonia Hartmann, Susanna Luzi, Kurt Murer, Rob A. de Bie, and Eling D. de Bruin. Concurrent validity of a trunk tri-axial accelerometer system for gait analysis in older adults. *Gait & Posture*, 29(3):444–448, April 2009.

[67] Chihiro Hayashi, Yu Enokibori, and Kenji Mase. Harmless line-oriented sensing point reduction for non-categorical sitting posture score. In *Proceedings of the 2017 ACM International Joint Conference on Pervasive and Ubiquitous Computing and Proceedings of the 2017 ACM International Symposium on Wearable Computers*, pages 61–64, 2017.

[68] Jennifer Healey. Gsr sock: A new e-textile sensor prototype. In *2011 15th Annual International Symposium on Wearable Computers*, pages 113–114, 2011.

[69] Jae Sang Heo, Hossein Hamidi Shishavan, Rahim Soleymanpour, Jiwon Kim, and Insoo Kim. Textile-based stretchable and flexible glove sensor for monitoring upper extremity prosthesis functions. *IEEE Sensors Journal*, 20(4):1754–1760, 2020.

[70] Hermie J Hermens, Bart Freriks, Catherine Disselhorst-Klug, and Günter Rau. Development of recommendations for semg sensors and sensor placement procedures. *Journal of Electromyography and Kinesiology*, 10(5):361–374, 2000.

[71] Aodhán Hickey, Eleanor Gunn, Lisa Alcock, Silvia Del Din, Alan Godfrey, Lynn Rochester, and Brook Galna. Validity of a wearable accelerometer to quantify gait in spinocerebellar ataxia type 6. *Physiological Measurement*, 37(11):N105–N117, November 2016.

[72] T. Higuchi. Approach to an irregular time series on the basis of the fractal theory. *Physica D: Nonlinear Phenomena*, 31(2):277–283, June 1988.

[73] Jean-Yves Hogrel. Clinical applications of surface electromyography in neuromuscular disorders. *Neurophysiologie Clinique/Clinical Neurophysiology*, 35(2):59–71, 2005.

[74] Thomas Holleczek, Alex Rüegg, Holger Harms, and Gerhard Tröster. Textile pressure sensors for sports applications. In *2010 IEEE SENSORS*, pages 732–737, November 2010. ISSN: 1930-0395.

[75] Ming-Chun Huang, Wenyao Xu, Jason Liu, Lauren Samy, Amir Vajid, Nabil Alshurafa, and Majid Sarrafzadeh. Inconspicuous on-bed respiratory rate monitoring. In *Proceedings of the 6th International Conference on PErvasive Technologies Related to Assistive Environments*, PETRA '13, New York, NY, USA, 2013. Association for Computing Machinery.

[76] Heikki V. Huikuri, Timo H. Mäkikallio, Chung-Kang Peng, Ary L. Goldberger, Ulrik Hintze, and Mogens Møller. Fractal Correlation Properties of R-R Interval Dynamics and Mortality in Patients With Depressed Left Ventricular Function After an Acute Myocardial Infarction. *Circulation*, 101(1):47–53, January 2000.

[77] Ezgi Ismar, Xuyuan Tao, Francois Rault, Francois Dassonville, and Cedric Cochrane. Towards Embroidered Circuit Board From Conductive Yarns for E-Textiles. *IEEE Access*, 8:155329–155336, 2020.

[78] Julia F. Item-Glatthorn, Nicola C. Casartelli, Jeannette Petrich-Munzinger, Urs K. Munzinger, and Nicola A. Maffiuletti. Validity of the Intelligent Device for Energy Expenditure and Activity Accelerometry System for Quantitative Gait Analysis in Patients With Hip Osteoarthritis. *Archives of Physical Medicine and Rehabilitation*, 93(11):2090–2093, November 2012.

[79] Yutong Jiang, Kewen Pan, Ting Leng, and Zhirun Hu. Smart textile integrated wireless powered near field communication body temperature and sweat sensing system. *IEEE Journal of Electromagnetics, RF and Microwaves in Medicine and Biology*, 4(3):164–170, 2020.

[80] Hanbit Jin, Md Osman Goni Nayeem, Sunghoon Lee, Naoji Matsuhisa, Daishi Inoue, Tomoyuki Yokota, Daisuke Hashizume, and Takao Someya. Highly durable nanofiber-reinforced elastic conductors for skin-tight electronic textiles. *ACS nano*, 13(7):7905–7912, 2019.

[81] Gaeul Kim, Chi Cuong Vu, and Jooyong Kim. Single-Layer Pressure Textile Sensors with Woven Conductive Yarn Circuit. *Applied Sciences*, 10(8):2877, April 2020.

[82] Siyeon Kim, Sojung Lee, and Wonyoung Jeong. EMG Measurement with Textile-Based Electrodes in Different Electrode Sizes and Clothing Pressures for Smart Clothing Design Optimization. *Polymers*, 12(10):2406, October 2020.

[83] Felix Kluge, Heiko Gaßner, Julius Hannink, Cristian Pasluosta, Jochen Klucken, and Björn Eskofier. Towards Mobile Gait Analysis: Concurrent Validity and Test-Retest Reliability of an Inertial Measurement System for the Assessment of Spatio-Temporal Gait Parameters. *Sensors*, 17(7):1522, June 2017.

[84] James F. Knight and Chris Baber. A tool to assess the comfort of wearable computers. *Human Factors*, 47(1):77–91, 2005.

[85] James F. Knight, Daniel Deen-Williams, Theodoros N. Arvanitis, Chris Baber, Sofoklis Sotiriou, Stamatina Anastopoulou, and Michael Gargalakos. Assessing the Wearability of Wearable Computers. In *2006 10th IEEE International Symposium on Wearable Computers*, pages 75–82, October 2006. ISSN: 2376-8541.

[86] Anke I.R. Kottink, Linda J.M. Oostendorp, Jacob H. Buurke, Anand V. Nene, Hermanus J. Hermens, and Maarten J. IJzerman. The Orthotic Effect of Functional Electrical Stimulation on the Improvement of Walking in Stroke Patients with a Dropped Foot: A Systematic Review. *Artificial Organs*, 28(6):577–586, June 2004.

[87] Tomohiro Kuroda, Kikuo Hirano, Kazushige Sugimura, Satoshi Adachi, Hidetsugu Igarashi, Kazuo Ueshima, Hideo Nakamura, Masayuki Nambu, and Takahiro Doi. Applying nishijin historical textile technique for e-textile. In *2013 35th Annual International Conference of the IEEE Engineering in Medicine and Biology Society (EMBC)*, pages 1226–1229, 2013.

[88] Alper Köse, Andrea Cereatti, and Ugo Della Croce. Bilateral step length estimation using a single inertial measurement unit attached to the pelvis. *Journal of NeuroEngineering and Rehabilitation*, 9(1):9, December 2012.

[89] Katherine Le, Amir Servati, Frank Ko, and Peyman Servati. Signal quality analysis of electrocardiogram textile electrodes for smart apparel applications. In *2019 IEEE International Flexible Electronics Technology Conference (IFETC)*, pages 1–3, 2019.

[90] Braden M Li, Inhwan Kim, Ying Zhou, Amanda C Mills, Tashana J Flewwellin, and Jesse S Jur. Kirigami-inspired textile electronics: Kite. *Advanced Materials Technologies*, 4(11):1900511, 2019.

[91] Menglong Li, Russel Torah, Helga Nunes-Matos, Yang Wei, Steve Beeby, John Tudor, and Kai Yang. Integration and testing of a three-axis accelerometer in a woven e-textile sleeve for wearable movement monitoring. *Sensors*, 20(18), 2020.

[92] Yudong Li, Yanan Li, Meng Su, Wenbo Li, Yifan Li, Huizeng Li, Xin Qian, Xingye Zhang, Fengyu Li, and Yanlin Song. Electronic textile by dyeing method for multiresolution physical kineses monitoring. *Advanced Electronic Materials*, 3(10):1700253, 2017.

[93] Yunlu Lian, He Yu, Mingyuan Wang, Xiaonan Yang, Zhe Li, Fan Yang, Yang Wang, Huiling Tai, Yulong Liao, Jieyun Wu, Xiangru Wang, Yadong Jiang, and Guangming Tao. A multifunctional wearable e-textile via integrated nanowire-coated fabrics. *J. Mater. Chem. C*, 8:8399–8409, 2020.

[94] An Liang, Rebecca Stewart, Rachel Freire, and Nick Bryan-Kinns. Effect of bonding and washing on electronic textile stretch sensor properties. In *Adjunct Proceedings of the 2019 ACM International Joint Conference on Pervasive and Ubiquitous Computing and Proceedings of the 2019 ACM International Symposium on Wearable Computers*, pages 121–124, London United Kingdom, September 2019. ACM.

[95] Haipeng Liu, John Allen, Dingchang Zheng, and Fei Chen. Recent development of respiratory rate measurement technologies. *Physiological Measurement*, 40(7):07TR01, aug 2019.

[96] Jason J. Liu, Ming-Chun Huang, Wenyao Xu, Xiaoyi Zhang, Luke Stevens, Nabil Alshurafa, and Majid Sarrafzadeh. Breathsens: A continuous on-bed respiratory monitoring system with torso localization using an unobtrusive pressure sensing array. *IEEE Journal of Biomedical and Health Informatics*, 19(5):1682–1688, 2015.

[97] Rong Liu, Shuxiao Wang, and Terence T. Lao. A novel solution of monitoring incontinence status by conductive yarn and advanced seamless knitting techniques. *Journal of Engineered Fibers and Fabrics*, 7(4):155892501200700415, 2012.

[98] N. R. Lomb. Least-squares frequency analysis of unequally spaced data. *Astrophysics and Space Science*, 39(2):447–462, February 1976.

[99] Gregorio Lopez, Victor Custodio, and Jose Ignacio Moreno. Location-aware system for wearable physiological monitoring within hospital facilities. In *21st Annual IEEE International Symposium on Personal, Indoor and Mobile Radio Communications*, pages 2609–2614, 2010.

[100] Sue Lord, Lynn Rochester, Katherine Baker, and Alice Nieuwboer. Concurrent validity of accelerometry to measure gait in Parkinsons Disease. *Gait & Posture*, 27(2):357–359, February 2008.

[101] Federico Lorussi, Irene Lucchese, Alessandro Tognetti, and Nicola Carbonaro. A wearable system for remote monitoring of the treatments of musculoskeletal disorder. In *2018 IEEE International Conference on Smart Computing (SMARTCOMP)*, pages 362–367, 2018.

[102] Pasindu Lugoda, Theodore Hughes-Riley, Carlos Oliveira, Rob Morris, and Tilak Dias. Developing novel temperature sensing garments for health monitoring applications. *Fibers*, 6(3), 2018.

[103] Gerard M. Lyons, Thomas Sinkjaer, Jane H. Burridge, and David J. Wilcox. A review of portable FES-based neural orthoses for the correction of drop foot. *IEEE transactions on neural systems and rehabilitation engineering: a publication of the IEEE Engineering in Medicine and Biology Society*, 10(4):260–279, December 2002.

[104] Gregorio López, Víctor Custodio, and José Ignacio Moreno. Lobin: E-textile and wireless-sensor-network-based platform for healthcare monitoring in future hospital environments. *IEEE Transactions on Information Technology in Biomedicine*, 14(6):1446–1458, 2010.

[105] Shadi Mahdiani, Vala Jeyhani, Mikko Peltokangas, and Antti Vehkaoja. Is 50 Hz high enough ECG sampling frequency for accurate HRV analysis? In *2015 37th Annual International Conference of the IEEE Engineering in Medicine and Biology Society (EMBC)*, pages 5948–5951, Milan, August 2015. IEEE.

[106] A Malliani, M Pagani, F Lombardi, and S Cerutti. Cardiovascular neural regulation explored in the frequency domain. *Circulation*, 84(2):482–492, August 1991.

[107] Hitoshi Maruyama and Hiroshi Nagasaki. Temporal variability in the phase durations during treadmill walking. *Human Movement Science*, 11(3):335–348, May 1992.

[108] A Mason, S Wylie, Olga Korostynska, LE Cordova-Lopez, and AI Al-Shamma'a. Flexible e-textile sensors for real-time health monitoring at microwave frequencies. *International Journal on Smart Sensing and Intelligent Systems*, 7(1), 2017.

[109] Keyu Meng, Shenlong Zhao, Yihao Zhou, Yufen Wu, Songlin Zhang, Qiang He, Xue Wang, Zhihao Zhou, Wenjing Fan, Xulong Tan, Jin Yang, and Jun Chen. A Wireless Textile-Based Sensor System for Self-Powered Personalized Health Care. *Matter*, 2(4):896–907, April 2020.

[110] Saumendra K Mohapatra and Mihir N Mohanty. Ecg analysis: A brief review. *Recent Advances in Computer Science and Communications (Formerly: Recent Patents on Computer Science)*, 14(2):344–359, 2021.

[111] Sarah A. Moore, Aodhan Hickey, Sue Lord, Silvia Del Din, Alan Godfrey, and Lynn Rochester. Comprehensive measurement of stroke gait characteristics with a single accelerometer in the laboratory and community: a feasibility, validity and reliability study. *Journal of Neuroengineering and Rehabilitation*, 14(1):130, December 2017.

[112] Rosie Morris, Samuel Stuart, Grace McBarron, Peter C. Fino, Martina Mancini, and Carolin Curtze. Validity of Mobility Lab (version 2) for gait assessment in young adults, older adults and Parkinson's disease. *Physiological Measurement*, 40(9):095003, September 2019.

[113] R. Nayak, L. Wang, and R. Padhye. Electronic textiles for military personnel. In *Electronic Textiles*, pages 239–256. Elsevier, 2015.

[114] K.M. Newell. 30 The Speed-Accuracy Paradox in Movement Control: Errors of Time and space. In *Advances in Psychology*, volume 1, pages 501–510. Elsevier, 1980.

[115] Andrea Nicolò, Carlo Massaroni, Emiliano Schena, and Massimo Sacchetti. The importance of respiratory rate monitoring: From healthcare to sport and exercise. *Sensors*, 20(21), 2020.

[116] Arinobu Niijima, Takashi Isezaki, Ryosuke Aoki, Tomoki Watanabe, and Tomohiro Yamada. hitoecap: Wearable emg sensor for monitoring masticatory muscles with pedot-pss textile electrodes. In *Proceedings of the 2017 ACM International Symposium on Wearable Computers*, pages 215–220, 2017.

[117] Arinobu Niijima, Takashi Isezaki, Ryosuke Aoki, Tomoki Watanabe, and Tomohiro Yamada. Biceps fatigue estimation with an e-textile headband. In *Proceedings of the 2018 ACM International Symposium on Wearable Computers*, pages 222–223, 2018.

[118] Masahiko Okada. A Digital Filter for the QRS Complex Detection. *IEEE Transactions on Biomedical Engineering*, BME-26(12):700–703, December 1979.

[119] Ozberk Ozturk and Murat Kaya Yapici. Muscular activity monitoring and surface electromyography (semg) with graphene textiles. In *2019 IEEE SENSORS*, pages 1–4, 2019.

[120] Ozberk Ozturk and Murat Kaya Yapici. Surface electromyography with wearable graphene textiles. *IEEE Sensors Journal*, 21(13):14397–14406, 2021.

[121] Giulia Pacini Panebianco, Maria Cristina Bisi, Rita Stagni, and Silvia Fantozzi. Analysis of the performance of 17 algorithms from a systematic review: Influence of sensor position, analysed variable and computational approach in gait timing estimation from IMU measurements. *Gait & Posture*, 66:76–82, October 2018.

[122] Sungmee Park and Sundaresan Jayaraman. Smart Textiles: Wearable Electronic Systems. *MRS Bulletin*, 28(8):585–591, August 2003.

[123] Sungmee Park and Sundaresan Jayaraman. The wearables revolution and Big Data: the textile lineage. *The Journal of The Textile Institute*, 108(4):605–614, April 2017.

[124] H. Passing and W. Bablok. A New Biometrical Procedure for Testing the Equality of Measurements from Two Different Analytical Methods. Application of linear regression procedures for method comparison studies in Clinical Chemistry, Part I. *Clinical Chemistry and Laboratory Medicine*, 21(11), 1983.

[125] Matthew R. Patterson, William Johnston, Niamh O'Mahony, Sam O'Mahony, Eimear Nolan, and Brian Caulfield. Validation of temporal gait metrics from three IMU locations to the gold standard force plate. *Annual International Conference of the IEEE Engineering in Medicine and Biology Society. IEEE Engineering in Medicine and Biology Society. Annual International Conference*, 2016:667–671, August 2016.

[126] P. Hunter Peckham and Jayme S. Knutson. Functional Electrical Stimulation for Neuromuscular Applications. *Annual Review of Biomedical Engineering*, 7(1):327–360, August 2005.

[127] Federica Petraglia, Luca Scarcella, Giuseppe Pedrazzi, Luigi Brancato, Robert Puers, and Cosimo Costantino. Inertial sensors versus standard systems in gait analysis: a systematic review and meta-analysis. *European Journal of Physical and Rehabilitation Medicine*, 55(2), May 2019.

[128] Francesco Picariello, Grazia Iadarola, Eulalia Balestrieri, Ioan Tudosa, and Luca De Vito. A novel compressive sampling method for ECG wearable measurement systems. *Measurement*, 167:108259, January 2021.

[129] O. Postolache, V. Viegas, J. M. Dias Pereira, D. Vinhas, P. Silva Girão, and G. Postolache. Toward developing a smart wheelchair for user physiological stress and physical activity monitoring. In *2014 IEEE International Symposium on Medical Measurements and Applications (MeMeA)*, pages 1–6, 2014.

[130] T. E. Prieto, J. B. Myklebust, R. G. Hoffmann, E. G. Lovett, and B. M. Myklebust. Measures of postural steadiness: differences between healthy young and elderly adults. *IEEE transactions on bio-medical engineering*, 43(9):956–966, September 1996.

[131] Muhammad Wasim Raad, Mohamed A Deriche, A Bin Hafeedh, H Almasawa, K Bin Jofan, H Alsakkaf, A Bahumran, and M Salem. An iot based wearable smart glove for remote monitoring of rheumatoid arthritis patients. *Biosignals*, 2019:224–228, 2019.

[132] Raul I. Ramos-Garcia, Fernanda Da Silva, Yashvanth Kondi, Edward Sazonov, and Lucy E. Dunne. Analysis of a coverstitched stretch sensor for monitoring of breathing. In *2016 10th International Conference on Sensing Technology (ICST)*, pages 1–6, 2016.

[133] Alexander Rampp, Jens Barth, Samuel Schülein, Karl-Günter Gaßmann, Jochen Klucken, and Björn M. Eskofier. Inertial sensor-based stride parameter calculation from gait sequences in geriatric patients. *IEEE transactions on bio-medical engineering*, 62(4):1089–1097, April 2015.

[134] Samuel Reinfelder, Felix Durlak, Jens Barth, Jochen Klucken, and Bjoern M. Eskofier. Wearable static posturography solution using a novel pressure sensor sole. *Annual International Conference of the IEEE Engineering in Medicine and Biology Society. IEEE Engineering in Medicine and Biology Society. Annual International Conference*, 2014:2973–2976, 2014.

[135] Sandy Rolfe. The importance of respiratory rate monitoring. *British Journal of Nursing*, 28(8):504–508, 2019.

[136] Laura Romeo, Roberto Marani, Nicola Lorusso, Maria Teresa Angelillo, and Grazia Cicirelli. Vision-based Assessment of Balance Control in Elderly People. In *2020 IEEE International Symposium on Medical Measurements and Applications (MeMeA)*, pages 1–6, Bari, Italy, June 2020. IEEE.

[137] Sigrid Rotzler, Christine Kallmayer, Christian Dils, Malte von Krshiwoblozki, Ulrich Bauer, and Martin Schneider-Ramelow. Improving the

washability of smart textiles: influence of different washing conditions on textile integrated conductor tracks. *The Journal of The Textile Institute*, 111(12):1766–1777, December 2020.

[138] Arash Salarian, Heike Russmann, François J. G. Vingerhoets, Catherine Dehollain, Yves Blanc, Pierre R. Burkhard, and Kamiar Aminian. Gait assessment in Parkinson's disease: toward an ambulatory system for long-term monitoring. *IEEE transactions on bio-medical engineering*, 51(8):1434–1443, August 2004.

[139] Horacio J. Salavagione, Peter S. Shuttleworth, Juan P. Fernández-Blázquez, Gary J. Ellis, and Marián A. Gómez-Fatou. Scalable graphene-based nanocomposite coatings for flexible and washable conductive textiles. *Carbon*, 167:495–503, October 2020.

[140] Syaidah Md. Saleh, Syafiqah Md. Jusob, Fauzan Khairi Che Harun, Leny Yuliati, and Dedy H. B. Wicaksono. Optimization of Reduced GO-Based Cotton Electrodes for Wearable Electrocardiography. *IEEE Sensors Journal*, 20(14):7774–7782, July 2020.

[141] Andrew J. Sama, Howard Hillstrom, Aaron Daluiski, and Aviva Wolff. Reliability and agreement between two wearable inertial sensor devices for measurement of arm activity during walking and running gait. *Journal of Hand Therapy*, 2020.

[142] Lauren Samy, Ming-Chun Huang, Jason J. Liu, Wenyao Xu, and Majid Sarrafzadeh. Unobtrusive sleep stage identification using a pressure-sensitive bed sheet. *IEEE Sensors Journal*, 14(7):2092–2101, 2014.

[143] Sofia Scataglini, Giuseppe Andreoni, and Johan Gallant. A Review of Smart Clothing in Military. In *Proceedings of the 2015 workshop on Wearable Systems and Applications*, pages 53–54, Florence Italy, May 2015. ACM.

[144] Georg Schmidt, Marek Malik, Petra Barthel, Raphael Schneider, Kurt Ulm, Linda Rolnitzky, A John Camm, J Thomas Bigger, and Albert Schömig. Heart-rate turbulence after ventricular premature beats as a predictor of mortality after acute myocardial infarction. *The Lancet*, 353(9162):1390–1396, April 1999.

[145] Tanja Schmitz-Hübsch, Alexander U. Brandt, Caspar Pfueller, Leonora Zange, Adrian Seidel, Andrea A. Kühn, Friedemann Paul, Martina Minnerop, and Sarah Doss. Accuracy and repeatability of two methods of gait analysis – GaitRite™ und Mobility Lab™ – in subjects with cerebellar ataxia. *Gait & Posture*, 48:194–201, July 2016.

[146] Mohamed Adel Serhani, Hadeel T. El Kassabi, Heba Ismail, and Alramzana Nujum Navaz. Ecg monitoring systems: Review, architecture, processes, and key challenges. *Sensors*, 20(6), 2020.

[147] Hasan Shahariar, Inhwan Kim, Raj Bhakta, and Jesse S Jur. Direct-write printing process of conductive paste on fiber bulks for wearable textile heaters. *Smart Materials and Structures*, 29(8):085018, August 2020.

[148] Mahmuda Akter Shathi, Minzhi Chen, Nazakat Ali Khoso, Md Taslimur Rahman, and Bidhan Bhattacharjee. Graphene coated textile based highly flexible and washable sports bra for human health monitoring. *Materials & Design*, 193:108792, 2020.

[149] Abdella Ahmmed Simegnaw, Benny Malengier, Gideon Rotich, Melkie Getnet Tadesse, and Lieva Van Langenhove. Review on the Integration of Microelectronics for E-Textile. *Materials*, 14(17):5113, September 2021.

[150] Sneh K Sinha, Hugo F Posada-Quintero, Yeonsik Noh, Christopher Allen, Robert Daniels, Ki H Chon, Laurie Sloan, and Gregory A Sotzing. Integrated dry poly (3, 4-ethylenedioxythiophene): polystyrene sulfonate electrodes on finished textiles for continuous and simultaneous monitoring of electrocardiogram, electromyogram and electrodermal activity. *Flexible and Printed Electronics*, 5(3):035009, 2020.

[151] D Stegeman and H Hermens. Standards for surface electromyography: The european project surface emg for non-invasive assessment of muscles (seniam). *Enschede: Roessingh Research and Development*, pages 108–12, 2007.

[152] Matteo Stoppa and Alessandro Chiolerio. Wearable Electronics and Smart Textiles: A Critical Review. *Sensors*, 14(7):11957–11992, July 2014.

[153] Fabio A. Storm, Christopher J. Buckley, and Claudia Mazzà. Gait event detection in laboratory and real life settings: Accuracy of ankle and waist sensor based methods. *Gait & Posture*, 50:42–46, October 2016.

[154] Zhenhua Tang, Dijie Yao, Donghe Du, and Jianyong Ouyang. Highly machine-washable e-textiles with high strain sensitivity and high thermal conduction. *Journal of Materials Chemistry C*, 8(8):2741–2748, 2020.

[155] Meseret N. Teferra, David A. Hobbs, Robyn A. Clark, and Karen J. Reynolds. Preliminary Analysis of a Wireless and Wearable Electronic-Textile EASI-Based Electrocardiogram. *Frontiers in Cardiovascular Medicine*, 8:806726, December 2021.

[156] Meseret N. Teferra, David A. Hobbs, Robyn A. Clark, and Karen J. Reynolds. Electronic-Textile 12-Lead Equivalent Diagnostic Electrocardiogram Based on the EASI Lead Placement. *IEEE Sensors Journal*, 22(6):5994–6001, March 2022.

[157] Luca Della Toffola, Shyamal Patel, Muzaffer Y. Ozsecen, Ravi Ramachandran, and Paolo Bonato. A wearable system for long-term monitoring of knee kinematics. In *Proceedings of 2012 IEEE-EMBS International Conference on Biomedical and Health Informatics*, pages 188–191, 2012.

[158] Kaiyu Tong and Malcolm H Granat. A practical gait analysis system using gyroscopes. *Medical Engineering & Physics*, 21(2):87–94, March 1999.

[159] Diana Trojaniello, Andrea Cereatti, Elisa Pelosin, Laura Avanzino, Anat Mirelman, Jeffrey M Hausdorff, and Ugo Della Croce. Estimation of step-by-step spatio-temporal parameters of normal and impaired gait using shank-mounted magneto-inertial sensors: application to elderly, hemiparetic, parkinsonian and choreic gait. *Journal of NeuroEngineering and Rehabilitation*, 11(1):152, 2014.

[160] Diana Trojaniello, Andrea Ravaschio, Jeffrey M. Hausdorff, and Andrea Cereatti. Comparative assessment of different methods for the estimation of gait temporal parameters using a single inertial sensor: application to elderly, post-stroke, Parkinson's disease and Huntington's disease subjects. *Gait & Posture*, 42(3):310–316, September 2015.

[161] Granch Berhe Tseghai, Benny Malengier, Kinde Anlay Fante, Abreha Bayrau Nigusse, and Lieva Van Langenhove. Integration of Conductive Materials with Textile Structures, an Overview. *Sensors*, 20(23):6910, December 2020.

[162] Can Tunca, Nezihe Pehlivan, Nağme Ak, Bert Arnrich, Gülüstü Salur, and Cem Ersoy. Inertial Sensor-Based Robust Gait Analysis in Non-Hospital Settings for Neurological Disorders. *Sensors*, 17(4):825, April 2017.

[163] I. N. Tyurin, V. V. Getmantseva, and E. G. Andreeva. Van der Pauw Method for Measuring the Electrical Conductivity of Smart Textiles. *Fibre Chemistry*, 51(2):139–146, July 2019.

[164] Shahood uz Zaman, Xuyuan Tao, Cédric Cochrane, and Vladan Koncar. Launderability of Conductive Polymer Yarns Used for Connections of E-textile Modules: Mechanical Stresses. *Fibers and Polymers*, 20(11):2355–2366, November 2019.

[165] Louise Valentine, Jen Ballie, Joanna Bletcher, Sara Robertson, and Frances Stevenson. Design Thinking for Textiles: let's make it meaningful. *The Design Journal*, 20(sup1):S964–S976, July 2017.

[166] Erik Vanegas, Raul Igual, and Inmaculada Plaza. Sensing systems for respiration monitoring: A technical systematic review. *Sensors*, 20(18), 2020.

[167] Chi Cuong Vu and Jooyong Kim. Highly sensitive e-textile strain sensors enhanced by geometrical treatment for human monitoring. *Sensors*, 20(8):2383, 2020.

[168] Chicuong Vu and Jooyong Kim. Human motion recognition using e-textile sensor and adaptive neuro-fuzzy inference system. *Fibers and Polymers*, 19(12):2657–2666, 2018.

[169] Lie Wang, Xuemei Fu, Jiqing He, Xiang Shi, Taiqiang Chen, Peining Chen, Bingjie Wang, and Huisheng Peng. Application Challenges in Fiber and Textile Electronics. *Advanced Materials (Deerfield Beach, Fla.)*, 32(5):e1901971, February 2020.

[170] Edward P. Washabaugh, Tarun Kalyanaraman, Peter G. Adamczyk, Edward S. Claflin, and Chandramouli Krishnan. Validity and repeatability of inertial measurement units for measuring gait parameters. *Gait & Posture*, 55:87–93, June 2017.

[171] P. Welch. The use of fast Fourier transform for the estimation of power spectra: A method based on time averaging over short, modified periodograms. *IEEE Transactions on Audio and Electroacoustics*, 15(2):70–73, June 1967.

[172] Yi-Zhi Wu, Jia-Xin Sun, Long-Fei Li, Yong-Sheng Ding, and Hong-An Xu. Performance evaluation of a novel cloth electrode. In *2010 4th International Conference on Bioinformatics and Biomedical Engineering*, pages 1–5, 2010.

[173] Shanshan Yao, Ji Yang, Felipe R Poblete, Xiaogang Hu, and Yong Zhu. Multifunctional electronic textiles using silver nanowire composites. *ACS applied materials & interfaces*, 11(34):31028–31037, 2019.

[174] Chao Ye, Jing Ren, Yanlei Wang, Wenwen Zhang, Cheng Qian, Jun Han, Chenxin Zhang, Kai Jin, Markus J. Buehler, David L. Kaplan, and Shengjie Ling. Design and fabrication of silk templated electronic yarns and applications in multifunctional textiles. *Matter*, 1(5):1411–1425, 2019.

[175] J.S. Yeap, R. Birch, and D. Singh. Long-term results of tibialis posterior tendon transfer for drop-foot. *International Orthopaedics*, 25(2):114–118, April 2001.

[176] Julia Yeung, Davis Catolico, Niko Fullmer, Russell Daniel, Ryan Lovell, Ruiqi Tang, Elise M. Pearson, and Sheila S. Rosenberg. Evaluating the Sensoria Smart Socks Gait Monitoring System for Rehabilitation Outcomes. *PM&R*, 11(5):512–521, May 2019.

[177] Rafdzah Zaki, Awang Bulgiba, Roshidi Ismail, and Noor Azina Ismail. Statistical methods used to test for agreement of medical instruments measuring continuous variables in method comparison studies: a systematic review. *PloS One*, 7(5):e37908, 2012.

[178] Shahood uz Zaman, Xuyuan Tao, Cédric Cochrane, and Vladan Koncar. Understanding the Washing Damage to Textile ECG Dry Skin Electrodes, Embroidered and Fabric-Based; set up of Equivalent Laboratory Tests. *Sensors*, 20(5):1272, February 2020.

[179] Chen Zhao, Xiao Li, Qiyang Wu, and Xinyu Liu. A thread-based wearable sweat nanobiosensor. *Biosensors and Bioelectronics*, page 113270, 2021.

[180] Huiru Zheng, Norman D Black, and Nigel D Harris. Position-sensing technologies for movement analysis in stroke rehabilitation. *Medical and biological engineering and computing*, 43(4):413–420, 2005.

Author's Publications

Amitrano, F., Donisi, L., Coccia, A., Biancardi, A., Pagano, G., & D'Addio, G. (2020). Experimental Development and Validation of an E-Textile Sock Prototype. 2020 IEEE International Symposium on Medical Measurements and Applications (MeMeA), 1–5. https://doi.org/10.1109/MeMeA49120.2020.9137302

Coccia, A., Lanzillo, B., Donisi, L., Amitrano, F., Cesarelli, G., & D'Addio, G. (2020). Repeatability of Spatio-Temporal Gait Measurements in Parkinson's Disease. 2020 IEEE International Symposium on Medical Measurements and Applications (MeMeA), 1–6. https://doi.org/10.1109/MeMeA49120.2020.9137357

Donisi, L., Coccia, A., Amitrano, F., Mercogliano, L., Cesarelli, G., & D'Addio, G. (2020). Backpack Influence on Kinematic Parameters related to Timed Up and Go (TUG) Test in School Children. 2020 IEEE International Symposium on Medical Measurements and Applications (MeMeA), 1–5. https://doi.org/10.1109/MeMeA49120.2020.9137198

Donisi, L., Ricciardi, C., Cesarelli, G., Pagano, G., Amitrano, F., & D'Addio, G. (2020). Machine Learning applied on Poincaré Analyisis to discriminate different cardiac issues. 2020 11th Conference of the European Study Group on Cardiovascular Oscillations (ESGCO), 1–2. https://doi.org/10.1109/ESGCO49734.2020.9158144

Donisi, L., Cesarelli, G., Amitrano, F., Coccia, A., Gargiulo, P., & D'Addio, G. (2020, settembre 18). An overall agreement evaluation between two measuring systems for gait analysis through a machine learning approach. Nordic Baltic Conference on Biomedical Engineering and Medical Physics 2020 - NBC 2020.

Amitrano, F., Coccia, A., Ricciardi, C., Donisi, L., Cesarelli, G., Capodaglio, E. M., & D'Addio, G. (2020). Design and Validation of an E-Textile-Based Wearable Sock for Remote Gait and Postural Assessment. Sensors, 20(22), 6691. https://doi.org/10.3390/s20226691

Donisi, L., Amitrano, F., Coccia, A., Mercogliano, L., Cesarelli, G., & D'Addio,

G. (2021). Influence of the Backpack on School Children's Gait: A Statistical and Machine Learning Approach. In T. Jarm, A. Cvetkoska, S. Mahnič-Kalamiza, & D. Miklavcic (A c. Di), 8th European Medical and Biological Engineering Conference (Vol. 80, pp. 682–688). Springer International Publishing. https://doi.org/10.1007/978-3-030-64610-3_76

Donisi, L., Pagano, G., Cesarelli, G., Coccia, A., Amitrano, F., & D'Addio, G. (2021). Benchmarking between two wearable inertial systems for gait analysis based on a different sensor placement using several statistical approaches. Measurement, 173, 108642. https://doi.org/10.1016/j.measurement.2020.108642

Amitrano, F., Coccia, A., Donisi, L., Biancardi, A., Pagano, G., & D'Addio, G. (2021, giugno 9). Experimental Validation of an E-Textile T-Shirt for ECG Monitoring. VIII Congress of National Group of Bioengineering – GNB2021.

Donisi, L., Coccia, A., Amitrano, F., Ricciardi, C., Cesarelli, G., & D'Addio, G. (2021, giugno 9). Benchmarking between a Sensorized E-textile Sock for Remote Monitoring and a Stereophotogrammetric System. VIII Congress of National Group of Bioengineering – GNB2021.

Amitrano, F., Coccia, A., Donisi, L., Pagano, G., Cesarelli, G., & D'Addio, G. (2021). Gait Analysis using Wearable E-Textile Sock: An Experimental Study of Test-Retest Reliability. 2021 IEEE International Symposium on Medical Measurements and Applications (MeMeA), 1–6.
https://doi.org/10.1109/MeMeA52024.2021.9478702

Coccia, A., Amitrano, F., Balbi, P., Donisi, L., Biancardi, A., & D'Addio, G. (2021). Analysis of Test-Retest Repeatability of Gait Analysis Parameters in Hereditary Spastic Paraplegia. 2021 IEEE International Symposium on Medical Measurements and Applications (MeMeA), 1–6.
https://doi.org/10.1109/MeMeA52024.2021.9478743

Donisi, L., Moretta, P., Coccia, A., Amitrano, F., Biancardi, A., & D'Addio, G. (2021). Distinguishing Stroke patients with and without Unilateral Spatial Neglect by means of Clinical Features: A Tree-based Machine Learning Approach. 2021 IEEE International Symposium on Medical Measurements and Applications (MeMeA), 1–5. https://doi.org/10.1109/MeMeA52024.2021.9478727

Coccia, A., Amitrano, F., Donisi, L., Cesarelli, G., Pagano, G., Cesarelli, M., & D'Addio, G. (2021). Design and validation of an e-textile-based wearable system for remote health monitoring. ACTA IMEKO, 10(2), 220.
https://doi.org/10.21014/acta_imeko.v10i2.912

Amitrano, F., Coccia, A., Donisi, L., Cesarelli, G., Pagano, G., & D'Addio, G. (2021). Benchmarking of Novel Wearable Smart Socks with Optoelectronic Gait Analysis System in Assessing Walking Cadence. Proceedings XXI Congresso SIAMOC 2021, 85. https://doi.org/10.6092/unibo/amsacta/6846

Cesarelli, G., Donisi, L., Scioli, M., Di Caprio, G., Amitrano, F., & D'Addio,

G. (2021). Gait analysis as a potential indicator of the rehabilitation outcome for obese patients. Proceedings XXI Congresso SIAMOC 2021, 65. https://doi.org/10.6092/unibo/amsacta/6846

Coccia, A., Amitrano, F., Pagano, G., Bosco, V., Losavio, E., & D'Addio, G. (2021). Quantitative Outcome Assessment of Ankle Foot Orthosis Using Biomechanical Modelling and Simulation of Gait: A Case Study. Proceedings XXI Congresso SIAMOC 2021, 92. https://doi.org/10.6092/unibo/amsacta/6846

D'Addio, G., Donisi, L., Cesarelli, G., Amitrano, F., Coccia, A., La Rovere, M. T., & Ricciardi, C. (2021). Extracting Features from Poincaré Plots to Distinguish Congestive Heart Failure Patients According to NYHA Classes. Bioengineering, 8(10), 138. https://doi.org/10.3390/bioengineering8100138

Donisi, L., Capodaglio, E. M., Amitrano, F., Cesarelli, G., Pagano, G., & D'Addio, G. (2021). A multiple linear regression approach to extimate lifted load from features extracted from inertial data. Giornale Italiano Di Medicina Del Lavoro Ed Ergonomia, 43(4), 373–378.

Cesarelli, G., Donisi, L., Coccia, A., Amitrano, F., D'Addio, G., & Ricciardi, C. (2021). The E-Textile for Biomedical Applications: A Systematic Review of Literature. Diagnostics, 11(12), 2263. https://doi.org/10.3390/diagnostics11122263

Donisi, L., Ricciardi, C., Cesarelli, G., Coccia, A., Amitrano, F., Adamo, S., & D'Addio, G. (2022). Bidimensional and Tridimensional Poincaré Maps in Cardiology: A Multiclass Machine Learning Study. Electronics, 11(3), 448. https://doi.org/10.3390/electronics11030448

Amitrano, F., Coccia, A., Pagano, G., Dileo, L., Losavio, E., Tombolini, G., & D'Addio, G. (2022a). Study of Gait and Posture Kinematic Indices for the Evaluation of Ankle-Foot Orthoses. Proceedings XXII Congresso SIAMOC 2022, 38. https://doi.org/10.6092/unibo/amsacta/7027

Amitrano, F., Macagno, M., Rossotti, S., Viganò, D., Cesarelli, M., & D'Addio, G. (2022). E-Textile smart socks for gait analysis: A preliminary validation study. Proceedings XXII Congresso SIAMOC 2022, 44. https://doi.org/10.6092/unibo/amsacta/7027

Coccia, A., Amitrano, F., Pagano, G., Dileo, L., Marsico, V., Tombolini, G., & D'Addio, G. (2022a). Kinematic analysis of ankle joint during gait in drop foot patients wearing passive Ankle-Foot Orthosis. Proceedings XXII Congresso SIAMOC 2022, 37. https://doi.org/10.6092/unibo/amsacta/7027

Amitrano, F., Coccia, A., Pagano, G., Dileo, L., Losavio, E., Tombolini, G., & D'Addio, G. (2022b). The Impact of Ankle-Foot Orthoses on Spatio-Temporal Gait Parameters in Drop-Foot Patients. 2022 IEEE International Symposium on Medical Measurements and Applications (MeMeA), 1–6. https://doi.org/10.1109/MeMeA54994.2022.9856440

Cesarelli, G., Donisi, L., Coccia, A., Amitrano, F., Biancardi, A., Lanzillo, B., & D'Addio, G. (2022). Ataxia and Parkinson's disease patients classification using tree-based machine learning algorithms fed by spatiotemporal features: A pilot study. 2022 IEEE International Symposium on Medical Measurements and Applications (MeMeA), 1–6. https://doi.org/10.1109/MeMeA54994.2022.9856460

Coccia, A., Amitrano, F., Pagano, G., Dileo, L., Marsico, V., Tombolini, G., & D'Addio, G. (2022b). Biomechanical modelling for quantitative assessment of gait kinematics in drop foot patients with ankle foot orthosis. 2022 IEEE International Symposium on Medical Measurements and Applications (MeMeA), 1–6. https://doi.org/10.1109/MeMeA54994.2022.9856549

Donisi, L., Capodaglio, E., Pagano, G., Amitrano, F., Cesarelli, M., Panigazzi, M., & D'Addio, G. (2022). Feasibility of Tree-based Machine Learning algorithms fed with surface electromyographic features to discriminate risk classes according to NIOSH. 2022 IEEE International Symposium on Medical Measurements and Applications (MeMeA), 1–6. https://doi.org/10.1109/MeMeA54994.2022.9856521

Amitrano, F., Coccia, A., Cesarelli, G., Donisi, L., Pagano, G., Cesarelli, M., & D'Addio, G. (2022, ottobre 26). The Impact of Ankle-Foot Orthosis on Walking Features of Drop Foot Patients. 2022 IEEE International Conference on Metrology for Extended Reality, Artificial Intelligence and Neural Engineering (MetroXRAINE), 2022, Rome, Italy.